THE UNIVERSITY OF CALGARY

CYCLOPHOSPHATHIAZENES: UNSATURATED PHOSPHORUS, NITROGEN AND SULFUR CONTAINING HETEROCYCLES WITH TWO COORDINATE SULFUR

by

NEIL BURFORD

A THESIS

SUBMITTED TO THE FACULTY OF GRADUATE STUDIES

IN PARTIAL FULFILLMENT OF THE REQUIREMENTS FOR THE DEGREE

OF DOCTOR OF PHILOSOPHY

DEPARTMENT OF CHEMISTRY

CALGARY, ALBERTA

JUNE, 1983

THE UNIVERSITY OF CALGARY

FACULTY OF GRADUATE STUDIES

The undersigned certify that they have read, and recommend to the Faculty of Graduate Studies for acceptance, a thesis entitled, "Cyclophosphathiazenes: Unsaturated Phosphorus, Nitrogen and Sulfur Containing Heterocycles With Two Coordinate Sulfur" submitted by Neil Burford in partial fulfillment of the requirements for the degree of Doctor of Philosophy.

T. Chivers.

Dr. T. Chivers (Chairman)
Department of Chemistry

P.M. Boorman

Dr. P.M. Boorman
Department of Chemistry

K.A. Kerr

Dr. K.A. Kerr
Department of Chemistry

P. Bayliss

Dr. P. Bayliss
Department of Geology

A.H. Cowley

Dr. A.H. Cowley
Department of Chemistry
University of Texas at Austin

Date: June 17, 1983

ABSTRACT

The complex reaction mixtures obtained from the nucleophilic degradation of S_4N_4 by certain phosphines possessing labile ligands (Ph_2PH, $Ph_2P\text{-}PPh_2$, $Me_2P\text{-}PMe_2$) were examined by ^{31}P NMR spectroscopy. In addition to the respective phosphine sulfides, the major products are three unsaturated phosphorus, nitrogen and sulfur containing heterocycles with two coordinate sulfur. The distinctive colors of these compounds allowed simple chromatographic separation. The deep purple species was characterized as $(R_2PN)(SN)_2$ (I). An X-ray structural study of the phenyl derivative shows it to be planar in the S_2N_3 region with the phosphorus displaced from the plane by 0.28 Å. Fluoro and phenoxy derivatives of I

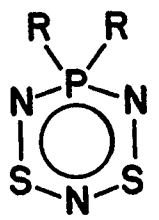

I

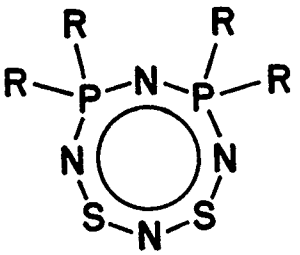

II

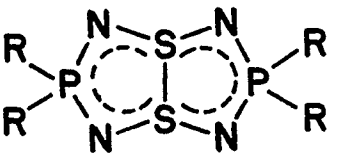

III

have also been prepared and are blue in color. The deep orange and pale yellow compounds were characterized as the two structural isomers of an eight- membered ring, 1,3-$(R_2PN)_2(SN)_2$ (II) and 1,5-$(R_2PN)_2(SN)_2$ (III). The molecular structures of the phenyl derivatives of II (R = 0.054) and III (R = 0.045) and the methyl derivative of III (R = 0.033) were determined by X-ray crystallographic methods. The structure of the S_2N_3 unit of II is similar to the same unit of I, and the phosphorus atoms are displaced on opposite sides of the S-N plane by 0.69 Å. In contrast, III has a folded conformation with a short cross-ring S-S contact of 2.528(1) Å in the phenyl derivative and 2.551(2) Å in the methyl

derivative.

At the simple Hückel level, an internal salt model was used to describe the π-structures of I and II. In both cases the low energy π*-MO is occupied. The strong visible absorption observed at 550 nm for I and 460 nm for II was assigned to the same π*(HOMO)-π*(LUMO) electronic transition. The opposite positions of the sulfur atoms in III allows the possibility of a cross-ring S-S σ-bonding interaction.

The two antibonding electrons are readily removed from I and II by halogenation. The dichloride of I was characterized by elemental analysis and spectroscopic data. Chlorination of II produces the six-membered $(R_2PN)_2(NSCl)$, whilst bromination and iodination yield a twelve-membered dicationic heterocycle $(R_2PN)_4(NS)_2^{2+}$ $(X_3^-)_2$ (X = Br, I). The molecular structure of the tribromide derivative of the dication was determined by X-ray methods (R = 0.048). Oxidation of III with chlorinating agents and bromine results in cleavage of the cross-ring S-S bond to give a dihalide. An X-ray crystallographic study of 1,5-$(Ph_2PN)_2(NSBr)_2$ (R = 0.043) indicates a trans covalent addition tothe sulfur atoms effecting a flattening of the P-N-S ring.

Both $(Ph_2PN)(NSCl)_2$ and 1,5-$(Ph_2PN)_2(NSCl)_2$ undergo a metathesis reaction with $Me_3SiNSNSiMe_3$ to give a bicyclic system and a cage system, respectively. The former can be quantitatively transformed back into I by a thermal degradation involving reductive elimination of an N_2S unit.

Rapid cycloaddition reactions of I and II with norbornadiene give 1:1 adducts. An X-ray crystallographic examination indicates an exo stereochemistry for the addition. The reaction between an olefin and an $S_2N_3^-$ unit has been shown to be an $8\pi_s + 2\pi_s$ thermally allowed reaction.

ACKNOWLEDGEMENTS

Special thanks go to my supervisor, Dr. T. Chivers, whose guidance and assistance were outstanding. It was a pleasure working with him.

Thanks also go to a variety of coworkers, who have provided additional assistance in many ways. In particular, Dr. R. T. Oakley, for his friendship, help and many long stimulating discussions; I will always be grateful. Dr. J. F. Richardson, for his patience and guidance with much of the crystallographic work. Dr. P. W. Codding, for her instruction during my first attempt at crystallography. Dr. R. Yamdagni, for obtaining NMR spectra. Drs. R. A. Kydd and C. Lau for measuring the Raman spectra. Dr. M. N. S. Rao, for many useful discussions.

Thanks go to the Department of Chemistry at the University of Calgary and the Alberta Research Council for financial support.

Finally, I would like to thank my family and friends for their encouragement, particularly my wife, for her constant support, patience and perseverance in typing this thesis.

With Love

To My

Loving Wife and

Caring Parents

TABLE OF CONTENTS

LIST OF TABLES

LIST OF FIGURES

LIST OF ABBREVIATIONS

cm^{-1}	:	wavenumbers
nm	:	nanometres
Å	:	angstroms
ml	:	millilitres
mm	:	millimetres
mmol	:	millimoles
g	:	grams
^{o}C	:	degrees Celsius
eV	:	electron volts
Kcal	:	kilocalories
D	:	Density
V	:	volume
Z	:	number of molecules in the unit cell
UV	:	ultra-violet
(vs)	:	very strong
(s)	:	strong
(m)	:	medium
(w)	:	weak
(vw)	:	very weak
sh	:	shoulder
I	:	intensity
MO	:	molecular orbital
M	:	molarity
λ	:	wavelength
ε	:	extinction coefficient

Structural parameters (bond lengths and angles, atomic coordinates, etc.) are presented with estimated standard deviations in parentheses.

CHAPTER 1

UNSATURATED INORGANIC HETEROCYCLES

1.1 GENERAL INTRODUCTION

Catenation is probably the most important single feature of carbon responsible for the large number of organic compounds. Although certain non-metals (Si[1], S[2], Se[2]) do form a significant number of chains and rings, none compare with the extensive series of known carbon compounds. However, many non-metallic elements (B, O, N, Si, P, S, etc.) exhibit various types of heterocatenation (chains built up of alternating atoms of different elements). Compounds such as polyphosphates[3], silicates[4] and phosphorus sulfides[5], are relatively thermodynamically stable. In contrast, heterochains and rings containing nitrogen (borazines, phosphazenes and thiazenes) are very reactive and all have rich chemistries. One of their most interesting features is that they form a wide range of unsaturated heterocycles and cages. Borazine (1),‡ first prepared in 1926[6], is the best known of these compounds. However, it was in 1834 that Liebig and Wöhler discovered the first inorganic heterocycle, hexachlorocyclotriphosphazene (2)[7,8]. Since then a comprehensive series of unsaturated cyclic compounds known as the cyclophosphazenes or phosphonitriles have been prepared. These phosphorus-nitrogen (P-N) heterocycles are made up of ($R_2P{=}N$) units (R is an exocyclic ligand) with phosphorus in a pentavalent

‡ Many of the compounds discussed in this thesis are represented by some form of structural figure. Valence bond designations are used for certain molecules. However, in cases where cyclic π-electron delocalization is evident, a circle is used to represent the π-bonds within the heterocycle. The structural framework of complex cage molecules are symbolized without π-bonding illustrations.

oxidation state. There have been no reports of cyclophosphazenes containing phosphorus in a trivalent oxidation state. The first unsaturated sulfur-nitrogen (S-N) heterocycle, tetrasulfur tetranitride (3), was discovered in 1835 by Gregory[9]. Surprisingly, it is only in the last couple

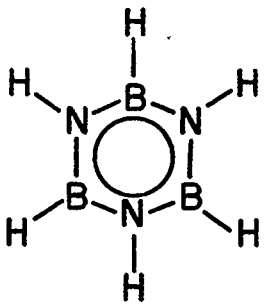

1

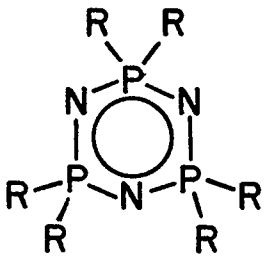

2

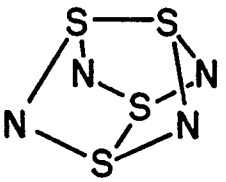

3

of decades that S-N chemistry has attracted attention. Anionic, cationic and neutral S-N compounds have now been discovered, ranging in size from simple four atom open chains (4)[10,11] and rings (5),[12] to more complex ten atom rings (6)[13,14,15,16] and eleven atom cages (7)[17,18,19]. A large

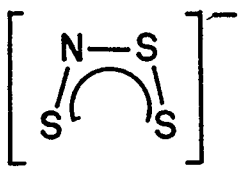

4

5

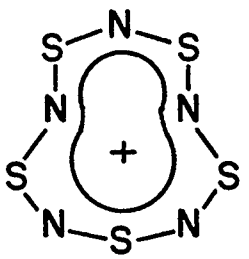

6

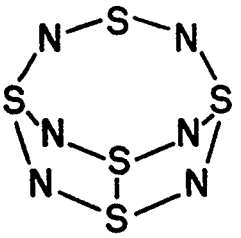

7

variety of S-N heterocycles have been prepared, but unlike the phosphorus analogs, the wide oxidation range exhibited by sulfur results in compounds containing two (8)[20,21], three (9)[22] and four (10)[23,24] coordinate sulfur centers. The compounds of primary interest in this thesis are those containing sulfur in a low oxidation state (II or IV).

Comparisons are continually drawn between the P-N and S-N heterocyclic series and there are a number of mixed P-N-S heterocycles containing

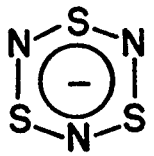

8

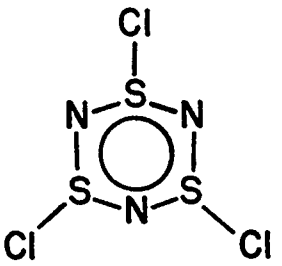

9

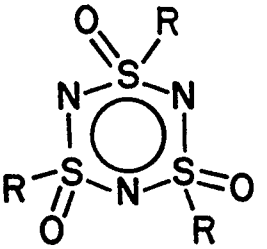

10

four coordinate sulfur (11,12)[25,26]. These compounds have been examined thoroughly with principal interest concentrating on their nucleophilic substitution reactions and anticancer properties[27]. However, there are only two examples of mixed or hybrid P-N-S heterocycles containing sulfur in a low oxidation state (13,14),[28,29,30,31] and neither has been examined in detail. As a natural expansion of P-N and S-N heterocyclic chemistry,

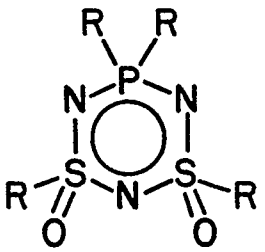

11

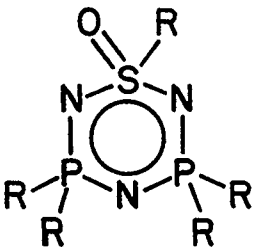

12

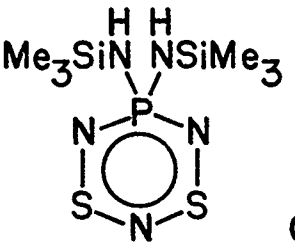

13

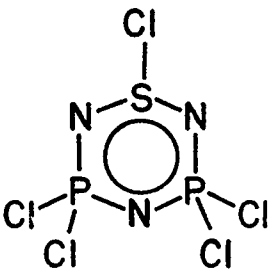

14

it should be possible to develop a series of unsaturated P-N-S rings of various sizes. The structures available for eight-membered P-N-S heterocycles containing sulfur in a low oxidation state are shown (15,16,17,18).

Before investigating the P-N-S systems any further, it is useful to briefly examine the parent systems, the cyclothiazenes and the cyclophos-

phazenes. A large number of up-to-date reviews covering S-N[32,33,34,35 36,37] and P-N[38,39,40,41] compounds, along with a recent book by Heal[42]

15

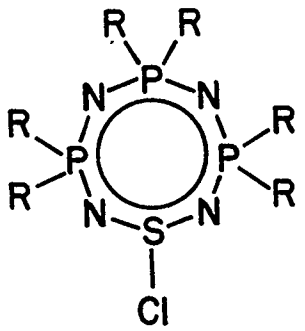

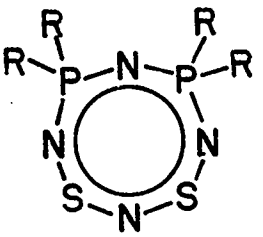

16

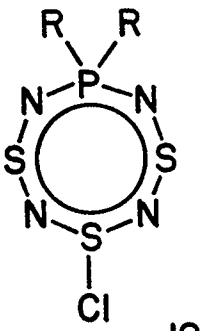

18

17

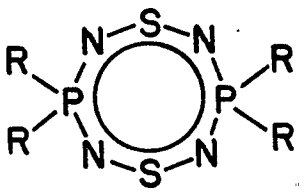

dealing with both areas, are available. A literature survey here would therefore be repetitive. Nevertheless, it is important to discuss the relevant aspects of the chemistry, structure and bonding in the binary S-N and P-N heterocycles, as a foundation for discussion in later chapters. The various bonding concepts available to describe inorganic systems are first inspected, in order to appreciate the properties and difficulties encountered with heterocycles. This is followed by a study of the S-N heterocyclic system containing low oxidation state sulfur and then, for comparison, a general examination of the cyclophosphazenes.

1.2 BONDING IN UNSATURATED INORGANIC HETEROCYCLES

Homonuclear single bonds are common for many non-metallic elements. Molecular oxygen has a strong double bond and N_2 has the strongest (triple) bond known. However, $p\pi$-$p\pi$ multiple bonds between non-metallic elements of the second-period are rare. It is only very recently that a compound

containing a P=P double bond has been reported[43]. The second-row elements are not able to approach close enough to achieve good overlap of $p\pi$ atomic orbitals, due to the large repulsive forces resulting from overlapping of their filled inner shells. The small compact inner shell of the first-row elements does not produce this repulsion.

There are a variety of examples of heteronuclear π-bonding between first and second-row elements. In such cases the second-row elements must employ an atomic orbital from the third shell. Dicoordinate sulfur and phosphorus utilize $3p_z$ orbitals, however, tricoordinate and tetracoordinate sulfur and tetracoordinate phosphorus have the 3s and 3p orbitals incorporated into σ-bonds and must make use of 3d orbitals for π-bonding[44]. Four d orbitals are capable of π-overlap (d_z^2 does not have π-symmetry). The d_{xz} and d_{yz} orbitals have the potential of out of plane interaction and the d_{xy} and $d_{x^2-y^2}$ may interact in a π-fashion with nitrogen lone-pair orbitals, within the plane of the molecule. It is believed that the out of plane π-structure is the most significant because the orbitals are directed towards the lobes of the neighbouring π-type orbitals. The behavior of the d_{xz} and d_{yz} orbitals in the local molecular site group

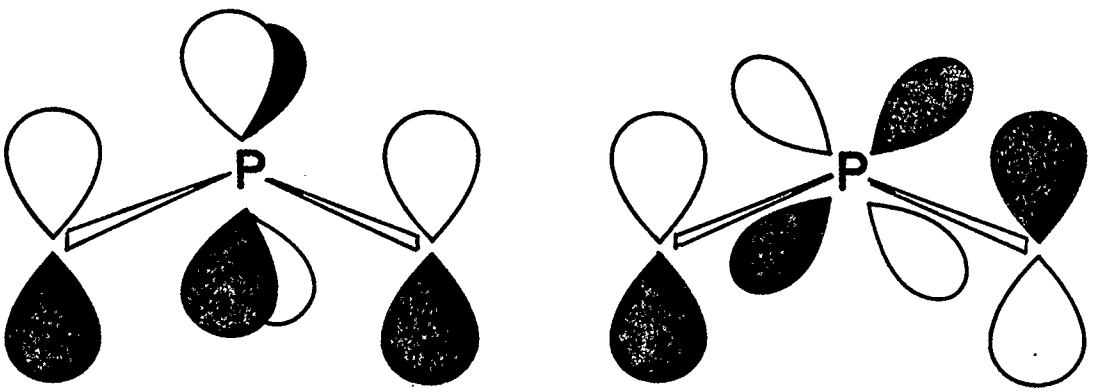

d_{yz} d_{xz}

directly governs their mode of π-interaction, as illustrated for phos-

phorus. The d_{yz} orbital is antisymmetric with respect to a molecular C_2 axis and only interacts with molecular orbitals of the same symmetry. An overlap of this type is referred to as a homomorphic interaction[40]. The d_{xz} orbital is symmetric with respect to the same C_2 axis and the interaction is termed heteromorphic[40].

Naturally, the different sizes of the orbitals results in a less effective overlap compared to a 2pπ-2pπ interaction. Moreover, the difference in electronegativities of the atomic centers polarizes the π-electron density towards the more electronegative atom. Therefore, the form of the π-cloud may be an almost even electron distribution between the atoms, an internal salt arrangement (in which one center donates its π-electron to the other center) or any intermediate. This description can be extended to include the heterocatenated cyclic environment of an $(AB)_n$ type system. Many compounds of this nature have features reminiscent of a homocyclic system such as benzene. Short equivalent bond lengths, ring planarity and chemical and spectroscopic properties are all evidence for a degree of circumannular π-electron delocalization. The structure of the π-manifold depends mainly on the difference in electronegativity between the atoms and the extent of overlap afforded by the atomic orbitals having π-symmetry. When the atoms have similar electronegativities the π-structure may be viewed in the same context as benzene. Alternatively, a large electronegativity difference allows a description involving an internal salt with π-donation back through the electropositive nuclei.

Simple valence bond (VB) representations[45] are very useful as a superficial description of the bonding in inorganic heterocycles. They account for connectivity and determine local geometries (tetrahedral or

trigonal arrangement of bonds around an atom). In addition VB structures predetermine the number of electrons in σ-bonds, π-bonds and lone-pairs. However, they do not distinguish between bonding, antibonding and non-bonding electrons, making it difficult to obtain bond orders. Further inadequacies of the VB approach include no effective measure of electron distribution (charge densities) and an inability to examine the excited state properties of a system. A number of empirical electron count methods have been developed for specific types of compounds[46], and although they may provide minor improvements, they lack important features.

The employment of molecular orbital (MO) theory has vastly improved the understanding of bonding in heterocyclic compounds. Inorganic heterocycles of all kinds have now been studied at various levels of sophistication, from simple Hückel[47] (HMO) to rigorous *ab initio* approaches. In many cases, promising agreement of results has been observed between the HMO approach and the sophisticated methods, and this has encouraged application of the simpler procedures to large systems. The extended Hückel method (EHMO) contains all the required parameters for the various elements and produces useful results for inorganic systems including eigenvalues, overlap populations and charge densities. Provided adjustments are made, the simple HMO method also yields useful approximations of the relative orbital energies and wavefunctions[48,49,50]. The Coulomb integrals are directly related to the electronegativity of the orbitals of the atoms and for an $(AB)_n$ type system can be equated by $\alpha_B = \alpha_A + \rho\beta$, where ρ is a parameter that measures the difference between the electronegativities of A and B. When $\rho=0$, the π-structure is the same as that for homocyclic systems (i.e. benzene). The choice of Coulomb parameter is arbitrary, one may use the atomic electronegativities from the Pauling scale[45] or the

orbital electronegativities proposed by Streitweiser[51]. The selection is not obvious for unsaturated inorganic heterocycles, because unlike unsaturated carbon systems, the lower energy π-levels of the more electronegative systems are buried in energy into the upper occupied σ-levels. The result is that the π-MOs of inorganic systems all behave as if they experience a different potential field and cannot be handled accurately by a one electron calculation[52]. Nevertheless, useful information concerning composition and ordering of the frontier orbitals may still be obtained, and with suitable changes of the parameters, π-charge densities may be estimated. However, it may be dangerous to obtain such delicate information from a simple calculation.

The majority of the theoretical discussion in this thesis will be developed from simple HMO calculations. Justification for the validity of the results will be obtained by comparison with results from sophisticated calculations on related systems.

1.3 THE HETEROCYCLIC SULFUR-NITROGEN ENVIRONMENT WITH SULFUR IN A LOW OXIDATION STATE

1.3.1 OXIDATION STATES OF SULFUR IN S-N HETEROCYCLES

Sulfur is one of the most interesting elements. Its comprehensive chemistry has been extensively studied and yet new areas are still being uncovered. The wide range of chemical properties observed for sulfur is a function of the broad oxidation limits available. As mentioned in the general introduction, S-N compounds are known containing many different oxidation states for sulfur, the most common being II, IV and VI. However, it is the lower oxidation states (II and IV) which provide the most unusual

and diverse series of compounds. When the sulfur is two coordinate, the low oxidation states result in a large number of electrons in the π-system, as discussed below. This makes the systems susceptible to oxidative electrophilic attack. Nevertheless, the high electronegativity of both nitrogen and sulfur affords a relatively low energy for all the MOs of the system, including the virtual levels, and allows for reductive nucleophilic attack at the sulfur centers.

When the sulfur centers are restricted to low oxidation states there are a number of structural possibilities for a particular system. For a heterocycle with an even number of sulfur atoms, the formal oxidation states must be different (II and IV) giving an average oxidation state of III. In heterocycles containing an odd number of sulfur atoms, at least one sulfur center must be fixed in an oxidation state of IV and have an exocyclic ligand, in order that simple electron pairing rules are obeyed. The interesting chemical, structural and electronic properties of compounds of this nature can be appreciated by examination of some examples. The most obvious example is S_4N_4, whose chemistry also provides an excellent introduction to other pertinent S-N systems.

1.3.2 S_4N_4

A large part of S-N chemistry has been found to revolve around S_4N_4, and for this reason it is the most well known binary S-N compound. In recent years, the molecular structure, electronic structure and chemistry of this novel and interesting system have been studied in great detail[42] It is still prepared by the method first used; the reaction between sulfur monochloride and gaseous ammonia[53], although other methods are known. It

has also been observed as a by-product in a number of reactions involving S-N compounds[54,55]. The molecular structure of S_4N_4 (deep orange crystals) was first determined in 1944[56], although there are more recent reports[57,58] including a low temperature study[59]. The eight-membered ring is folded into an unusual cage conformation (3). All the S-N bond lengths are equal (1.61 Å), which is shorter than an average single S-N bond (1.74 Å)[60]. The cross-ring S-S bonds (2.58 Å) are longer than the average single (S-S bond (2.05 Å)[61], however, they are well within the sum of the Van der Waals' radii (3.64 Å)[58]. The folded cage structure of S_4N_4 is a consequence of the low oxidation state of the sulfur centers, and a detailed rationale in terms of the electronic structure is given in 1.3.5.4.

1.3.3 THE FORMATION OF S-N HETEROCYCLES FROM S_4N_4

The chemistry of S_4N_4 is complex and extremely diverse. As illustrated in Figure 1.1, many S-N heterocycles have been discovered from its unusual reactions including oxidation, reduction, addition and dissociation. Electrophilic attack of S_4N_4 usually occurs at the electronegative nitrogen center, although there are exceptions (eg. $S_4N_4Cl_2$ (19)[62,63,64]).

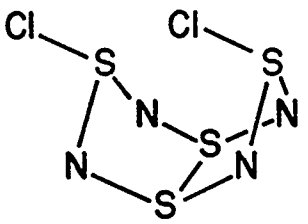

19

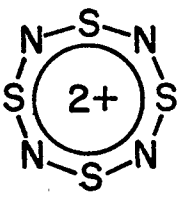

20

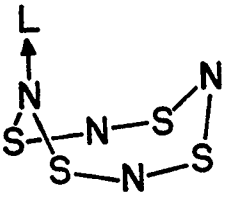

21

In all cases, the products of oxidation are very dependent on the reagent

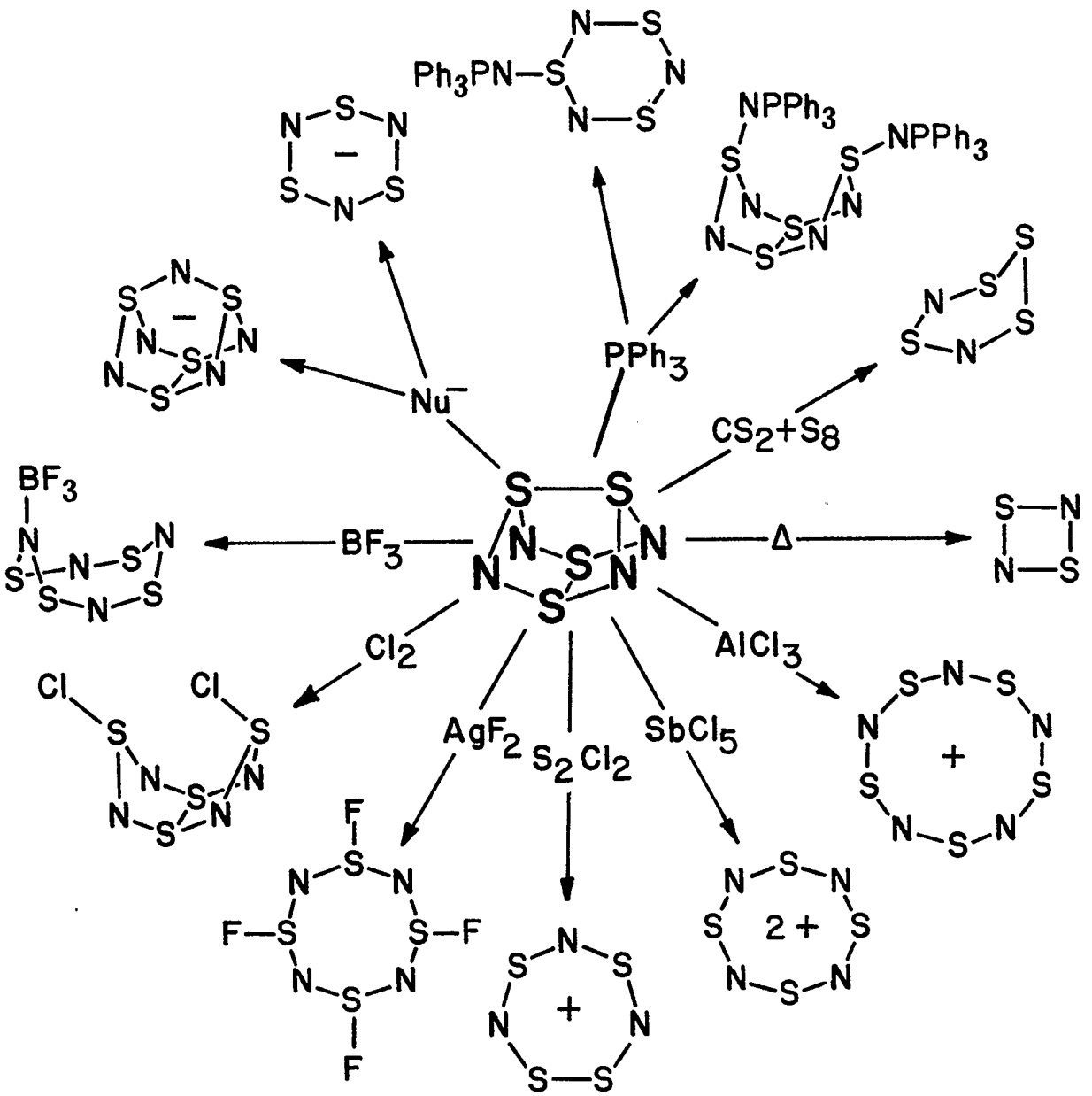

Figure 1.1 The diverse chemistry of S_4N_4.

employed. Strong Lewis acids, such as $SbCl_5$ (under certain conditions), effect the removal of two electrons to give $S_4N_4^{2+}$ (20)[65,66], an almost planar eight-membered ring. In contrast, other Lewis acids (eg. BF_3[67], SO_3[68], $FeCl_3$[69] and AsF_5[70]) form adducts with S_4N_4, in which the acid is bound to a nitrogen atom of a saddle-shaped eight-membered ring (21). Oxidizing agents such as F_3CSO_3H and S_2Cl_2 lead to the formation of various cationic S-N heterocycles, $(S_3N_2^+)_2$ (22)[71,72] and $S_4N_3^+$ (23)[73], respectively.

A series of S-N halides is obtained from the halogenation reactions of S_4N_4. Although the mechanisms of these reactions are complex, the initial step for chlorination and fluorination involves the formation of 1,5-$X_2S_4N_4$ (19)[62,63,74,75]. This is the result of oxidation of one S-S

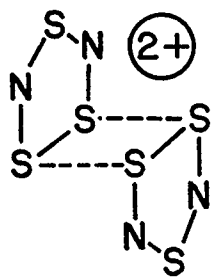

22

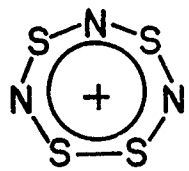

23

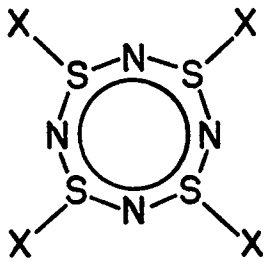

24

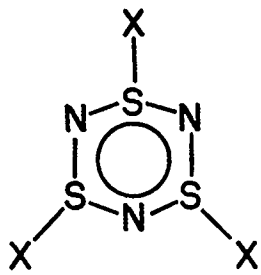

25

cross-ring bond. The fluorination reaction continues, to form $S_4N_4F_4$ (24)[76] and $S_3N_3F_3$ (25)[77]. The fully chlorinated derivative of 24 has never been isolated, instead $S_3N_3Cl_3$ (25)[75,78,79] is observed in high yield This apparent ring contraction indicates the release of an NSX unit, the reason for which is unclear. $S_3N_3F_3$[80] and $S_3N_3Cl_3$[81] have very similar structures as determined by X-ray crystallography. The six-membered ring adopts a chair conformation with equal ring bond lengths and the halogen atoms in axial positions. In contrast to the chair-shaped $S_3N_3F_3$, the

puckered and quite compact structure of $S_4N_4F_4$ has been attributed to the identical bond angles at nitrogen and sulfur. In addition, the S-N bond lengths alternate in $S_4N_4F_4$ and only two fluorine atoms occupy axial positions[76]. Under certain conditions bromination of S_4N_4 gives $S_4N_3^+Br_3^-$[82]. $S_3N_3Br_3$ and $S_3N_3I_3$ are unknown.

Nucleophilic degradation of S_4N_4 results in the formation of very novel, unexpected products. In many cases, the two major components of

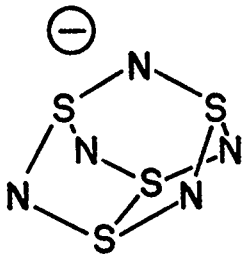

26

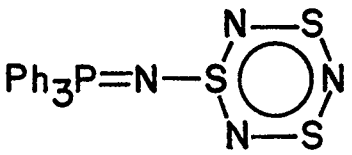

27

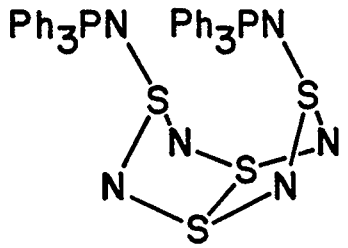

28

the reaction mixture are $S_3N_3^-$ (8)[20,21,83,84] and/or $S_4N_5^-$ (26)[83,84,85]. The reaction with Ph_3P is anomalous, although $S_4N_5^-$ has been observed under certain conditions, the products obtained are $Ph_3P{=}N{-}S_3N_3$ (27) and 1,5-$(Ph_3P{=}N)_2S_4N_4$ (28)[86,87]. These reactions are obviously complex, but the basic mechanism is believed to involve initial attack of the nucleophile at the sulfur center, followed by ring opening. The poly(sulfur-nitrogen) chain may then recyclize to form an S_3N_3 ring[88,89,90,91].

1.3.4 THERMAL INSTABILITY OF S-N COMPOUNDS

All S-N compounds, including S_4N_4, have an inherent thermodynamic instability with respect to their constituent elements. In most cases (eg. S_5N_6) they have a low kinetic barrier to decomposition[18].

consequently, compounds of this nature have explosive tendencies and should be handled with great care[53,92]. Thermal decomposition can be carried out under controlled conditions and the compounds examined so far have been observed to decompose by either the release of an S_2N_2 (5) (e.g. from S_4N_4)[12,93,94,95], or an N_2S unit (e.g. from $S_4N_5^-$)[96,97,98,99]. The volatile S_2N_2 species can be isolated and has been fully characterized[12]. Under suitable conditions it can be polymerized into the well known poly(sulfur nitride) or $(SN)_x$[100]. However, N_2S has never been isolated.

1.3.5 ELECTRONIC STRUCTURES OF S-N HETEROCYCLES CONTAINING SULFUR IN A LOW OXIDATION STATE

VALENCE BOND REPRESENTATIONS

The first attempt to investigate the electronic environment of unsaturated S-N compounds was made by Banister[101,102]. Using a VB approach, he developed a number of simple rules imposing a formal σ and π-designation to the valence electrons of the constituent atoms. For a binary S-N monocycle, the six valence electrons of each sulfur atom and five valence electrons of each nitrogen atom are divided in such a way that each atom contributes one electron to each σ-bond and two electrons to a lone-pair. Thus two electrons remain on each sulfur atom and one on each nitrogen atom, available for π-bonding. VB theory is not able to explain how or where this large number of π-electrons is accommodated by these compounds, which Banister refers to as "Electron-rich systems". In order to rationalize this phenomenon, he has postulated that the

unsaturated S-N heterocycles conform with the Hückel 4n + 2 rule employed for aromatic organic systems. Indeed, all the known binary S-N heterocycles (top Figure 1.2) excepting $S_3N_2^+$[72,104,105], contain (4n + 2) π-electrons. However, many of these heterocycles do not have the high symmetry of the homocyclic carbon systems. It can be argued that for lower symmetries (C_{2v}) the distinction between 4n and (4n + 2)π-electrons is not fundamental, since the Hückel rule is based upon Hund's rule of maximum multiplicity coupled with the presence of degenerate levels in the cyclic hydrocarbons for which it is normally invoked. There are no degenerate levels in C_{2v} systems[106].

MOLECULAR ORBITAL DESCRIPTIONS

In an attempt to overcome the inadequacies encountered in the VB approach (see Section 1.2) and improve the bonding descriptions for unsaturated S-N heterocycles, a number of MO approaches have been employed. Figure 1.2 [107] shows an energy level diagram of the π-structures of the known binary S-N heterocycles, obtained from simple HMO calculations[108]. In all cases, antibonding π^*-levels are occupied to some extent, giving these molecules an inherent instability. In comparison with the π-energy levels of benzene, the relative stability of these systems appears to be dependent mainly on the higher electronegativity of nitrogen and sulfur compared to carbon. This has the effect of lowering the antibonding energy levels towards the region of the bonding energy levels of benzene. A number of important aspects of the electronic structures of these systems are illustrated below by inspection of some specific examples.

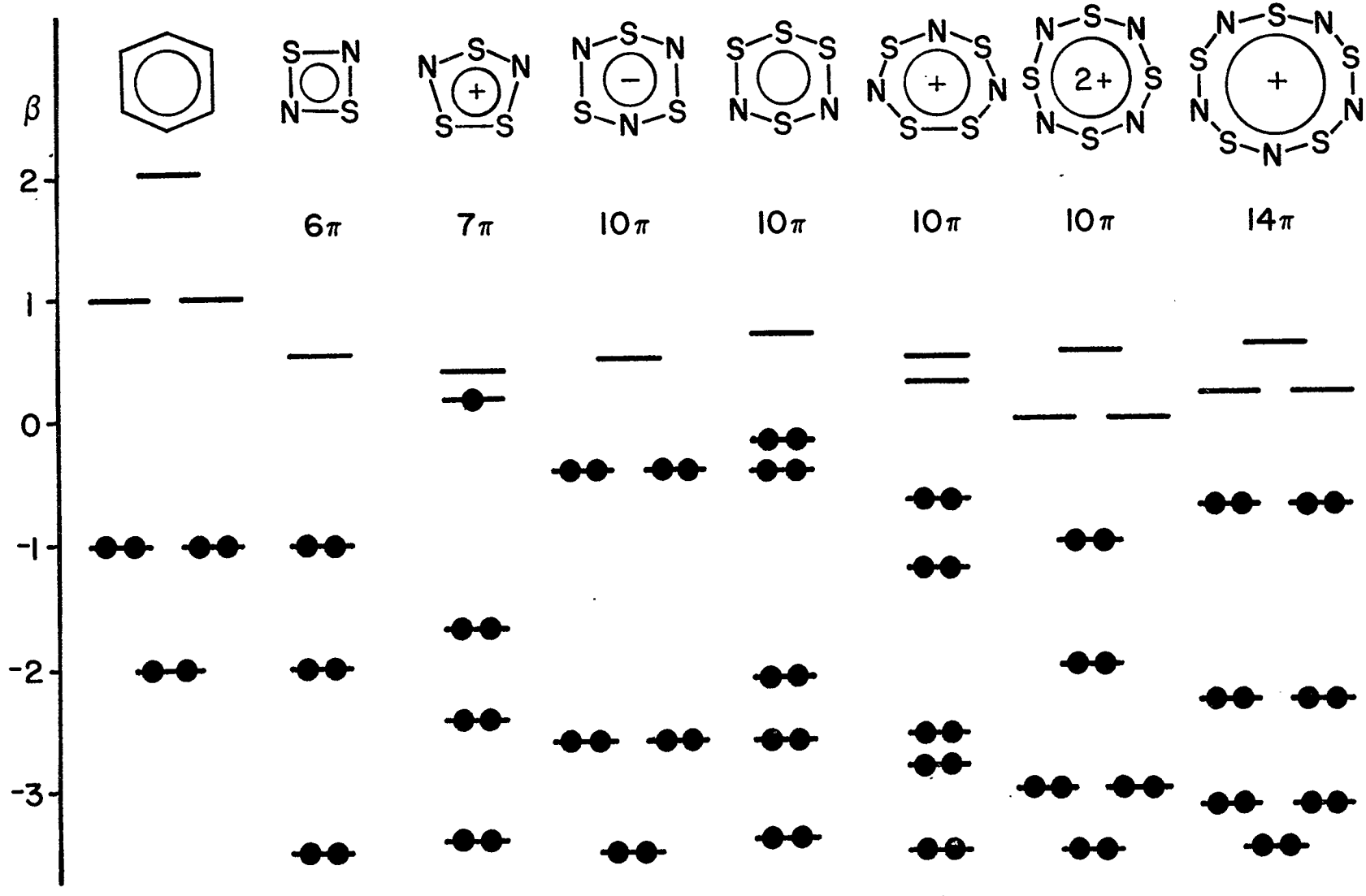

Figure 1.2 Hückel π-levels for known S-N heterocycles compared to benzene.

$S_3N_3^-$

$S_3N_3^-$[20,21] is the most fascinating of the binary unsaturated S-N heterocycles. The molecular structure of $(n\text{-}Bu_4N)^+(S_3N_3)^-$ was determined by X-ray techniques[21], and the anion was found to be planar with all the S-N bond lengths within a narrow range (1.580(12)-1.626(12) Å). A theoretical calculation at an *ab initio* level[21] has shown $S_3N_3^-$ to have a π-system containing ten electrons in agreement with Banister's prediction[101,102]. The D_{3h} symmetry of the ring demands that the π-structure contains two degenerate levels, reminiscent of the π-structure of benzene. However, unlike benzene, the upper degenerate π^*-levels of $S_3N_3^-$ are occupied (Figure 1.2), and this considerably weakens the framework of $S_3N_3^-$ (S-N π-bond order = 0.3) compared to benzene (C-C π-bond order = 0.5).

The substantial antibonding character in $S_3N_3^-$ is accommodated by effective π-electron delocalization around the planar ring (29) and the relative stabilizing effect of the highly electronegative nitrogen atoms.

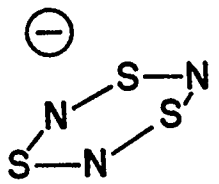

29

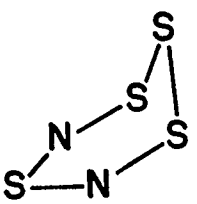

30

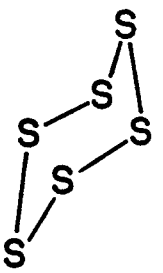

31

This is illustrated by comparison with S_4N_2 (30)[109,110,111], where one of the nitrogen centers in $S_3N_3^-$ has been replaced by a sulfur atom. The π-structure of S_4N_2 is comparatively destabilized both energetically, due to the lower electronegativity of sulfur, and structurally, because of the ineffective π-overlap afforded between two $3p_z$ orbitals. Therefore

the π^*-electrons are rearranged into sulfur lone-pair orbitals, the mutual repulsion of which results in the folded conformation. However, planarity and effective π-bonding is maintained at the N_2S section of the molecule. The poor π-interaction between sulfur centers is further illustrated by the structure of S_6 (31)[112]. The twelve electrons available for π-bonding in S_6 are contained in non-bonding lone-pair orbitals. The electron-electron repulsive forces experienced between the twelve electrons surpass the attractive forces between these electrons and the atomic nuclei. An effective spatial distribution of the lone-pair orbitals is achieved by the chair conformation.

The excited state properties of $S_3N_3^-$ have also been thoroughly investigated. Calculated transition moments and estimated energies have indicated that the intense visible absorption observed at 360nm, is due to a π^*(HOMO)$\rightarrow\pi^*$(LUMO) electronic transition[21]. This assignment has been confirmed by measurement of the magnetic circular dichroism (MCD)† spectrum of $S_3N_3^-$[113], which shows a shape characteristic of a negative A term. The MCD activity of $S_3N_3^-$ demonstrates the effective circumannular π-electron delocalization. An A term signifies that the electronic transition is occuring from a singlet ground state to a degenerate excited state, and the sign of the term indicates that the transition originates from a pair of degenerate molecular orbitals.

There have been a number of attempts to oxidize $S_3N_3^-$, in the hope of isolating $S_3N_3^+$ or S_3N_3X[115,116,117,118,119]. However, the products are S_4N_4 and common S-N halides ($S_3N_3Cl_3$)[120]. The latter is probably a result of oxidation of S_4N_4[75,78,79]. The reason $S_3N_3^+$ has not yet been

---

† For a full description of the MCD experiment see reference 114.

isolated is not clear. However, predictions can be made about its structure. Retention of a planar ring structure with D_{3h} symmetry following a two electron oxidation of $S_3N_3^-$ would result in the formation of an orbitally degenerate ground state. One would expect a Jahn-Teller distortion (chair conformation) to remove the degeneracy and relieve the multiplicity.

S_4N_4

The unique structure and extensive chemistry of S_4N_4 has attracted a large amount of theoretical interest[121,122,123,124,125,126]. In 1970 Gleiter was able to rationalize the cage conformation of S_4N_4 using an EHMO approach[121]. The results are summarized in Figure 1.3, showing an energy level diagram of the π-MOs for a hypothetical planar structure correlated with those of the cage structure observed experimentally. A planar S_4N_4 has 12 π-electrons and therefore the non-bonding b_{2u} MO is occupied and the degenerate antibonding π*-levels (e_g) each contain one electron, giving the molecule an orbitally degenerate ground state. The triplet ground state can be avoided by a Jahn-Teller distortion to either break the degeneracy or destabilize the e_g level and stabilize the a_{2u} level. Puckering of the ring into a crown (cf. S_8[127]) was found to have little effect on the multiplicity of the ground state. However, adjustment into a cradle or cage bringing together opposite sulfur atoms, allows S-S σ-interactions to take place. This causes more pronounced effects on the overall bonding scheme. The result is a singlet ground state containing two cross-ring S-S σ-bonds. Although Figure 1.3 shows the HOMO of the cage structure to be a bonding S-S σ-MO, more sophisticated calculations

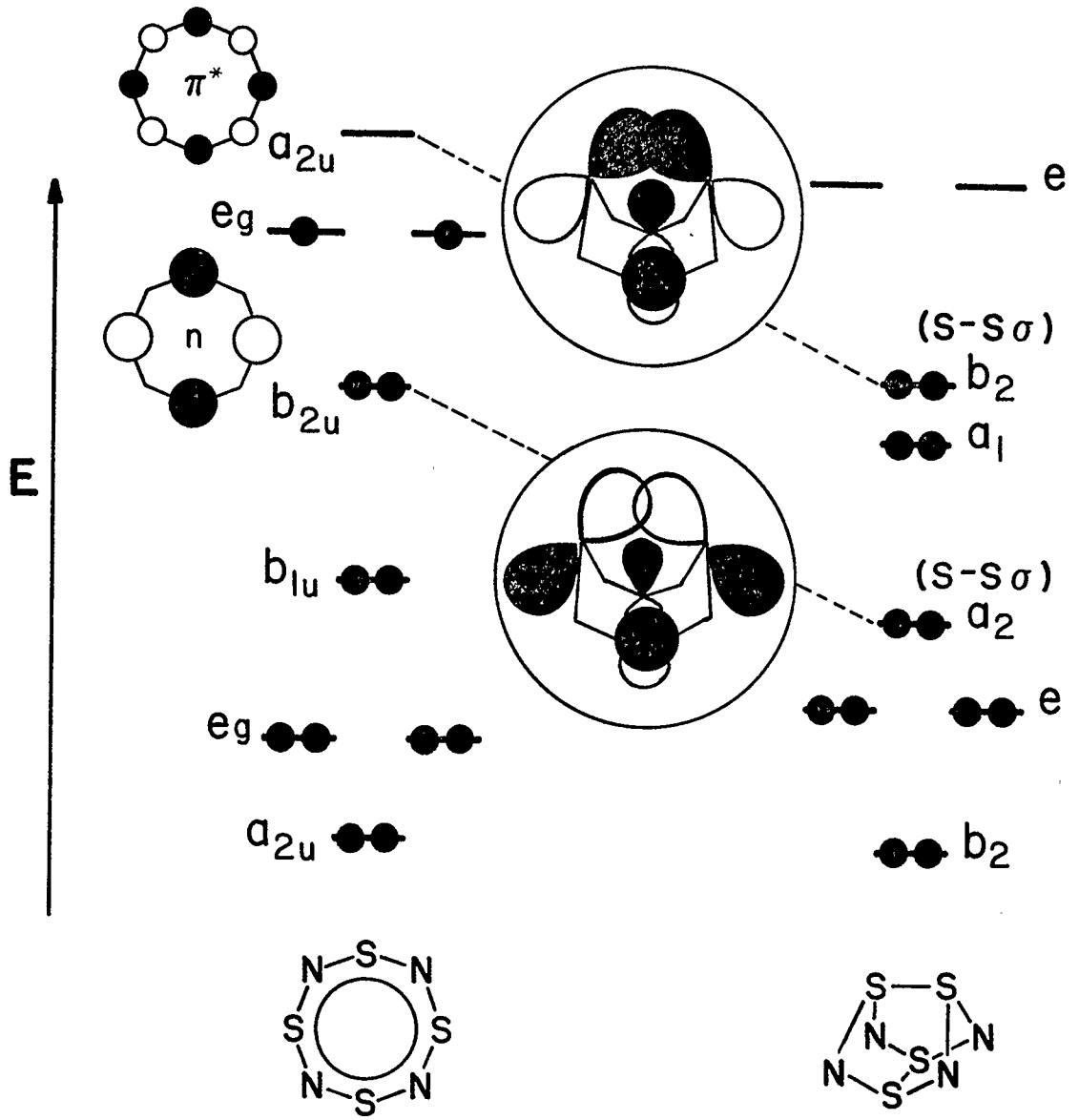

Figure 1.3 Energy correlation diagram for the π-structure of a hypothetical planar S_4N_4 system and the upper levels of the observed cage structure. Shading in the MOs indicates the sign of the wavefunction.

have shown this orbital to be slightly lower in energy than a non-bonding orbital based on nitrogen[126,128]. In many cases, it is an orbital of this nature that is involved in the oxidation of S_4N_4, as illustrated by the formation of the Lewis acid adducts (21)[67,68,69,70]. However, the open structure of the adduct[67] and the planar conformation of $S_4N_4^{2+}$[65,66], suggest an involvement of the electrons contained in the cross-ring S-S σ-bonds. It would appear that activation of the HOMO renders the cage conformation unstable with respect to the open or planar structure.

$S_4N_4^{2+}$

The electronic structure of the $S_4N_4^{2+}$ cation has a number of interesting features. It has been shown to be a 10 π-electron system[129]. However, a recent *ab initio* study[52] indicated that, unlike other unsaturated S-N heterocycles containing sulfur in a low oxidation state, the π-structure is so low in energy that the HOMO is a non-bonding σ-MO and not a π-type orbital. The frontier orbitals of $S_4N_4^{2+}$ are shown in Figure 1.4. In view of the folded structure of $S_4N_4Cl_2$ (19)[64], the planar structure of $S_4N_4^{2+}$ is surprising. It would appear that the delocalization energy of the π-structure of $S_4N_4^{2+}$ accommodates the electron density more efficiently than the folded structure. In addition, the positive charge effects a general stabilization of all the energy levels, in comparison to a neutral system.

The two major absorptions (λ_{max} = 346 nm and 262 nm) observed in the UV-visible spectrum of $S_4N_4^{2+}$[52], have been assigned from results obtained from transition moment calculations. The HOMO→LUMO transition is symm etry forbidden. Instead, the two highest occupied π-type MOs ($1b_{1u}(n\pi)$

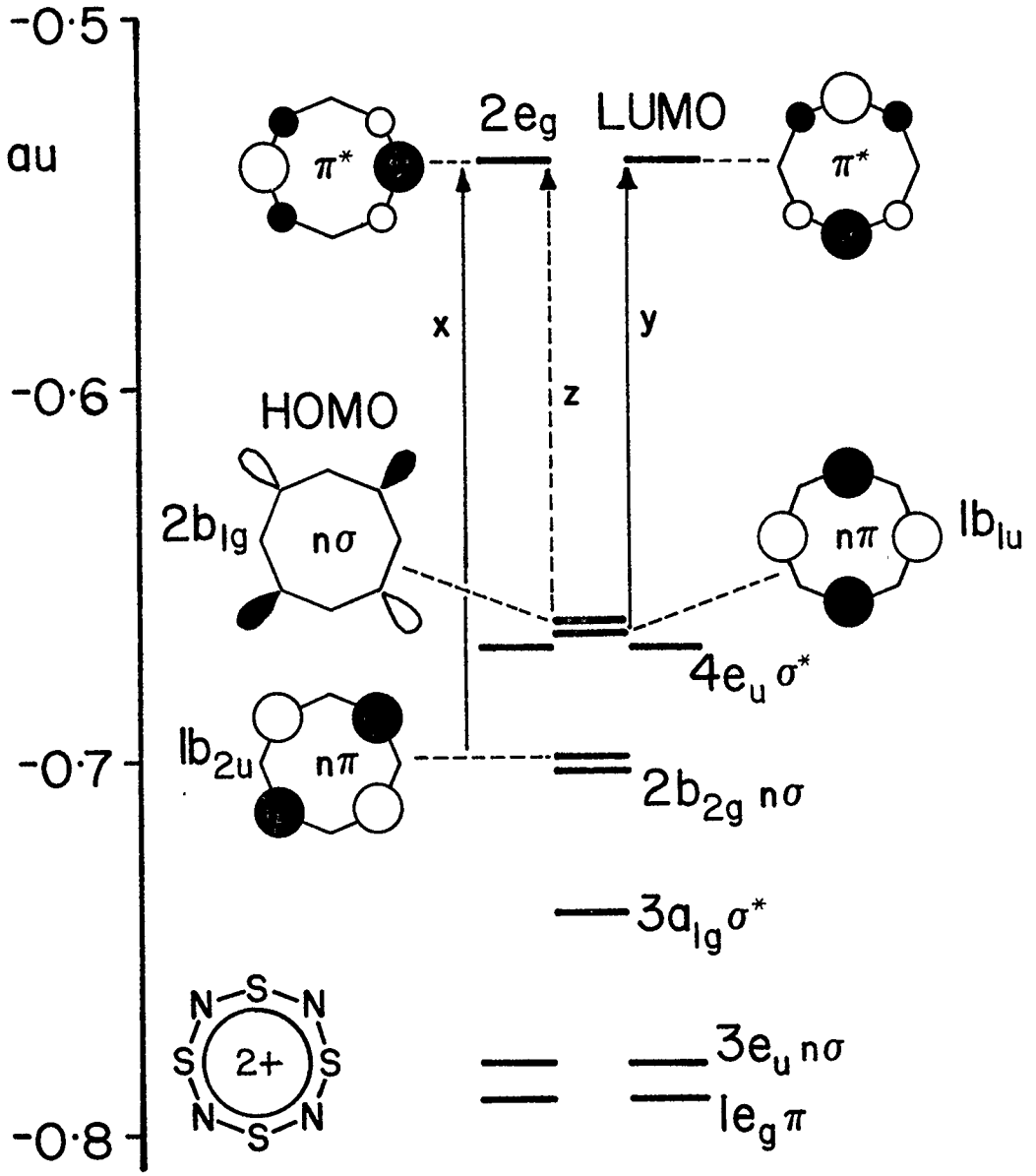

Figure 1.4 Upper energy levels of $S_4N_4^{2+}$. X corresponds to a visible absorption at 346 nm, Y corresponds to an absorption at 262 nm, and Z is symmetry forbidden ($n\sigma$ = non-bonding, σ-symmetry; $n\pi$ = non-bonding, π-symmetry).

and $1b_{2u}$ ($n\pi$)) are responsible for these two transitions, as illustrated in figure 1.4. Michl has predicted a positive A term in the MCD spectrum of $S_4N_4^{2+}$, corresponding to each of the electronic transitions[114]. In contrast to $S_3N_3^-$, the positive sign of both A terms would be indicative of electronic transitions originating from a non-degenerate level and terminating at a degenerate level.

1.4 UNSATURATED PHOSPHORUS-NITROGEN HETEROCYCLES

1.4.1 INTRODUCTION

Cyclophosphazenes of the type $(R_2PN)_x$ have been investigated far more extensively than the cyclothiazenes. A large number of cyclophosphazenes has been fully characterized from relatively simple six-membered rings to complex molecules containing up to seventeen units, $(R_2PN)_{17}$. The series is further extended by the variety of exocyclic groups available, as illustrated by the examples shown in Figure 1.5. Unlike the thiazenes, simple anions and cations are rare[136].

The most well known derivative is hexachlorocyclotriphosphazene (2). It was first prepared by the action of gaseous ammonia on phosphorus pentachloride[7,8] and this is still the basis of most preparations. Ammonium chloride is routinely used nowadays with PCl_5 to give a range of ring sizes[137,138,139]. Cyclophosphazenes can also be prepared by the reaction between aminochlorophosphoranes and triethylamine[38] and from phosphorus (III) halides by formation of an unstable phosphorus (III) azide, the intermediate to phosphazene polymer formation[38]. In addition, the cyclochlorophosphazenes act as a useful synthetic starting material for other phosphazenes via nucleophilic substitution of the exocyclic groups.

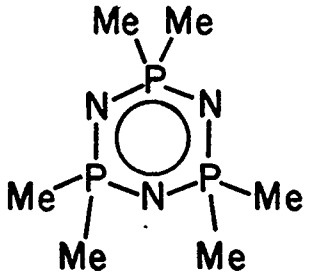

Ref 130

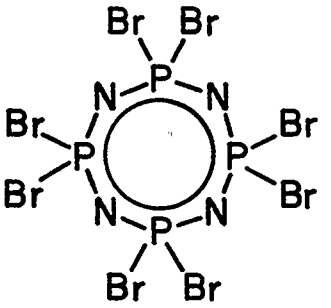

Ref 131

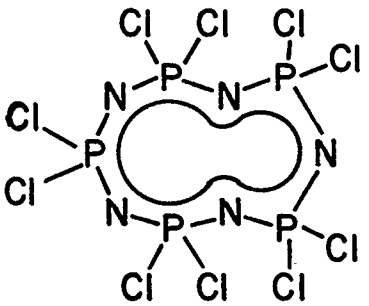

Ref 132

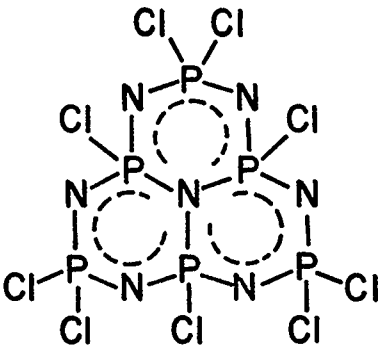

Ref 132,133

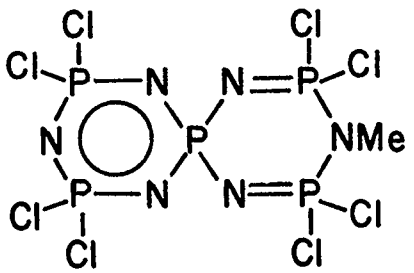

Ref 134

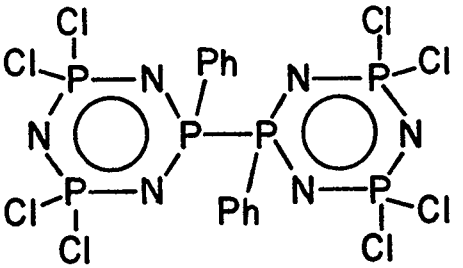

Ref 135

Figure 1.5 Examples of cyclophosphazenes demonstrating the variety in ring size, exocyclic ligand, and form.

1.4.2 CHEMICAL PROPERTIES

The majority of cyclophosphazene chemistry involves the exocyclic ligands attached to the phosphorus centers; the P-N skeleton is quite robust[40]. Nucleophilic substitutions are easily effected and their course can be rationalized by the same concepts successfully used with organic rings, such as inductive and steric effects. As would be expected the reactivity is very dependent on the electron distribution around the ring. Indeed, results from reactivity studies have complemented the conclusions made concerning the π-structure of the cyclophosphazenes.

In contrast to the easy oxidation observed for the cyclothiazenes, removal of electrons from the cyclophosphazenes has not yet been reported. However, the phosphazenes do act as bases, the degree of basicity being dependent on the electronegativity of the exocyclic groups. Nitrogen lone-pairs are used for donation to various types of acceptor ions and molecules. Methyl phosphazenes have enough basic strength to add a proton

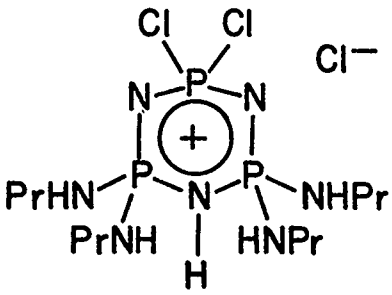

32

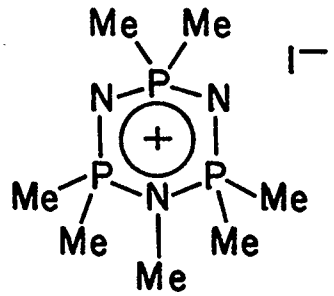

33

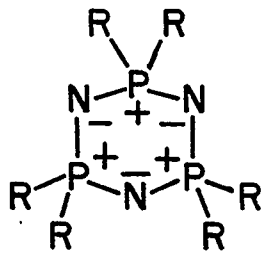

34

and salts have been prepared, in which a positively charged moiety is bound to one of the ring nitrogen atoms (32,33)[40,140]. Covalent donor-acceptor compounds are also known of the type $(NPCl_2)_3.AlBr_3$[141]. It is important to note that in many of the reactions of cyclophosphazenes the ring is left intact.

1.4.3 STRUCTURE AND BONDING

An immense amount of structural information has been collected for the cyclophosphazenes, including the determination of hundreds of molecular structures by X-ray methods. The structure of $(Cl_2PN)_3$ (2)[142] consists of an almost planar six-membered P_3N_3 ring, in which all the bond lengths are equal (≃1.59 Å) and the endocyclic angle at phosphorus ($\hat{NPN}$) is ≃ 120°. In general, symmetrically substituted cyclophosphazenes have equal P-N bond lengths in the range 1.47-1.62 Å (cf. P-N single bond value in $(O_3PNH_3)^-$ of 1.769(19) Å[143,144]) depending on the exocyclic ligand on phosphorus. Tetramers and larger rings tend to be puckered, maintaining $\hat{NPN}$ close to 120°[38,40,41]. Angles at nitrogen ($\hat{PNP}$) are observed to be more flexible, ranging from 119.7° for $(Cl_2PN)_3$[142] to 147.5° for $((NMe_2)_2PN)_6$[145]. Octafluorocyclotetraphosphazene is one exception having a planar structure (D_{4h})[146].

The electronic structures of the cyclophosphazenes have proven more difficult to understand than those of the cyclothiazenes. Various models have been proposed to describe the π-structure in cyclophosphazenes, including internal salts (34) and fully delocalized systems having aromatic characteristics, involving d orbital contributions from phosphorus. The most truthful picture is a combination of these, involving a strong polarization towards the nitrogen centers with π-interaction back through the phosphorus d orbitals (see section 1.2). Although the contribution of d orbitals in the π-structure may be small, the effects are significant. Structural features such as short, equal ring bond lengths and ring planarity are indicative of an effective π-electron delocalization, however, they can also be rationalized by the internal

salt definition. Further illustration of d orbital involvement is seen in the wide $\hat{NPN}$ angles (120^{o}), which would have tetrahedral geometries in an sp^3 hybridized environment. The vibrational spectra of various cyclophosphazenes also provide important evidence for d orbital participation. The wavenumber of the P-N stretches, for one particular ring size, has been observed to increase as the electronegativity of the substituents at the phosphorus increases. A trend of this nature is consistent with the concept that the d orbitals will contract in the presence of electronegative ligands to allow more efficient π-interaction[40]. Chemical characteristics of π-electron delocalization are apparent in a number of forms. For example, nucleophilic substitution activation energies, calculated from reaction rates for cyclophosphazenes, show a considerable dependence on the size of the phosphazene ring[147]. The π-electrons are obviously influenced by the size of the heterocycle, a feature which cannot be rationalized by a localization of π-electron density.

The complexity of the electronic environment of the cyclophosphazenes stems from the different symmetries of the two d orbitals available on phosphorus for π-interaction (see Section 1.2). Although both d orbitals are involved to some degree, there is a significant amount of experimental evidence to indicate that the homomorphic (d_{yz}) interaction predominates. The symmetry aspects of a heteromorphic (d_{xz}) system demand that the HOMO is solely nitrogen based and the LUMO is phosphorus based, both nonbonding in nature. Therefore, these orbitals would have a constant energy irrespective of ring size. However, measured ionization potentials of homogeneously substituted phosphazenes oscillate with ring size, indicating that the HOMO involves some bonding interaction and must therefore possess some homomorphic character[40]. This property is also evident in

the electronic spectra of the pyrrole derivatives of the cyclic phosphazenes, which provide a unique probe into the electronic structure of the P-N heterocycles[148] (The $\pi \rightarrow \pi^*$ electronic transitions of the cyclophosphazenes occur at high energy and are difficult to measure). The pyrryl group is a strong electron donor and effects a charge transfer into the π-LUMO of the phosphazene. The corresponding ultraviolet absorption observed for these compounds at about 240 nm and can be easily measured. In accordance with the conclusions made above, the energy of the absorption alternates with ring size of the phosphazene. Although the variations in the energies of the absorptions are small, they indicate some bonding character in the phosphorus based LUMO of the cyclophosphazene.

1.5 OBJECTIVES AND OUTLINE OF THE THESIS

The extensive series of cyclothiazene and cyclophosphazene compounds have been thoroughly investigated and their chemical and physical properties are well documented. Isolated examples of mixed or hybrid P-N-S heterocycles have been reported. However, the common nitrogen molecular framework in the phosphazenes and thiazenes suggests that a comprehensive series of hybrid systems should be possible, having the broad range of exocyclic groups seen in the phosphazenes and the ring size variation characteristic of both parent series. The properties of these systems would provide a useful comparison between the parent species.

Therefore, the ultimate objective of this work has been the synthesis and characterization of a number of unsaturated P-N-S heterocyclic compounds. The diverse chemistry already known for S_4N_4 makes it an obvious choice as a precursor. Nucleophilic attack by phosphines possessing

labile ligands may be expected to lead to incorporation of the phosphorus center into the unsaturated S-N heterocyclic environment.

CHAPTER 2 deals with an examination of these reactions, isolation of the products and spectroscopic and structural characterization of the new heterocyclic P-N-S species. The electronic structures of these systems are discussed in CHAPTER 3 by comparison with the pure P-N and S-N systems. CHAPTER 4 examines some of the chemistry of the P-N-S heterocycles containing two coordinate sulfur. All the experimental procedures are covered in CHAPTER 5.

CHAPTER 2

PREPARATION AND SPECTROSCOPIC AND STRUCTURAL CHARACTERIZATION OF UNSATURATED PHOSPHORUS, NITROGEN AND SULFUR CONTAINING HETEROCYCLES WITH TWO COORDINATE SULFUR

2.1 INTRODUCTION

As discussed in Chapter 1, the nucleophilic degradation of S_4N_4 usually produces the binary anions, $S_3N_3^-$[20,21] and $S_4N_5^-$[83,84,85]. Although the reaction between S_4N_4 and Ph_3P gives $(Ph_3P{=}N)_3S^+S_4N_5^-$, under certain conditions products include two S-N rings with phosphinimino exocyclic ligands, $Ph_3P{=}N{-}S_3N_3$ (27) and 1,5-$(Ph_3P{=}N)_2S_4N_4$[86,87] (28). The formation of 27 indicates a ring opening mechanism and oxidation of the tertiary phosphorus center. However, the chemical inertness of the P-C bonds restricts the mode of interaction of the phosphorus center with the unsaturated S-N system. Reactions of S_4N_4 with phosphines possessing only two inert ligands give radically different results. The presence of a labile ligand allows incorporation of the phosphorus center into the unsaturated environment as a member of the heterocycle. The result is a number of unsaturated heterocyclic systems containing phosphorus, nitrogen and sulfur. The coordination number of the sulfur centers is very dependent on the form of the ligand. When X = Cl, the major product (80% yield) of the reaction is an unsaturated P-N-S heterocycle containing an exocyclic S-Cl bond (35)[149]. However phosphines such as Ph_2PH, $Ph_2P{-}PPh_2$, $Me_2P{-}PMe_2$ and $(PhO)_3P$ allow the sulfur centers to retain the oxidation states carried in S_4N_4 . These reactions are very complex and result in

a wide range of products. Amongst the major components are three unsaturated P-N-S heterocycles containing two coordinate sulfur. One is a six-membered ring (36) made up of one pentavalent phosphorus unit, three nitrogen atoms and two dicoordinate sulfur atoms[150,151,152]. The

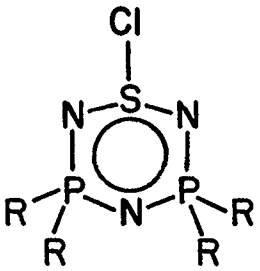

35

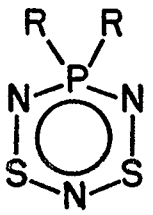

36

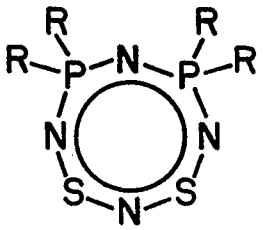

16

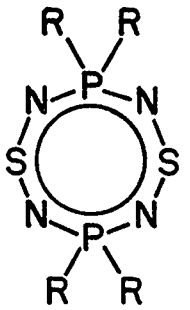

17

other two are structural isomers of an eight-membered ring containing two phosphorus units, four nitrogen atoms and two dicoordinate sulfur atoms[152,153,154]. The phosphorus atoms may be in the 1 and 3 positions, 1,3-$(R_2PN)_2(SN)_2$ (16), or 1 and 5 positions, 1,5-$(R_2PN)_2(SN)_2$ (17), of the eight-membered ring. The basic alternating nitrogen framework of these molecules is reminiscent of the unsaturated P-N and S-N systems, and they can be considered as hybrids or cyclophosphathiazenes.

This chapter deals with the formation and isolation of the new unsaturated P-N-S heterocycles. In addition the spectroscopic and structural properties of each type of system (16, 17) are examined and rationalized. All the experimental details for the work discussed in this chapter are presented in Sections 5.2 and 5.3

2.2 PREPARATION AND ISOLATION OF THE CYCLOPHOSPHATHIAZENES

2.2.1 REACTIONS OF S_4N_4 WITH PHOSPHINES

The complex reaction between Ph_3P and S_4N_4 has been examined by a number of workers[86,89,155], and recent results indicate that the mixture of the products is solvent and temperature dependent[87]. Although the reactions of S_4N_4 with phosphines containing labile ligands (Ph_2PH, $Ph_2P\text{-}PPh_2$, $Me_2P\text{-}PMe_2$ and $(PhO)_3P$) are also complex, the products are the same, irrespective of the experimental conditions. All of these phosphines react very readily with S_4N_4, indeed, the reaction between $Me_2P\text{-}PMe_2$ and S_4N_4 is sufficiently exothermic that care must be taken in the initial stages to avoid an explosion. Subsequently, all the reaction mixtures can be heated to reflux in toluene without any obvious effect on the form or yield of the products. Although the rates of reaction depend on the type of phosphine, they all appear to proceed in a universal fashion and can be monitored by their color changes. The yellow solution of S_4N_4 becomes an intense deep purple (Ph_2PH, $Ph_2P\text{-}PPh_2$, $Me_2P\text{-}PMe_2$) or black ($(PhO)_3P$) color. Stoichiometries of the reactions are not understood and have been chosen on the basis of the yields of the P-N-S heterocycles obtained ($2Ph_2PH{:}S_4N_4$, $R_2P\text{-}PR_2{:}S_4N_4$). In most cases the products are thermally stable and therefore the choice of reaction times is not critical and are long to ensure completion of reaction. However, care must be taken with the products containing methyl and phenoxy groups and the reflux time should be kept to a minimum.

2.2.2 ^{31}P NMR STUDY OF SELECTED PHOSPHINE/S_4N_4 REACTIONS AND CHROMATOGRAPHIC SEPARATION OF THE PRODUCTS

The complexity of these reactions is illustrated by the ^{31}P NMR spectra of the reaction mixtures. Figure 2.1 shows the relevant sections of the ^{31}P NMR spectrum of the $Ph_2P\text{-}PPh_2/S_4N_4$ reaction mixture in toluene. The ^{31}P NMR spectrum of the $2Ph_2PH/S_4N_4$ reaction mixture is identical, disregarding the relative peak intensities. It is not surprising that the spectrum of the $Me_2P\text{-}PMe_2/S_4N_4$ reaction mixture also compares very closely, if one allows for the slight chemical shift differences expected between a $Ph_2P\leqslant$ and $Me_2P\leqslant$ center. These signals imply the same products for reactions of both methyl and phenyl phosphines. A number of signals observed in Figure 2.1 have not been identified. However many of the components have been isolated from the reaction mixture by gel permeation chromatography. The intense colors of many of the products allow simple distinction between the various components of the reaction mixture during chromatographic separation. The strongest signal (B) in the ^{31}P NMR spectrum corresponds to tetraphenyldiphosphine disulfide $(Ph_2PS)_2$, and many of the fractions are contaminated with the respective phosphine sulfide. For this reason, purification of the required products involves repeated fractional crystallization procedures. Signals D and E correspond to $(Ph_2PN)_4$ and $(Ph_2PN)_3$, which have been isolated from the first yellow fraction. The deep orange fraction that follows yielded the two structural isomers of an eight-membered P-N-S heterocycle which are responsible for signals A (17) and C (16). A six-membered P-N-S ring (36) was obtained from the final deep purple fraction and is accountable for signal F.

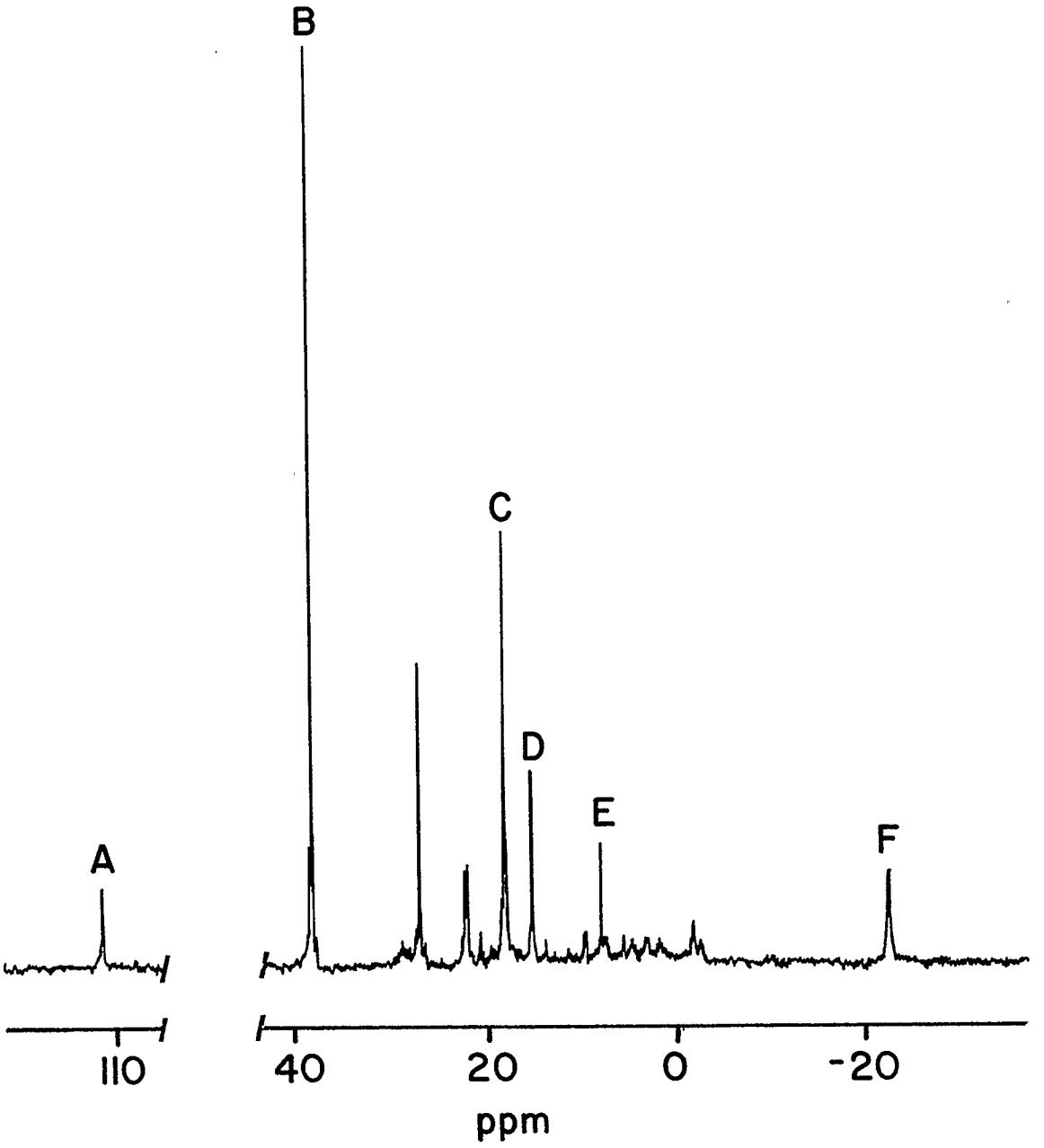

Figure 2.1 ^{31}P NMR spectrum of the $Ph_2P\text{-}PPh_2/S_4N_4$ reaction mixture in toluene. A corresponds to 1,5-$(Ph_2PN)_2(SN)_2$, B corresponds to $(Ph_2PS)_2$, C corresponds to 1,3-$(Ph_2PN)_2(SN)_2$, D corresponds to $(Ph_2PN)_4$, E corresponds to $(Ph_2PN)_3$ and F corresponds to $(Ph_2PN)(SN)_2$.

2.2.3 MECHANISM OF NUCLEOPHILIC DEGRADATION OF S_4N_4

In accordance with many of the reactions of S_4N_4, the phosphine reactions involve a network of possible mechanistic pathways. Nevertheless, it is possible to make a few basic statements regarding the initial mode of nucleophilic attack and alteration of the S-N framework, based on observations made on reactions of simple S-N compounds[156] and other phosphine/S_4N_4 reactions[87,90]. Kinetic evidence and tracer experiments on the reactions of sulfilimines with nucleophiles have shown that the first, rate-determining step of the reaction is nucleophilic attack at the sulfur atom with formation of a sulfurane-like structure[156]. The reactivity of sulfur diimides with nucleophiles is even more pronounced. The fast reaction of *bis*-tosyl-sulfur diimide with aliphatic sulfides gives a quantitative yield of the corresponding sulfilimines, indicating that both tosylimino groups are involved in their formation. Kresze has proposed a multistep process for the reaction[156], as illustrated in Figure 2.2(a). Following initial attack at the sulfur atom of the NSN compound the intermediate rearranges and loses a thianitroso compound to give the first molecule of sulfilimine. A second molecule is then produced either by reaction of the thianitroso compound by nucleophilic attack, rearrangement and extrusion of sulfur, or by decomposition of the thianitroso derivative to give a nitrene and subsequent reaction with the sulfide.

Chivers and co-workers have proposed a similar mechanism for the formation of $S_3N_3^-$ from S_4N_4, on the basis of experimental observations[88]. They suggested that the initial nucleophilic attack at the sulfur results in ring opening to give a poly(sulfur-nitrogen)chain. This intermediate

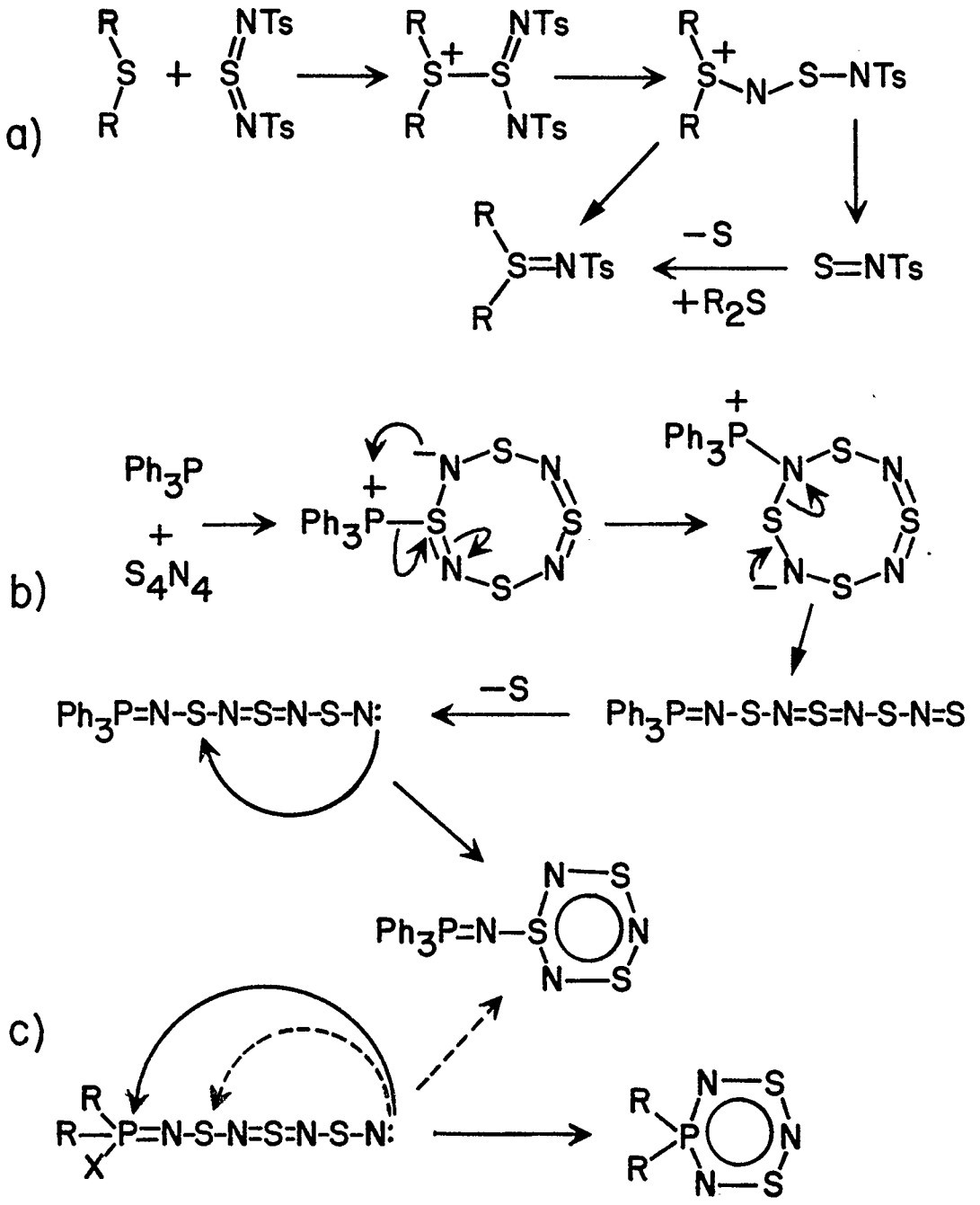

Figure 2.2 Mechanisms for nucleophilic degradation of unsaturated S-N systems. a) Reaction between sulfur diimide and aliphatic sulfides. b) Reaction between Ph_3P and S_4N_4. c) Reaction of S_4N_4 with phosphines containing labile ligands (X).

may then recyclize to a six-membered $S_3N_3^-$ ring. Chivers and Oakley extended this mechanism to the reaction between S_4N_4 and Ph_3P in the context of Kresze's work. As illustrated in Figure 2.2 (b), the phosphine is believed to attack the sulfur center and then undergo a 1,2-shift to a nitrogen atom. This is followed by ring opening and loss of a terminal sulfur atom to produce a nitrene intermediate, which recyclizes to form $Ph_3P{=}N{-}S_3N_3$. These concepts can be further extended to the systems in which the phosphine has a labile ligand (X), as illustrated in Figure 2.2(c). The initial steps will be identical to those for the Ph_3P system. However, the nitrene intermediate may either undergo recyclization in the manner observed for $Ph_3P{=}N{-}S_3N_3$, or a ring formation involving intramolecular nucleophilic substitution at the phosphorus center. The latter effects release of the labile ligand and allows the phosphorus to be incorporated into the unsaturated system. Prior release of an NS unit would account for the formation of the six-membered ring (36). However, the reason for this ring contraction is not clear. The formation of compounds containing more than one phosphorus unit can be rationalized by secondary nucleophilic attack of the unsaturated S-N heterocycle, in the initial stages, by another R_2PX unit. Concepts of this nature can also be used to account for the formation of the cyclophosphazenes in these reaction.

2.3 CHARACTERIZATION OF THE CYCLOPHOSPHATHIAZENES

2.3.1 SPECTROSCOPIC EXAMINATION OF S-N AND P-N COMPOUNDS.

One of the major difficulties experienced experimentally when dealing

with S-N compounds is the lack of a spectroscopic probe. Most S-N systems display simple distinctive infrared spectra, which are useful as a fingerprint but provide little structural information. S-N compounds have a reputation of exhibiting intense colors and indeed many have interesting visible spectra[10,11,20,21,157,158]. However, without a detailed electronic understanding, electronic spectra are difficult to rationalize. The advent of multinuclear NMR spectroscopy has enabled a number of structural uncertainties to be resolved. ^{15}N NMR is now considered routine, however, the poor solubility of S-N compounds and low natural abundance of ^{15}N (0.36%) requires that many samples be enriched with the ^{15}N nuclei (an expensive procedure) in order that a useful spectrum be obtained[159,160]. Nevertheless, the results are often informative.

Spectral inadequacies are not so great when studying the cyclophosphazenes. The NMR active ^{31}P nucleus is 100% abundant and provides an excellent alternative to ^{15}N NMR. In addition, when simple organic exocyclic groups (e.g. methyl) are attached to phosphorus, information can be obtained from ^{1}H NMR spectra. The infrared characteristics of phosphazenes are also easily correlated within a series and may provide comparative information[37,39]. However, the phosphazenes display no visible spectra. As hybrids of these two series of compounds, the cyclophosphathiazenes retain most of the spectroscopic characteristics of their parent systems. The result is a relative abundance of spectroscopic probes allowing detailed examination of their structural and electronic properties.

2.3.2 COMPOUNDS OF THE GENERAL FORMULA $(R_2PN)(SN)_2$

IDENTIFICATION

Four derivatives of $(R_2PN)(SN)_2$ have been prepared and isolated (R=Me, Ph, PhO and F (see Section 5.6.3.2)). Due to thermal or chemical instability, they each require a different purification technique. The phenyl derivative is crystalline and air stable at room temperature and can be handled very easily. However, the others are oils (Me, PhO) or vapors (F) and must be handled at low temperatures in an inert atmosphere. For this reason certain data were unobtainable for these derivatives and characterization is completed by reference to their norbornadiene adducts (Chapter 4). Therefore the majority of physical and chemical studies on all the unsaturated P-N-S heterocycles are centered around the more stable phenyl derivatives.

SPECTROSCOPIC CHARACTERIZATION

The vibrational spectra of the unsaturated P-N-S heterocycles containing two coordinate sulfur show an interesting compromise between the vibrational features well documented for the parent P-N and S-N systems. All the derivatives of $(R_2PN)(SN)_2$ show a very strong broad band in the region of 1100 cm^{-1} (R = Ph, 1123; R = Me, 1083; R = PhO, 1190 cm^{-1}). This can be confidently assigned to the P=N ring stretching vibration, by comparison with that vibration in the corresponding six-membered phosphazenes ($(Ph_2PN)_3$, 1190[161]; $(Me_2PN)_3$, 1180 cm^{-1} [162]). The slightly lower energy of the vibration in the hybrid species is an indication of the

destabilization of the NPN section by interaction with the S-N moiety. Vibrational bands originating from the S-N section of the molecule are masked by the phenyl vibrations in $(Ph_2PN)(SN)_2$ and $((PhO)_2PN)(SN)_2$. However, they can be clearly observed in $(Me_2PN)(SN)_2$ at 863 and 688 cm^{-1}. These values are consistent with the major stretches observed for $S_3N_3^-$ (925, 640, 380 cm^{-1})[21] and S_4N_4 (924, 699, 545, 350 cm^{-1})[163]. There are additional bands at 390 and 363 cm^{-1} observed for $(Me_2PN)(SN)_2$, however, because both S-N and P-N bands are normally seen in this region, assignment is difficult.

The most prominent characteristic of these compounds is their intense color. The phenyl and methyl derivatives are deep purple and the fluoro and phenoxy derivatives are deep blue. They all exhibit an intense visible absorption near 550-585 nm. Although additional absorptions are evident in the ultraviolet region between 250 and 300 nm, these can only be clearly seen in the spectrum of $(Me_2PN)(SN)_2$. In $(Ph_2PN)(SN)_2$ and $((PhO)_2PN)(SN)_2$ these higher energy absorptions are hidden by $\pi \longrightarrow \pi^*$ electronic absorptions of the phenyl groups. The UV- visible spectrum of $(Me_2PN)(SN)_2$ is illustrated in Figure 2.3. In Chapter 3 the nature of these electronic transitions will be discussed when the electronic structure of the unsaturated P-N-S system is examined.

NMR spectroscopy has provided important structural information for these compounds. Of course little data can be obtained from the characteristically broad multiplet associated with the proton resonances of the phenyl groups on $(Ph_2PN)(SN)_2$ and $((PhO)_2PN)(SN)_2$. However, for the methyl derivative the ^1H chemical shift (δ = 1.71 ppm) and two bond coupling constant to phosphorus ($^2J_{PH}$ = 14.4Hz) of the equivalent methyl protons, are similar to those reported for the methyl phosphazenes

($(Me_2PN)_3$, $\delta(CH_3)$ = 1.30 ppm, $^2J_{PH}$ = 14.0 Hz[164]; $Me_2F_4P_3N_3$, $\delta(CH_3)$ = 1.65 ppm, $^2J_{PH}$ = 14.0 Hz[165]). The ^{19}F chemical shift of the doublet observed for the equivalent fluorine atoms of $(F_2PN)(SN)_2$ (δ = -22.2 ppm is within the wide range of shifts reported for the fluorocyclophosphazenes (-18.0 to -71.9 ppm[40]). Strong P-F coupling is also observed (J_{PF} = 1054 Hz) again in agreement with the phosphazene values.

^{31}P NMR spectra of the cyclophosphadithiatriazenes all show singlets (R = Me, δ = 6.2 ppm; Ph, δ = -21.2 ppm; PhO, δ = -3.4 ppm) to high field of the characteristic resonances observed for the corresponding phosphazenes ($(R_2PN)_3$, R = Me, δ = 31.9 ppm[164]; Ph, δ = 14.3 ppm[166,167]; PhO, δ = 9 ppm[168]). The presence of the more electronegative sulfur atoms in place of two of the phosphorus units of the phosphazene systems would induce a deshielding of the phosphorus. However, the larger number of electrons probably leads to an increase in π-electron density at the phosphorus relative to $(R_2PN)_3$ (see Chapter 3).

The ^{15}N NMR spectra of the $(R_2PN)(SN)_2$ compounds unambiguously confirm the proposed heterocyclic structure. Figure 2.4 shows the ^{15}N NMR spectrum of a 100% ^{15}N enriched sample of the phenyl derivative. The signal corresponding to the nitrogen atoms bound to the phosphorus (N_A) is split by coupling to the phosphorus resonance and the unique nitrogen (N_B) to give a doublet of doublets. The signal corresponding to the unique nitrogen atom (N_B) is not only split by coupling to the equivalent nitrogen (N_A) resonance, but also by three bond coupling to phosphorus resonance, resulting in a doublet of triplets. Incorporation of the phosphorus center into the unsaturated system appears to enhance heteronuclear coupling. The P-N coupling constants are slightly greater than those observed for $Ph_3P{=}N{-}S_3N_3$ ($^1J_{PN}$ = 48.9 Hz, $^3J_{PN}$ = 4.3 Hz[160])

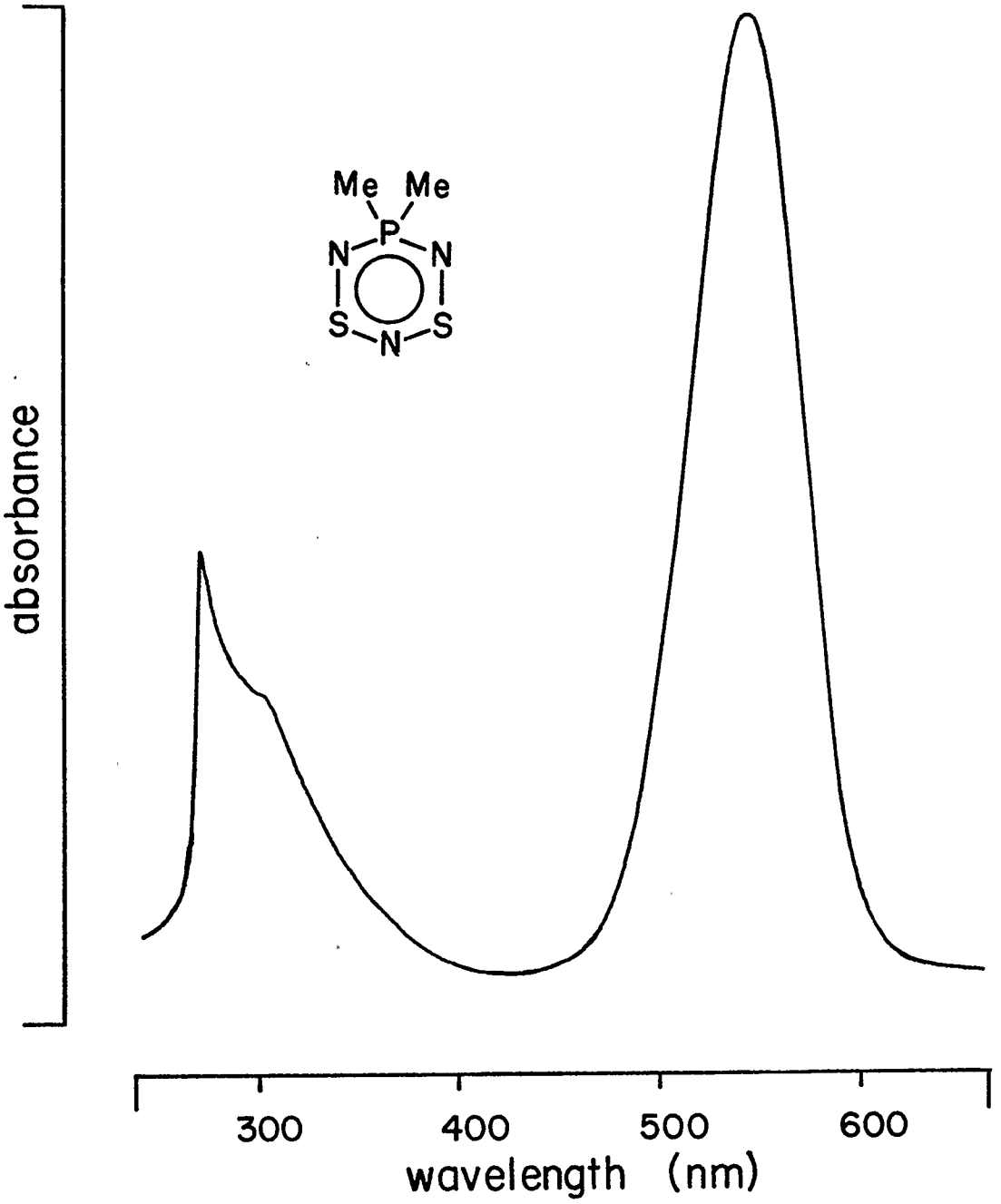

Figure 2.3 UV-visible spectrum of $(Me_2PN)(SN)_2$ in CH_2Cl_2.

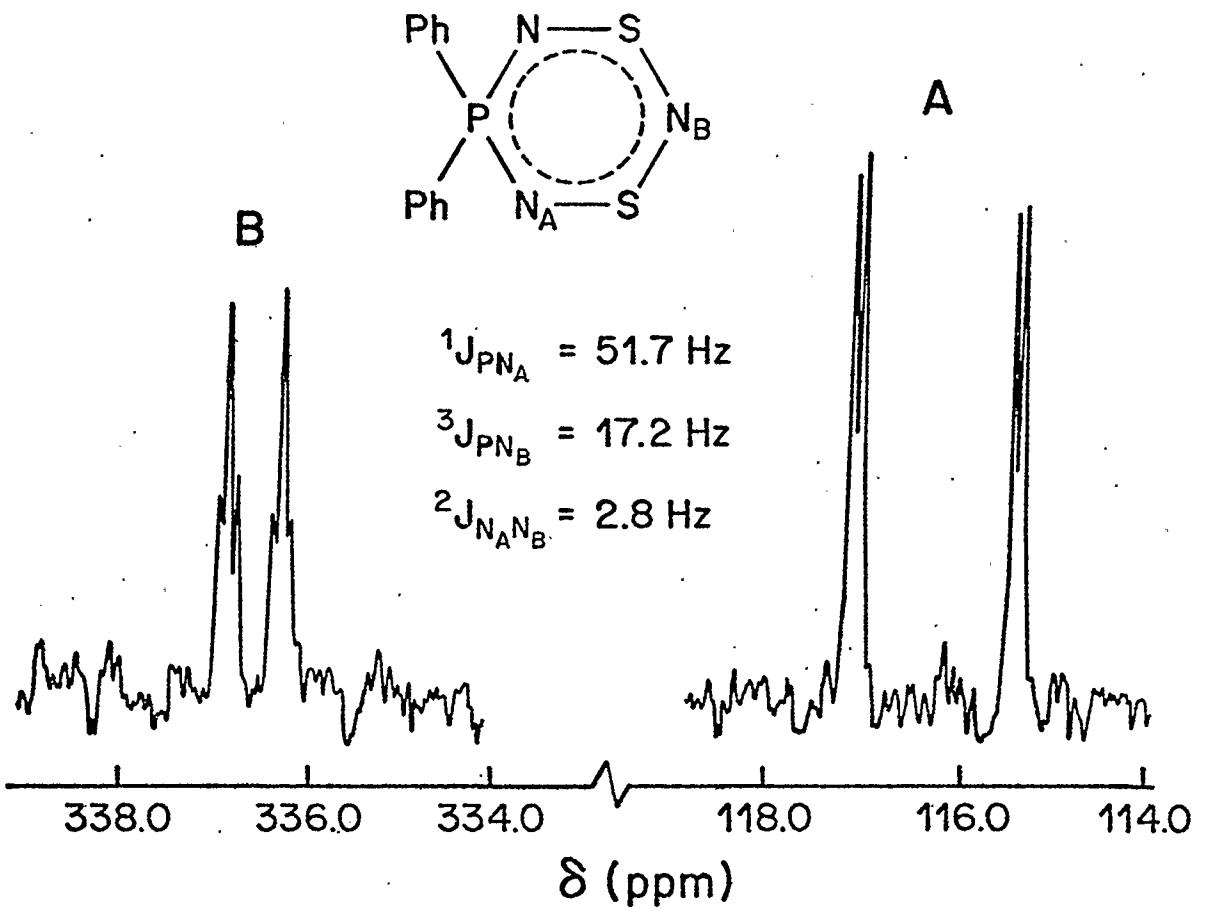

Figure 2.4 ^{15}N NMR spectrum of $(Ph_2PN)(SN)_2$ (99% enriched with ^{15}N).

and 1,5-$(Ph_3P{=}N)_2S_4N_4$ ($^1J_{PN}$ = 43.9 Hz, $^3J_{PN}$ = 4.3 Hz[160]), in which the phosphorus remains exocyclic to the unsaturated S-N ring. The N-N coupling constants are similar to those observed in other neutral conjugated S-N rings[160].

MOLECULAR STRUCTURE OF $(Ph_2PN)(SN)_2$

A schematic representation of the molecular structure† is shown in

† An X-ray crystallographic study was performed by Dr. P. N. Swepston and Dr. A. W. Cordes[150 151].

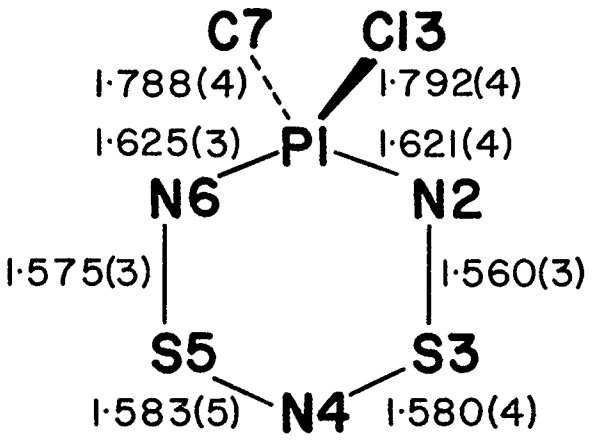

Atoms	Angle
N2-P1-C7	107.9(2)
N6-P1-C7	107.3(2)
N2-P1-C13	108.5(2)
N6-P1-C13	109.9(2)
C7-P1-C13	107.1(2)
N6-P1-N2	115.8(2)
P1-N2-S3	121.3(2)
N2-S3-N4	116.9(2)
S3-N4-S5	124.6(3)
N4-S5-N6	116.3(2)
S5-N6-P1	120.3(2)

Figure 2.5 Schematic representation of the molecular structure of $(Ph_2PN)(SN)_2$ with pertinent bond lengths (Å) and angles (Deg).

Figure 2.5 displaying the pertinent bond lengths and angles of the heterocycle and the α-carbons of the phenyl rings. The crystal structure consists of discrete molecular units and there are no unusual intermolecular contacts.

The molecular structure of $(Ph_2PN)(SN)_2$ consists of an almost planar (to within 0.05 A) S_2N_3 five-membered unit with the phosphorus atom displaced from this plane by 0.284(1) Å. Although significant, this departure from planarity is considerably less than the puckering observed in the silylated derivative reported by Weiss[28]. The latter has been found to have the two sulfur atoms (S3, -0.41 Å and S5, +0.53 Å) and phosphorus atom (P1, +0.27 Å) considerably removed from the plane defined by the three nitrogen atoms. In addition the latter structure has different bond lengths associated with the two sulfur atoms (S3-N2 = 1.564(7) Å, S3-N4 = 1.570(7) Å, S5-N4 = 1.615(8) Å, S5-N6 = 1.630(5) Å) suggesting that the sulfur atoms are permanently in different oxidation states (II and IV). In contrast, the phenyl derivative shows little difference between any of the S-N bond lengths, which indicates equivalent sulfur

centers and a delocalized electronic distribution around the heterocycle. The geometry at phosphorus is a distorted tetrahedron almost identical to that observed for the Ph_2P center in $Ph_2F_4P_3N_3$ (NPN = 115.5(3)^o, CPC = 107.9(3)^o[169]). One may expect this resemblance when considering the similar electronic effects imposed on the ring by S and F_2P.

2.3.3 COMPOUNDS OF THE GENERAL FORMULA $(R_2PN)_2(SN)_2$

IDENTIFICATION

Two compounds have been isolated from the bright orange fraction of the reaction mixtures involving Ph_2PH, $Ph_2P\text{-}PPh_2$ and $Me_2P\text{-}PMe_2$. These two compounds are structural isomers of an eight-membered $(PN)_2(SN)_2$ ring, introduced in Section 2.1. Despite the vastly different spectroscopic properties observed for these two isomers, their structures could not be unequivocally determined solely on the basis of analytical and spectroscopic data. X-ray techniques were therefore employed. These systems are far more thermally stable than the six-membered relatives, and both are air stable crystalline materials. 1,3-$(R_2PN)_2(SN)_2$ (16) is a deep orange color and 1,5-$(R_2PN)_2(SN)_2$ (17) pale yellow. The unique spectroscopic and structural properties of each of these isomers justify independent discussion.

SPECTROSCOPIC CHARACTERIZATION OF THE 1,3-$(R_2PN)_2(SN)_2$ COMPOUNDS

Like the $(R_2PN)(SN)_2$ species the vibrational spectra of these eight-

membered rings show characteristics reminiscent of phosphazenes and thiazenes. However, whereas the six-membered systems exhibit modified features, the spectra of the 1,3-$(R_2PN)_2(SN)_2$ compounds show properties almost identical to those of the series of compounds from which they are derived. 1,3-$(Ph_2PN)_2(SN)_2$ shows a very intense band at 1196 cm^{-1} which may be assigned to a P-N stretching mode, analogous to the same band observed for $(Ph_2PN)_4$ (1213 cm^{-1})[161]. The values are very similar and suggest that the PNP unit in the phosphathiazene is interchangeable with that same unit in the phosphazene. Stretches observed for 1,3-$(Me_2PN)_2$-$(SN)_2$ at 942 and 637 cm^{-1} can be assigned to S-N vibrations in accordance with the discussion for $(Me_2PN)(SN)_2$ (see section 2.3.2.2).

The intense orange color of both the phenyl and methyl derivatives of 1,3-$(R_2PN)_2(SN)_2$ is due to a strong visible absorption band at 460 nm (R = Ph) and 456 nm (R = Me). Although these absorption maxima are significantly higher in energy than the analogous absorptions observed for the six-membered $(R_2PN)(SN)_2$ species, they are of comparable intensity. In addition, the methyl derivative shows a further absorption in the ultraviolet region (350 nm) resembling $(Me_2PN)(SN)_2$. As will be discussed in Chapter 3, the origins of the electronic spectra of the six and eight membered systems are related.

Once again ^1H NMR spectroscopy provides little structural information for the phenyl derivative. Alternatively, the methyl derivative shows the expected doublet for the four equivalent methyl resonances split by coupling to the resonances of the equivalent phosphorus centers. The chemical shift (δ = 1.58 ppm) and coupling constant ($^2J_{PH}$ = 13.3 Hz) are similar to those values recorded for the six-membered relatives. The proton decoupled ^{31}P NMR spectra of the 1,3-$(R_2PN)_2(SN)_2$ systems

(R = Ph, δ = 18.7 ppm; R = Me, δ = 28.3 ppm) each show a singlet to lower field than seen for the $(R_2PN)(SN)_2$ systems (R = Ph, δ = -21.2 ppm; R = Me, δ = 6.2 ppm). Instead, they are of the same order as the ^{31}P NMR shifts recorded for the phosphazenes. On the basis of this spectroscopic data one may postulate that the P-N-P unit of this molecule is almost directly derived from the corresponding tetrameric cyclophosphazene and the interaction with an S_2N_3 unit appears to have little effect on the properties of the former.

MOLECULAR STRUCTURE OF 1,3-$(Ph_2PN)_2(SN)_2$

The crystal and molecular structure of 1,3-$(Ph_2PN)_2(SN)_2$ was determined by X-ray crystallographic methods[‡]. The crystal structure consists of discrete molecular units with no unusual intermolecular contacts. Bond lengths and angles of the asymmetric unit are given in Table 2.1, and the atomic numbering scheme of the inorganic ring and the α-carbon atoms of the phenyl groups is shown in the ORTEP drawing of the molecule in Figure 2.6.

The molecular structure of 1,3-$(Ph_2PN)_2(SN)_2$ consists of an almost planar S_2N_3 moiety analogous to $(Ph_2PN)(SN)_2$. A two-fold crystallographic axis passes through N1 and N3 forces the four nitrogen atoms to lie in a plane. The two sulfur atoms deviate from this plane by only 0.019 Å. The two phosphorus atoms lie on opposite sides of the S-N plane, displaced from the plane by 0.697 Å. The S-N bond lengths, although not equal, are very similar, and are almost identical to the S-N bond lengths observed for $(Ph_2PN)(SN)_2$. Indeed, the only difference between the S_2N_3 units in

---

[‡] The assistance of Dr. J. F. Richardson is gratefully acknowledged.

Table 2.1 Bond lengths (Å) and angles (deg) for the asymmetric unit of 1,3-$(Ph_2PN)_2(SN)_2$

Atoms	Distance	Atoms	Angle
P1-N1	1.585(3)	N1-P1-N2	118.1(2)
P1-N2	1.610(4)	N1-P1-C1	109.2(1)
P1-C1	1.814(5)	N1-P1-C7	106.6(2)
P1-C7	1.779(4)	N2-P1-C1	109.4(2)
N2-S1	1.562(4)	N2-P1-C7	104.1(2)
S1-N3	1.589(2)	C1-P1-C7	109.0(2)
C1-C2	1.385(5)	P1-N1-P1′	126.0(3)
C2-C3	1.394(6)	P1-N2-S1	134.5(2)
C3-C4	1.372(7)	N2-S1-N3	120.2(2)
C4-C5	1.381(6)	S1-N3-S1′	144.1(4)
C5-C6	1.399(7)	C6-C1-C2	119.1(4)
C6-C1	1.393(7)	C1-C2-C3	120.8(4)
C7-C8	1.386(5)	C2-C3-C4	119.9(3)
C8-C9	1.382(6)	C3-C4-C5	120.2(5)
C9-C10	1.375(7)	C4-C5-C6	120.4(5)
C10-C11	1.370(5)	C5-C6-C1	119.7(4)
C11-C12	1.383(6)	C12-C7-C8	118.4(4)
C12-C7	1.408(6)	C7-C8-C9	121.1(4)
		C8-C9-C10	119.8(4)
		C9-C10-C11	120.2(4)
		C10-C11-C12	120.8(4)
		C11-C12-C7	119.6(3)

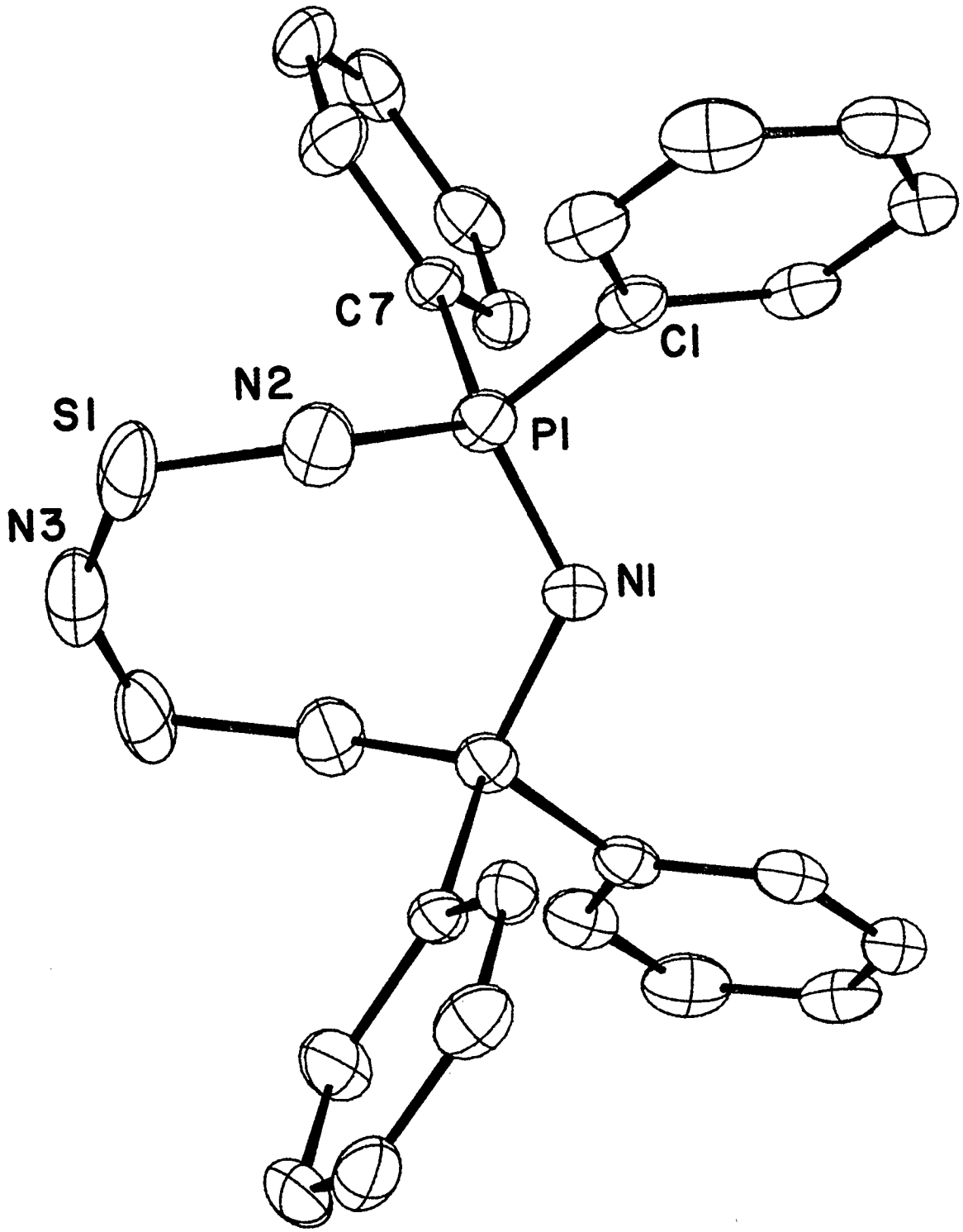

Figure 2.6 ORTEP view (50% probability ellipsoids) of 1,3-$(Ph_2PN)_2(SN)_2$ showing the atomic numbering scheme. A crystallographic two-fold axis passes through N1 and N3.

these two molecules is the wider bond angles at the nitrogen centers in the eight-membered ring. Despite these larger angles, a certain degree of ring puckering is required to accommodate the two extra atoms. The puckering observed at the phosphorus positions is of the nature commonly encountered in tetrameric phosphazenes, and allows retention of the general distorted tetrahedral geometry at phosphorus. The structure of the P-N-P unit is remarkably similar to the same unit in $(Ph_2PN)_4$[170], as predicted from spectroscopic data. Accordingly, the S_2N_3 unit has structural features reminiscent of $S_4N_4^{2+}$, although the bond lengths are slightly longer (mean d(S-N) in $S_4N_4^{2+}$ is 1.55 Å[65,66]). On this basis one may view 1,3-$(R_2PN)_2(SN)_2$ as two distinct units derived from these two species. The P-N bond lengths at the junction of the two units are significantly longer than the other P-N bonds,

SPECTROSCOPIC CHARACTERIZATION OF THE 1,5-$(R_2PN)_2(SN)_2$ COMPOUNDS

The spectroscopic properties of the 1,5-$(R_2PN)_2(SN)_2$ compounds are substantially different from those of the 1,3-isomer. The P-N stretch seen in the infrared spectrum is probably the most obvious example. Unlike the 1,3-isomer, this characteristically intense band is found at surprisingly low energy (R = Ph, 1053 cm^{-1}; R = Me, 1050 cm^{-1}). Whilst the 1,3-isomer is made up of a phosphazene segment and a thiazene segment, the 1,5-isomer may be viewed as a true hybrid of these two systems having no pure P-N-P or S-N-S units. Instead, 1,5-$(R_2PN)_2(SN)_2$ consists of P-N-S units. Therefore it is difficult to make useful comparative assignments for this isomer. The Raman spectra provide an important piece of

structural information. Whilst the 1,3-isomer displays no unusual Raman activity, the 1,5-isomer shows a strong band at 269 cm^{-1} (R = Ph). The observation of such a band in the Raman spectrum of S_5N_6 was tentatively assigned to the transannular S-S bond[18]. The fact that a strong band, whose frequency is dependent on the S-S bond length, is observed in the Raman spectra of related S-N compounds (Table 2.2) provides strong support for the same assignment in 1,5-$(R_2PN)_2(SN)_2$.

Another striking contrast between 1,3- and 1,5-isomers is evident from the very pale yellow color of both the methyl and phenyl derivatives of the 1,5-isomer. No visible spectrum is observed for the latter and although there are signs of absorptions in the ultraviolet region, they are not comparable to the intense visible bands measured for the 1,3-isomer. There is obviously a fundamental difference in the electronic structures of these isomers (see Chapter 3).

A number of interesting observations result from the NMR spectra of the 1,5-isomers. The ^1H NMR spectrum of the methyl derivative exhibits a complex multiplet which can be explained as an AB coupling pattern. This is clarified by the ^{31}P decoupled spectrum, which shows two singlets indicating two inequivalent methyl groups. On the basis of this and information obtained from the Raman spectra, one may expect a molecular structure with a fold centered about a cross-ring S-S bond (cf. 1,5-Cl_2-S_4N_4 and 1,5-$(Ph_3P{=}N)_2S_4N_4$). This structure appears to remain rigid in solution, the ^1H NMR spectrum is virtually unaltered up to 110^0C. The singlets observed in the ^{31}P NMR spectra of these compounds are particularly unusual, appearing at very low field (R = Ph, 113.9 ppm; R = Me, 110 ppm). The reason for this extreme deshielding is not clear.

Table 2.2 S-S bond lengths and Raman stretching frequencies in sulfur-nitrogen cages and bicyclic compounds

Compound	d(S-S), Å	ν(S-S), cm^{-1}
$1,5\text{-}(Me_2NCN)_2(SN)_2$	2.43 [a]	-
S_5N_6	2.43 [b]	269 [b]
$1,5\text{-}(Ph_3P{=}N)_2S_4N_4$	2.45 [c]	259 [d]
$1,5\text{-}Cl_2S_4N_4$	2.48 [e]	260 [d]
$1,5\text{-}(Ph_2PN)_2(SN)_2$	2.52 [f]	269 [f]
$1,5\text{-}(Me_2PN)_2(SN)_2$	2.55 [g]	250 [g]
S_4N_4	2.58 [h]	213 [i j]
$S_4N_5^-$	2.71 [k]	186 [d]
$S_4N_5O^-$	2.71 [j]	222 [j]
$S_4N_5^+$	4.01 [l]	-

[a]Ref 171 [b]Ref 18 [c]Ref 86,87 [d]Ref 172 [e]Ref 63 [f]Ref 153 [g]Ref 52 [h]Ref 55,56,57,58 [i]Ref 174 [j]Ref 163 [k]Ref 173 [l]Ref 125.

MOLECULAR STRUCTURE OF 1,5-$(Ph_2PN)_2(SN)_2$

The crystal and molecular structure of 1,5-$(Ph_2PN)_2(SN)_2$ was determined by X-ray crystallographic methods†. The crystal structure consists of discrete molecular units with no unusual intermolecular contacts. Bond lengths and angles of the asymmetric unit are given in Table 2.3, and the atomic numbering scheme of the inorganic ring and the α-carbon atoms of the phenyl groups is given in the ORTEP drawing of the molecule in Figure 2.7.

Simple structural conclusions based on spectroscopic data are confirmed by the X-ray structural determination. By analogy with related molecules, 1,5-$(Ph_3P{=}N)_2S_4N_4$[87] and $Me_2NC(NSN)_2CNMe_2$[171], 1,5-$(Ph_2PN)_2(SN)_2$ can be viewed as a bicyclic molecule in which two five-membered rings share a common S-S bond. A crystallographic two-fold axis passes through the center of the ring, perpendicular to the cross-ring S-S bond. As a result the two sulfur atoms and two nitrogen atoms form two four-membered planes (planar to within 0.013 Å), which intersect at an angle of 117.3° (cf. 114.0° in $Me_2NC(NSN)_2CNMe_2$ and 120.4° in 1,5-$(Ph_3P{=}N)_2S_4N_4$). The phosphorus atoms lie 0.214 Å below the respective planes. Both the P-N and S-N bond lengths are significantly longer than those of the analogous eight-membered phosphazene ($(Ph_2PN)_4$ average d(P-N) = 1.590(3) Å)[170] and thiazene ($S_4N_4^{2+}$ average d(S-N) = 1.55 Å)[65,66]. However, non-planarity of the system makes it difficult to rationalize these bond length differences in comparison with the parent systems. The endocyclic bond angles at phosphorus and nitrogen are considerably smaller than the average in both $(Ph_2PN)_3$ ($N\hat{P}N$ = 117.8(3)°; PNP = 122.1(7)°)[175] and $(Ph_2PN)_4$ ($N\hat{P}N$ =

---

† The assistance of Dr. J. F. Richardson is gratefully acknowledged.

Table 2.3 Bond lengths (Å) and angles (deg) for the asymmetric unit of 1,5-$(Ph_2PN)_2(SN)_2$

Atoms	Distance	Atoms	Angle
P1-N1	1.623(3)	N1-P1-N2	110.8(1)
P1-N2	1.620(3)	N1-P1-C1	108.6(1)
P1-C1	1.792(3)	N1-P1-C7	111.5(1)
P1-C7	1.796(3)	N1-P1-C1	107.5(1)
N1-S1	1.596(2)	N2-P1-C7	112.4(1)
N2-S1′	1.584(2)	C1-P1-C7	105.7(1)
S1-S1′	2.528(1)	P1-N1-S1	120.7(2)
C1-C2	1.402(4)	P1-N2-S1′	121.2(2)
C2-C3	1.387(4)	N1-S1-N2′	116.1(1)
C3-C4	1.376(4)	C6-C1-C2	119.6(3)
C4-C5	1.386(4)	C1-C2-C3	120.1(3)
C5-C6	1.396(4)	C2-C3-C4	119.9(3)
C6-C1	1.391(4)	C3-C4-C5	120.8(3)
C7-C8	1.398(4)	C4-C5-C6	119.8(3)
C8-C9	1.385(4)	C5-C6-C1	119.8(3)
C9-C10	1.392(4)	C12-C7-C8	120.0(3)
C10-C11	1.381(4)	C7-C8-C9	119.7(3)
C11-C12	1.389(4)	C8-C9-C10	120.0(3)
C12-C7	1.402(4)	C9-C10-C11	120.5(3)
		C10-C11-C12	120.2(3)
		C11-C12-C7	119.5(3)

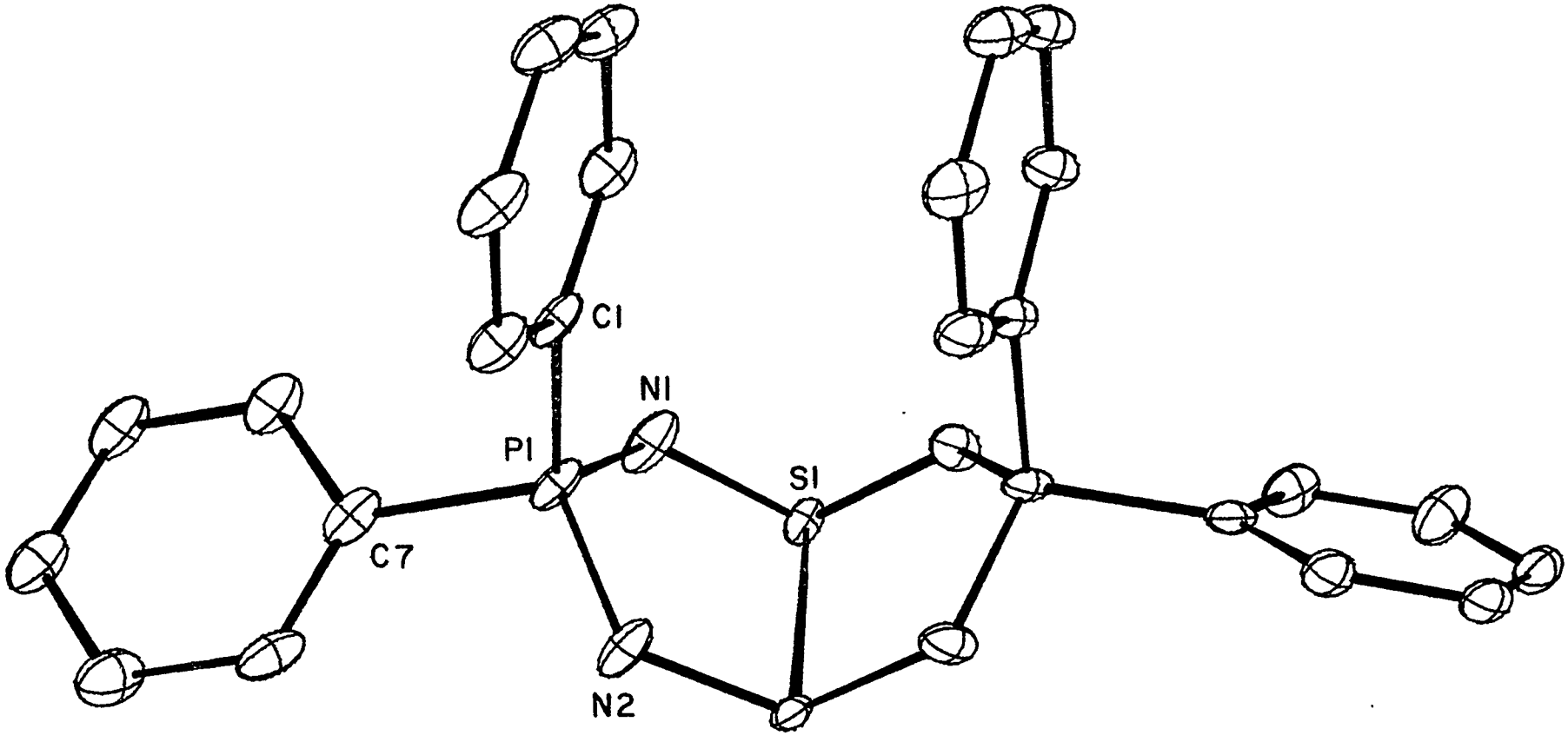

Figure 2.7 ORTEP view (50% probability ellipsoids) of 1,5-$(Ph_2PN)_2(SN)_2$ showing the atomic numbering scheme. A crystallographic two-fold axis passes perpendicularly through the S-S bond.

119.9(1)°; PNP = 127.9(2)°[170]). This is a function of the angle strain imposed by the close transannular S-S interaction.

MOLECULAR STRUCTURE OF 1,5-$(Me_2PN)_2(SN)_2$

The crystal and molecular structure of 1,5-$(Me_2PN)_2(SN)_2$ was determined by X-ray crystallographic methods†. Bond lengths and angles of the asymmetric unit are given in Table 2.4 and the atomic numbering scheme is given in the ORTEP drawing of the molecule in Figure 2.8.

The gross molecular structural features of the methyl derivative are very similar to those of the phenyl derivative, however, the different crystal symmetry imposes a number of crystallographic dissimilarities. The two phosphorus centers of the phenyl derivative are crystallography equivalent, due to a two-fold axis perpendicular to the cross-ring S-S bond. In contrast, the methyl derivative lies on a mirror plane passing through the two phosphorus atoms. A short intramolecular contact between C1 and C3 of 3.99 Å and short intermolecular contacts of the type C1-C3 ($\frac{1}{2}$-x, y, -$\frac{1}{2}$-z) of 3.64 Å and C2-C4 (1-x, y, z) of 3.61 Å effect a distortion, which renders the phosphorus atoms crystallographically inequivalent. One phosphorus is displaced above the four atom S1N2 plane by +0.194 Å and the other below the opposite four atom S1N1 plane by -0.479 Å. The spectroscopic equivalence of these two phosphorus centers is demonstrated by the singlet observed in the ^{31}P NMR spectrum (see Section 2.3.3.4). It is therefore reasonable to conclude the inequivalence of the phosphorus centers is a function of crystal packing and not a chemical phenomenon.

---

† The assistance of Dr. P. W. Codding is gratefully acknowledged.

Table 2.4 Bond lengths (Å) and angles (deg) for the asymmetric unit of 1,5-$(Me_2PN)_2(SN)_2$

Atoms	Distance	Atoms	Angle
P1-N2	1.630(3)	N2-P1-N2	110.0(2)
P2-N1	1.642(3)	N1-P2-N1	107.3(2)
P1-C3	1.795(6)	C3-P1-C4	104.8(3)
P1-C4	1.790(6)	C3-P1-N2	111.0(2)
P2-C1	1.797(5)	C4-P1-N2	110.0(1)
P2-C2	1.792(5)	C1-P2-C2	106.7(2)
N1-S1	1.594(3)	C1-P2-N1	113.3(1)
N2-S1	1.597(3)	C2-P2-N1	108.0(1)
S1-S1′	2.551(2)	N1-S1-N2	114.9(2)
		N1-S1-S1′	91.7(1)
		N2-S1-S1′	92.2(1)
		S1-N1-P2	119.4(2)
		S1-N2-P2	122.0(2)

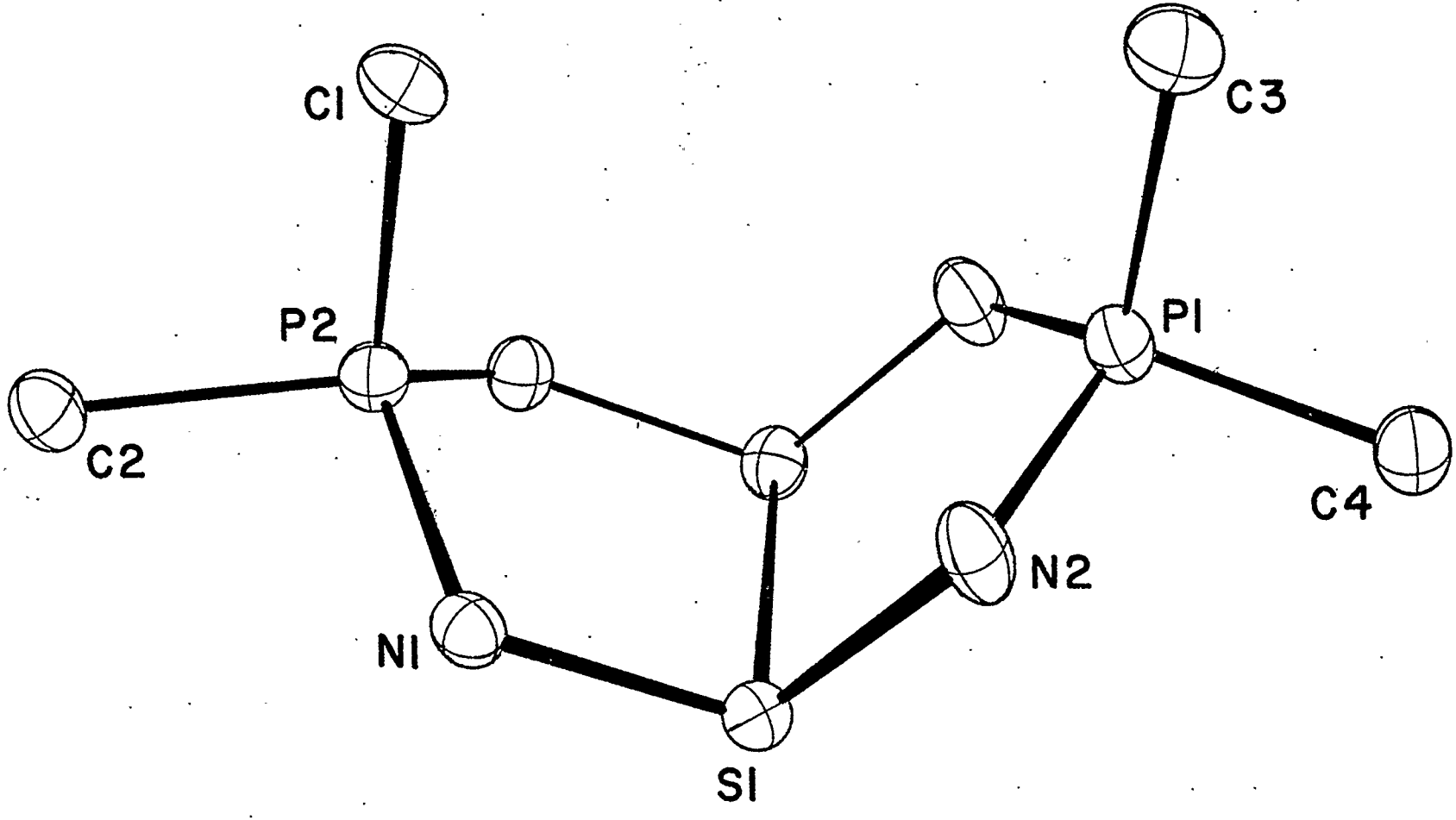

Figure 2.8 ORTEP view (50% probability ellipsoids) of 1,5-$(Me_2PN)_2(SN)_2$ showing the atomic numbering scheme. A crystallographic mirror plane passes through the four carbon and two phosphorus atoms.

CHAPTER 3

ELECTRONIC STRUCTURES OF UNSATURATED PHOSPHORUS, NITROGEN AND SULFUR CONTAINING HETEROCYCLES WITH SULFUR IN A LOW OXIDATION STATE

3.1 INTRODUCTION

The development of theoretical methods more advanced than simple VB approaches, on systems containing elements other than carbon and hydrogen, has been quite successful. Semi-empirical procedures on a variety of unsaturated heterocyclic main group systems have produced useful descriptive rationalizations of experimental results. In addition, where rigorous calculations have been possible, the results have provided encouraging confirmations of conclusions derived from the less sophisticated methods. Such results have prompted detailed investigation of relatively complex S-N heterocycles (e.g. $S_4N_5^-$[176,177], S_4N_4[121,122,123,124,125,126], $S_5N_5^+$[178, 179], $S_4N_4^{2+}$[52,129]). Although, an accurate bonding picture for the unsaturated P-N heterocycles is still in question, due to complication by d orbital involvement, an empirical description provides important rationalizations regarding structure and chemistry[40] (see Section 1.4.3).

The three unsaturated P-N-S heterocycles (36, 16, 17) introduced in Chapter 2 all contain two sulfur centers in oxidation states of II and IV. As discussed in Chapter 1, the unsaturated S-N heterocycles containing sulfur in such low oxidation states have unique chemical and physical properties. Similar physical properties have been discussed for these P-N-S heterocycles indicating that these systems may have related electronic

features. On this basis the bonding schemes for a series of known and unknown six- and eight-membered unsaturated P-N-S heterocycles containing sulfur in its lowest possible oxidation state (for a particular structure) have been examined. The results are discussed in this chapter. Before developing MO descriptions for these P-N-S systems it is worthwhile examining them from a VB viewpoint.

3.2 VALENCE BOND REPRESENTATIONS OF UNSATURATED P-N-S HETEROCYCLES

The universal application of VB representations, providing effective structural and electronic information, manifests their usefulness as a theoretical tool. They are very reliable and require little input to provide data pertaining to geometric arrangement of groups, viability of structures or compounds and electronic distribution within a molecular structure. Figure 3.1 shows some VB structures of all the possible six and eight-membered unsaturated P-N-S heterocycles containing sulfur in its lowest available oxidation state for a particular system. Systems containing two (even) sulfur atoms are neutral and the sulfur centers are dicoordinate in formal oxidation states of II and IV (A, D, E). Systems containing an odd number of sulfur atoms either have at least one tricoordinate sulfur center, or carry a charge (B, C, F).

Using the simple rules devised by Banister for the cyclothiazenes (see Section 1.3.5.1) it is possible to determine the number of electrons available for π-bonding in each of these P-N-S heterocycles (Figure 3.1). Certain of these compounds may be regarded as Hückel $(4n + 2)\pi$-electron systems, in accordance with the rationalization made by Banister for the S-N heterocycles. However, as discussed in Section 1.3.5.1, the Hückel

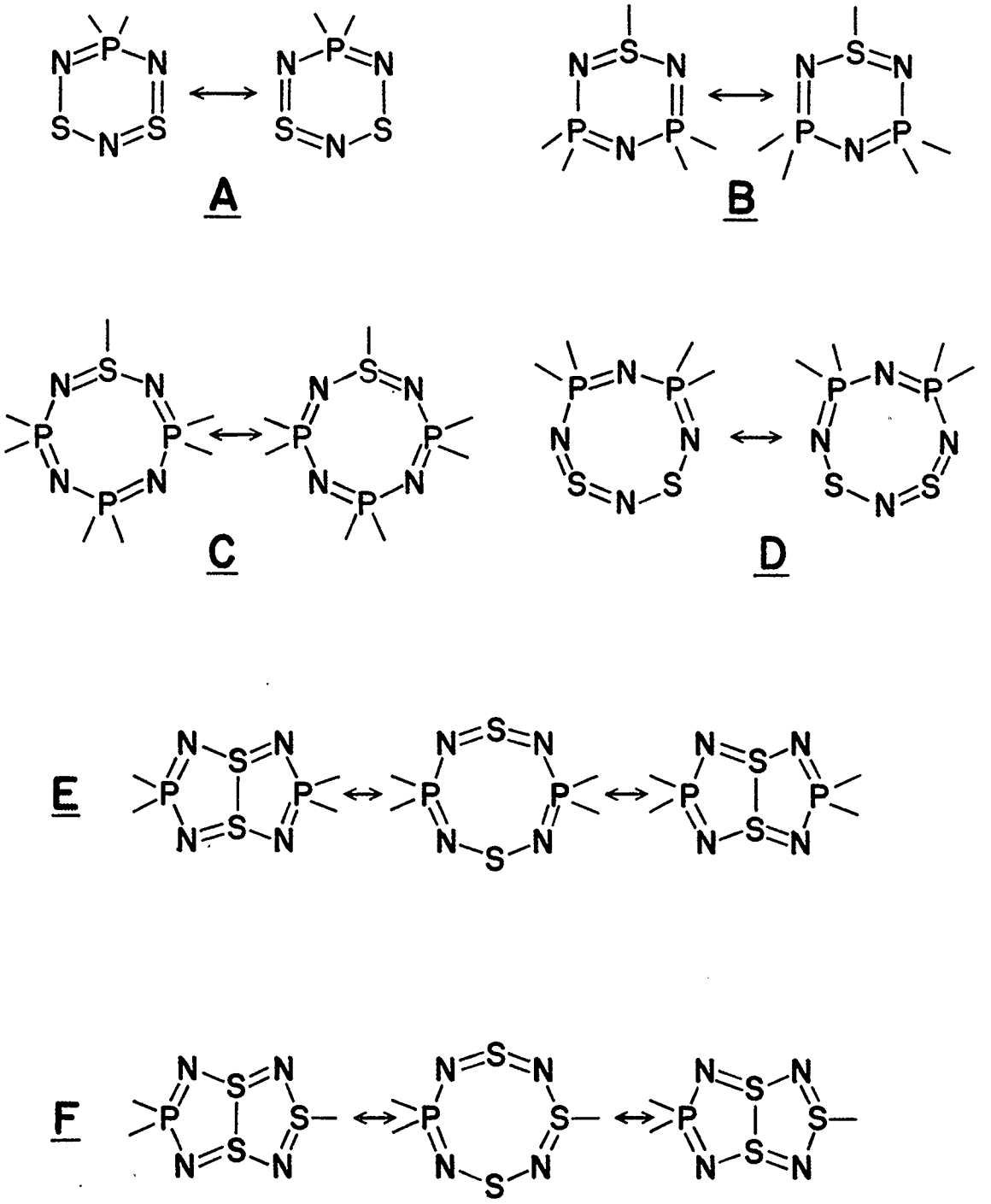

Figure 3.1 Some valence bond representations for all the possible six- and eight-membered P-N-S heterocycles containing sulfur in a low oxidation state.

rule should be handled with care for inorganic heterocyclic systems. Indeed, $(R_2PN)(SN)_2$ (A) is one of numerous examples of a six-atom $4n\pi$ - electron system. The stability and properties of these compounds appear to depend on more fundamental qualities.

Of the compounds exhibited in Figure 3.1, C and F are the only unknown species. A, D and E are presented in Chapter 2 and B was discovered by Roesky[30,31] and has been examined in detail more recently by Chivers and Rao[149,180,181,182,183]. The VB representations give a rationale for many of the gross features of these known systems, such as the planarity of A, B and D and the folded structure of E. However, they provide little predictive data. The general inadequacies of the VB description for inorganic heterocyclic systems were pointed out in Section 1.2.1 and many of them apply here. For this reason an MO approach has been employed to develop a more thorough understanding of the unsaturated P-N-S systems.

3.3 MOLECULAR ORBITAL STUDIES OF UNSATURATED P-N-S HETEROCYCLES CONTAINING SULFUR IN A LOW OXIDATION STATE

3.3.1 PROCEDURES

Simple HMO approaches used successfully for the unsaturated S-N and P-N heterocycles were employed to develop a picture for the π-structure in the hybrid unsaturated P-N-S compounds. In all the calculations the Coulomb parameters (α) were chosen to reflect the relative atomic electronegativities[45] of phosphorus, nitrogen and sulfur (which provide consistent results for the composition and ordering of the π-MOs), rather than the proposed orbital electronegativities[51] (see Section 1.2). They

are equated by $\alpha_N = \alpha_P + 4\beta$ and $\alpha_N = \alpha_S + \beta$, where β is also the resonance integral, assumed to be equal for all interactions. The two π-type d orbitals on phosphorus (d_{xz} and d_{yz}) were considered degenerate. Although both orbitals were considered in the calculations, in many cases inclusion of heteromorphic interactions (d_{xz}) provided little additional information. In view of the fact that the homomorphic interaction is believed to be the more substantial in the cyclophosphazenes (see Section 1.2), some of the discussions are developed on models possessing only a d_{yz} orbital on phosphorus. All systems presented in Figure 3.1 were investigated. Conclusions derived from the results are justified by comparison with results obtained from sophisticated calculations. Interpretation includes rationalization of experimental observations and correlation of results with parent S-N and P-N systems.

3.3.2 SIX-MEMBERED UNSATURATED P-N-S HETEROCYCLES

$(R_2PN)(SN)_2$

It was evident in Chapter 1 that the phosphazene and thiazene heterocycles both show some degree of π-electron delocalization. Many of the physical and chemical properties of these systems are also observed in the hybrid P-N-S systems. Therefore one may expect these mixed compounds to retain the basic electronic features of the parent systems.

Representations of the lower π-MOs of a $(PN)(SN)_2$ system are displayed in Figure 3.2 along with the calculated total π-bond orders. All of these orbitals are concentrated mainly on the S_2N_3 section of the molecule. Polarization of the π-structure is a function of the higher

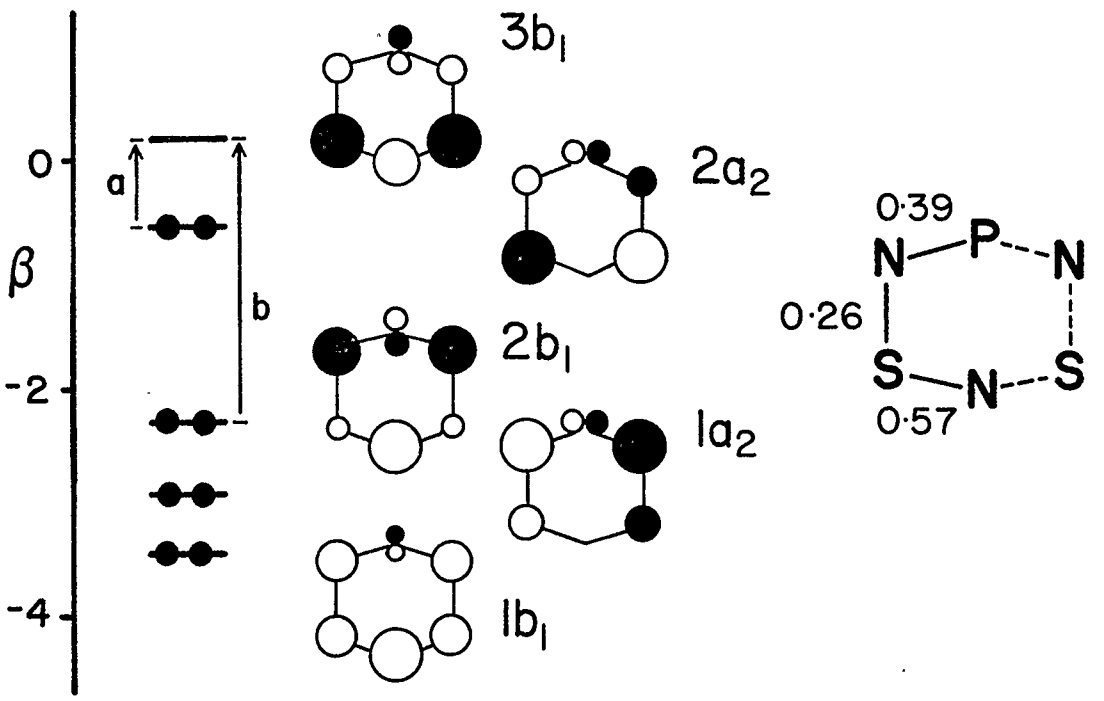

Figure 3.2 Relative energies and representations for the Hückel π-MOs of $(R_2PN)(SN)_2$ and calculated π-bond orders. a corresponds to a visible absorption at 560 nm and b corresponds to an absorption at 270 nm. Estimated atomic orbital contributions are viewed from above.

electronegativity of sulfur and nitrogen in comparison to phosphorus. The $1b_1$ and $1a_2$ MOs are strongly bonding in nature with respect to the S_2N_3 unit. On the other hand the $2a_2$ and $3b_1$ are strongly antibonding in the S-N region, whilst the $2b_1$ is a non-bonding orbital. The two π-type d orbitals on phosphorus interact with the S-N π-orbitals of suitable symmetry in a bonding fashion, irrespective of the bonding or antibonding character in the S_2N_3 moiety. However, the d orbital contribution is minor in the lower energy π-MOs. The higher energy π-MOs are based mainly on phosphorus. The eight electrons available for π-bonding in this system (see Section 3.2) occupy the four lowest energy π-MOs, including the $2a_2$ antibonding π*-MO.

Ab initio calculations carried out by Laidlaw[151] on a planar $(H_2PN)(SN)_2$ model have extended and quantified the picture. The results confirm the basic conclusions obtained from the simple method. In addition, an identical calculation on a non-planar model, with the phosphorus atom removed from the S-N plane by 0.28 Å (the structure observed experimentally, see Section 2.3.2.3), indicated that this structure has a total energy 15 kcal mol^{-1} lower than that of the planar model. However, the ordering and spacing of the energy levels remained essentially unchanged. In an attempt to establish the nature of the visible absorptions observed for these systems, transition moment calculations were carried out[151] for a number of transitions between the upper occupied energy levels and the virtual energy levels. The results revealed that the transitions $2b_1 \rightarrow 3b_1$ (estimated at 560 nm) and $2a_2 \rightarrow 3b_1$ (estimated at 280 nm) should both be two orders of magnitude more probable than any other transitions above 200 nm. On this basis the strong visible absorption observed for these systems at about 560 nm is assigned to a π^* (HOMO $2a_2$)$\rightarrow\pi^*$ (LUMO $3b_1$) transition (Figure 3.2(a)). The second less intense absorption observed in the spectrum of $(Me_2PN)(SN)_2$ at 270 nm is assigned to an $n\pi$ ($2b_1$)$\longrightarrow$ π^* (LUMO $3b_1$) transition Figure 3.2 (b)).

Oakley has developed an HMO description of the π-bonding in a $(PN)(SN)_2$ ring, viewing the heterocycle as a perturbation of the 10π-electron $S_3N_3^-$(8) system[151]. Replacement of a sulfur atom with a phosphonium cation (R_2P^+) has the effect of removing two electrons from the π-manifold, rendering the heterocycle an 8π-electron system. Such a system is isoelectronic with the unknown $S_3N_3^+$ cation (see Section 1.3.5.3) however, the D_{3h} symmetry of a planar $S_3N_3^+$ is lowered to C_{2v} in $(PN)(SN)_2$ removing the orbital degeneracy. Polarization of the π-electron density onto the S_2N_3 unit of

this system allows a comparison with λ^5-phosphorin (phosphabenzene)[44], which has been described as an "Internal salt" (38)[44]. The model requires that the phosphorus center donates its π-electron to the pentadienyl unit and there is no π-interaction back into the phosphorus d orbitals.

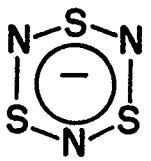

8

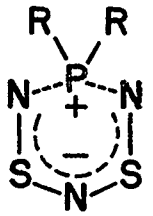

37

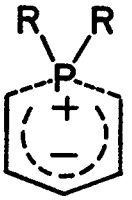

38

This picture can be extended to describe the P-N-S heterocycle (37), the major difference between the two systems being the extent of occupancy of the π-manifold (8π-electrons in $S_2N_3^-$ and 6π-electrons in $C_5H_5^-$).

This simple view allows some important conclusions to be made in the context of the more accurate results. In addition, the dependence of the absorption energies (λ_{max}, Table 5.2), observed for these compounds, on the nature of the exocyclic ligands attached to phosphorus, can be rationalized using this model. As illustrated in Figure 3.3 an interaction between the two high energy phosphorus d orbitals and the π-MOs of an open chain $S_2N_3^-$ anion results in a general stabilization of the latter. Concurrently, the former is destabilized. Naturally, the greater interaction of the d orbitals will be with those MOs which are of suitable symmetry and are nearest in energy (i.e. the HOMO and LUMO of $S_2N_3^-$). If we assume that two d orbitals are degenerate and their overlap with the π-MOs of the S_2N_3 fragment is equivalent, the stabilization of the LUMO (δE_L) will always be greater than the stabilization of the HOMO (δE_H). Consequently, the HOMO-LUMO energy separation (Δ) is intimately dependent

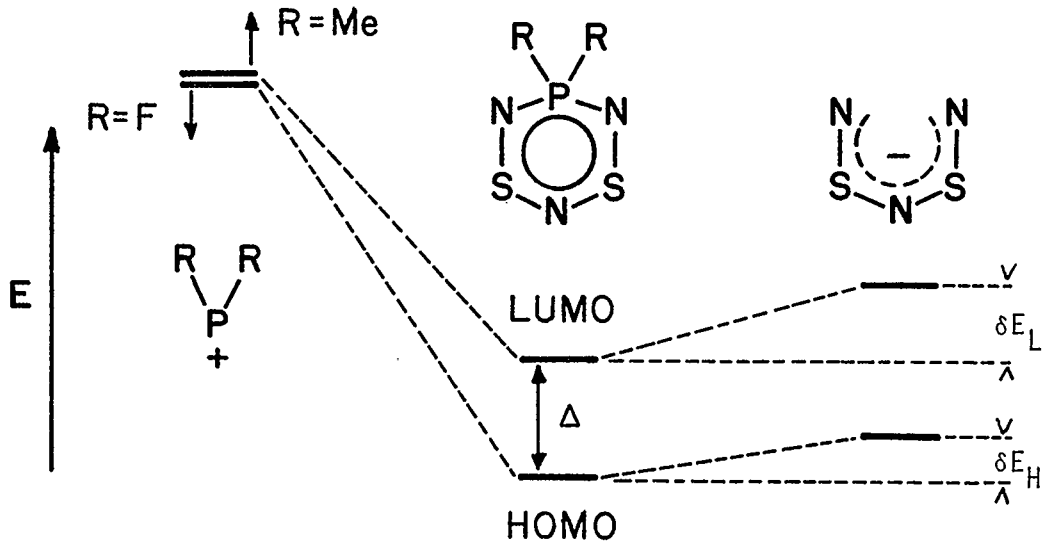

Figure 3.3 Effect of the exocyclic ligands attached to phosphorus on the HOMO-LUMO separation (Δ) of $(R_2PN)(SN)_2$. Qualitative view of the interaction between the phosphorus π-type d orbitals and the HOMO and LUMO of $S_2N_3^-$. δE_L and δE_H are relative stabilization energies.

on the energy of the d orbitals, which will vary with the electronegativity of the exocyclic ligands attached to phosphorus.

Electron donating (electropositive) groups (Me) on phosphorus will effect a relative increase in the energy of the d orbitals, so reducing the interaction and increasing Δ. Conversely, electronegative ligands (F) on phosphorus will lower the energy of the orbitals and allow a more effective interaction, resulting in a decrease in Δ. These conclusions help explain why the electronic absorption, corresponding to the π* (HOMO)-π* (LUMO) electronic transition in these compounds, occurs at higher energy (543 nm) in the methyl derivative than in the fluoro derivative (583 nm).

$(R_2PN)_2(NS)^+$

The encouraging agreement between simple HMO and *ab initio* descrip-

tions of the electronic structure of $(R_2PN)(SN)_2$ has prompted the investigation of unsaturated systems containing more than one phosphorus unit, using the simple approach. The electronic structures of the eight-membered rings will be discussed following an examination of the six-membered $(R_2PN)_2(NS)^+$ system[30,31]. Conclusions derived from studies on this cationic system can be extended to the derivatives which contain an exocyclic ligand attached to the sulfur center (X = Cl[149], Br[180], I[182], Ph[180], N_3[183], NMe_2[181])[183].

Representations of the lower π-MOs of a $(PN)_2(SN)$ system are shown in Figure 3.4 along with the calculated total π-bond orders. The d orbital involvement in the π-structure of this system is more complex than in $(R_2PN)(SN)_2$; however, it is the upper virtual orbitals which possess the major phosphorus contribution. The cationic species is a 6π-electron system and, in contrast to $(R_2PN)(SN)_2$, there are no occupied π*-MOs. The

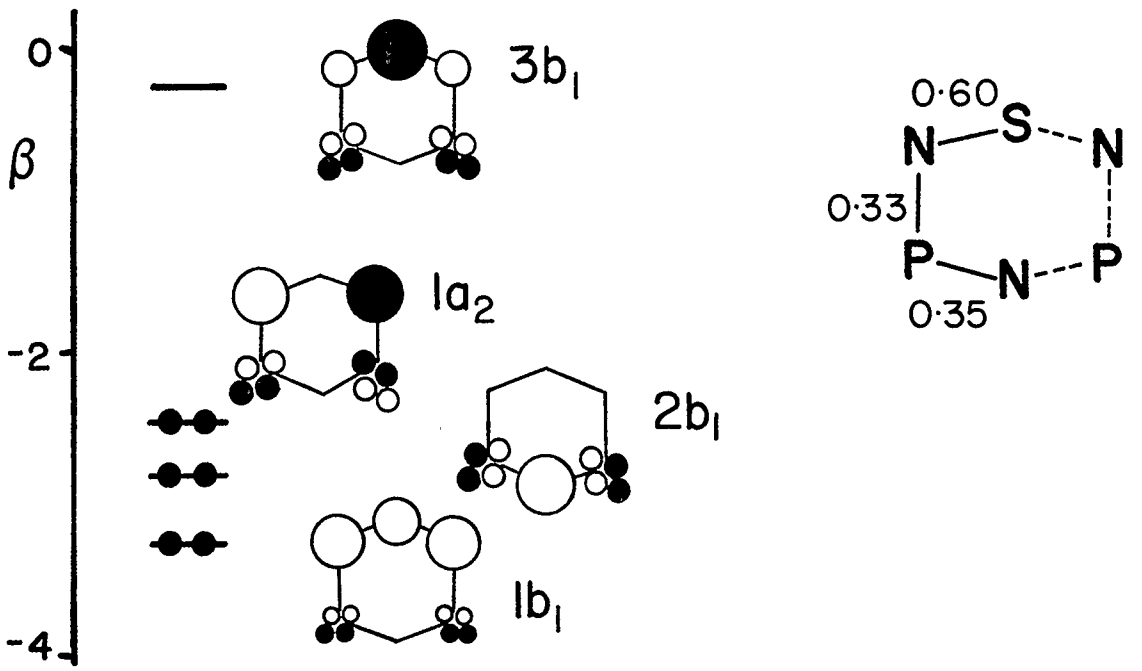

Figure 3.4 Relative energies and representations for the Hückel π-MOs of $(R_2PN)_2(NS)$ and calculated π-bond orders. Estimated atomic orbital contributions are viewed from above.

LUMO is a π^*-MO based mainly on the sulfur center, and is strongly antibonding with respect to the N-S-N unit. In contrast, the lowest energy π-MO associated with the ring is the $1b_1$ orbital, which is strongly bonding in nature over the N-S-N half of the molecule. The $2b_1$ π-MO is also bonding in nature, but is concentrated on the P-N-P unit. Above these is a π-MO almost non-bonding in character ($1a_2$) located on the equivalent nitrogen centers. This picture indicates that the π-bonding is polarized towards the NSN region of the ring.

Many of these electronic features have interesting effects on the molecular structure of the heterocycle. For easy reference, the pertinent bond length values obtained from X-ray crystallographic studies on various derivatives[30,31,149,180,182] are listed in Table 3.1. In most of the compounds the structure of the P-N-P unit resembles that same unit in the

Table 3.1 Pertinent bond length values for various derivatives of $(R_2PN)_2(NSX)$ (Å)

	R = Cl	R = Ph			
	X = +[a]	X = Cl[b]	X = Ph[c]	X = I[d]	X = NMe_2[c]
S-N1	1.556(12)	1.560(5)	1.622(6)	1.556(7)	1.587(5)
N1-P1	1.620(11)	1.660(6)	1.627(6)	1.667(9)	1.607(5)
P1-N2	1.500(11)	1.589(5)	1.595(4)	1.590(7)	1.595(5)
N2-P2	1.611(11)	1.582(5)	1.605(6)	1.582(7)	1.597(5)
P2-N3	1.646(10)	1.671(6)	1.627(5)	1.656(9)	1.608(5)
N3-S	1.564(10)	1.557(5)	1.613(4)	1.544(7)	1.607(5)

[a]Ref 30 [b]Ref 149 [c]Ref 180 [d]Ref 182

respective trimeric phosphazene. In contrast, the S-N bond lengths are significantly shorter than the mean bond length in a typical cyclic thiazyl system (eg. $S_3N_3Cl_3$, mean d(S-N) = 1.605 Å[22]). The calculated total π-bond orders are consistent with these observations. The dimethylamino and phenyl derivatives are exceptions, having unusually long S-N bond lengths. It would appear that these ligands π-donate into the π^*-LUMO of the ring. The antibonding character of this orbital in the N-S-N region, thereby weakens the S-N bonds. Indeed, the dimethylamino derivative is thermally unstable and undergoes a facile ring opening reaction at room temperature, involving S-N bond cleavage[181]. This characteristic is also evident in the reduction of $(Ph_2PN)_2(NSCl)$ by $SbPh_3$ which results in the formation of a dimeric twelve-membered heterocycle with a cross-ring S-S σ-bond[184]. One may conclude that the mechanism of the reduction involves population of the π^*-LUMO, once again resulting in rupture of the S-N bond. The P-N bonds which connect the two halves of the molecule (N1-P1 and P2-N2) are long in comparison to the P-N-P bond lengths, reflecting the π-electron deficiency in this region.

QUALITATIVE COMPARISON OF THE π-STRUCTURES OF $(R_2PN)(SN)_2$ AND $(R_2PN)_2(NS)^+$

$(R_2PN)(SN)_2$ and $(R_2PN)_2(NS)^+$ can each be viewed as a single atom (E) substitution of an $(AB)_n$ type six-membered ring (39). The former involves replacement of one sulfur atom of a thiazene system by a phosphorus unit, and the other is a phosphazene with one phosphorus unit substituted by a sulfonium cation. As already discussed for the former, the high energy of the phosphorus d orbitals effect a general stabilization of the π-MOs

of the S-N moiety (Figure 3.5(a)). Therefore, the ring retains many of the structural and electronic features of the original S-N system. In contrast, incorporation of a sulfur center into the phosphazene system results in more pronounced structural and electronic adjustments in comparison to the pure P-N ring. Figure 3.5(b) shows the characteristic energy spread for the π-MOs of a typical phosphazene-type P_2N_3 unit (see Section 1.4.3). The energy of the π-type sulfur orbital is intermediate between the two energy groups of the P_2N_3 π-MOs, and the interaction results in a stabilization of the lower energy nitrogen based orbitals and a destabilization of the upper phosphorus based orbital of suitable symmetry. For this reason the π-electron distribution around the ring

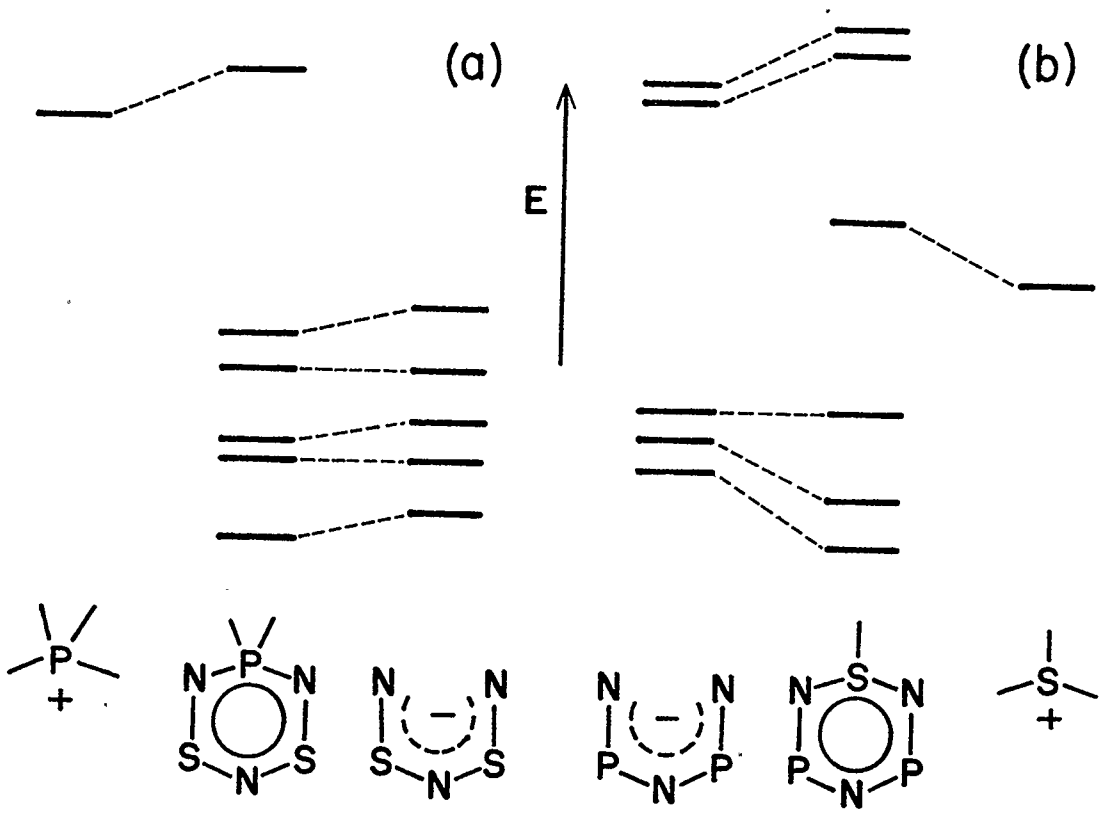

Figure 3.5 Single atom perturbation of a thiazene π-structure by a phosphorus orbital (a) and of a phosphazene π-structure by a sulfur orbital (b).

is localized and the bond order (bond length) variations in this system are greater than in the perturbed thiazene (ignoring π*-electrons).

Ring bond length variations of this type have been observed in geminally substituted phosphazenes, in which the geminal groups have significantly different electronic characteristics to the other ligands on the ring. For example in gem-$N_4P_4F_6Me_2$ (40)[184], the nearest bond to the Me_2P group is the longest bond in the ring and is adjacent to the shortest bond. The third bond is intermediate in length between the first two and the fourth between the second and third. This bond alternation

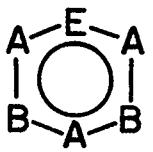

39

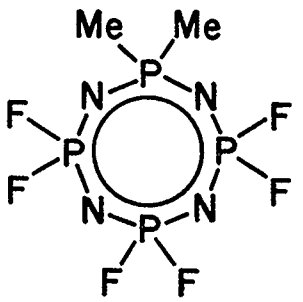

40

is not explicable in terms of σ-inductive effects which would cause the ring bonds to vary smoothly in length with distance from the perturbed center. Paddock has shown, using simple perturbation theory, that the bond length changes can be described in terms of the π-inductive effect of the methyl substituents[185]. Simple HMO calculations were carried out by adjusting the Coulomb parameter of the substituted atom, and the bond atom polarizabilities (δ(bond order)/ δ(Coulomb parameter of perturbed center))[186] were found to parallel the observed deviations. In addition the calculations demonstrated that the degree of the effect is dependent on the magnitude of the electronegativity differences between the non-substituted ring atoms. When the electronegativities of the ring

π-atomic orbitals are similar, the effect is smaller. At the other extreme, in systems which have π-type orbitals far removed in energy, the π-interaction is so poor that the perturbation is not transmitted.

All of these conclusions can be extended to account for the characteristics observed for the P-N-S systems. However, the perturbation in these systems is a consequence of the unique ring atom. The electropositive phosphorus center in $(PN)(SN)_2$ effects only small bond length alternations around the ring, due to the similar energies of the π-type sulfur and nitrogen orbitals. In contrast, large variations result from the sulfur perturbation of the P-N system in $(R_2PN)_2(NS)$.

3.3.3 EIGHT-MEMBERED UNSATURATED P-N-S HETEROCYCLES

$(R_2PN)(NS)_3^+$ AND $(R_2PN)_3(NS)^+$

Although neither of these systems has yet been prepared, isoelectronic species are known and various predictions can be made in the context of the other P-N-S heterocycles. $(R_2PN)(NS)_3^+$ (15) is a 10π-electron system and

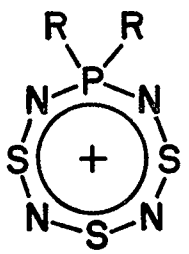

15

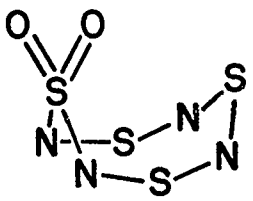

41

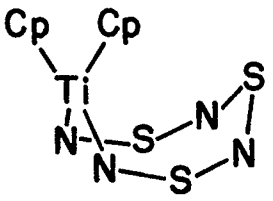

42

as such is isoelectronic with $O_2S_4N_4$ (41)[187] and $Cp_2TiS_3N_4$ (42)[188]. These systems can be viewed as a replacement of an S^{2+} center of $S_4N_4^{2+}$ (20) by

an R_2P^+, SO_2 or Cp_2Ti unit, respectively. The structures of 41 and 42 have been determined by X-ray crystallographic techniques[187,188] and both were found to have the boat-shaped conformation reminiscent of the Lewis acid adducts of S_4N_4 (21). On this basis it is tempting to suggest that 15 will have a similar structure. In all cases the π-structure will have the internal salt features seen in $(R_2PN)(SN)_2$ (see Section 3.3.2.1), involving an interaction between the π-MOs of a 10π-electron open chain S_3N_4 and the d orbitals of the unique unit. Consequently, the lower π-MOs are very similar in form and energy to those of $S_4N_4^{2+}$ (Figure 3.6 (a)). However, the HOMO is very different to the non-bonding sulfur based

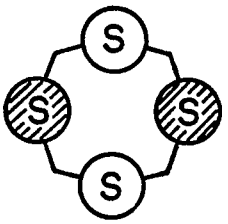

43

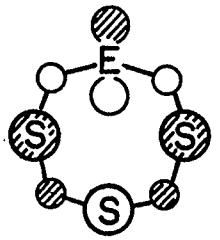

44

π-MO (43) of $S_4N_4^{2+}$. Substitution of one of the sulfur centers disrupts the symmetry of the molecule removing the degeneracy, and introducing some antibonding character into the orbital. This is illustrated in 44, which shows the adjustment of the nodal planes of the MO by the interaction of the unique atomic orbital (E = R_2P^+, SO_2, Cp_2Ti). Therefore, the orbital is destabilized with respect to 43. In addition, the circumannular π-electron delocalization is considerably reduced by the d orbital involvement, in comparison to $S_4N_4^{2+}$. It is conceivable that the molecule puckers into the boat form to relieve the antibonding character. Alternatively, 15 also has the capability to form a cross-ring S-S σ-bond

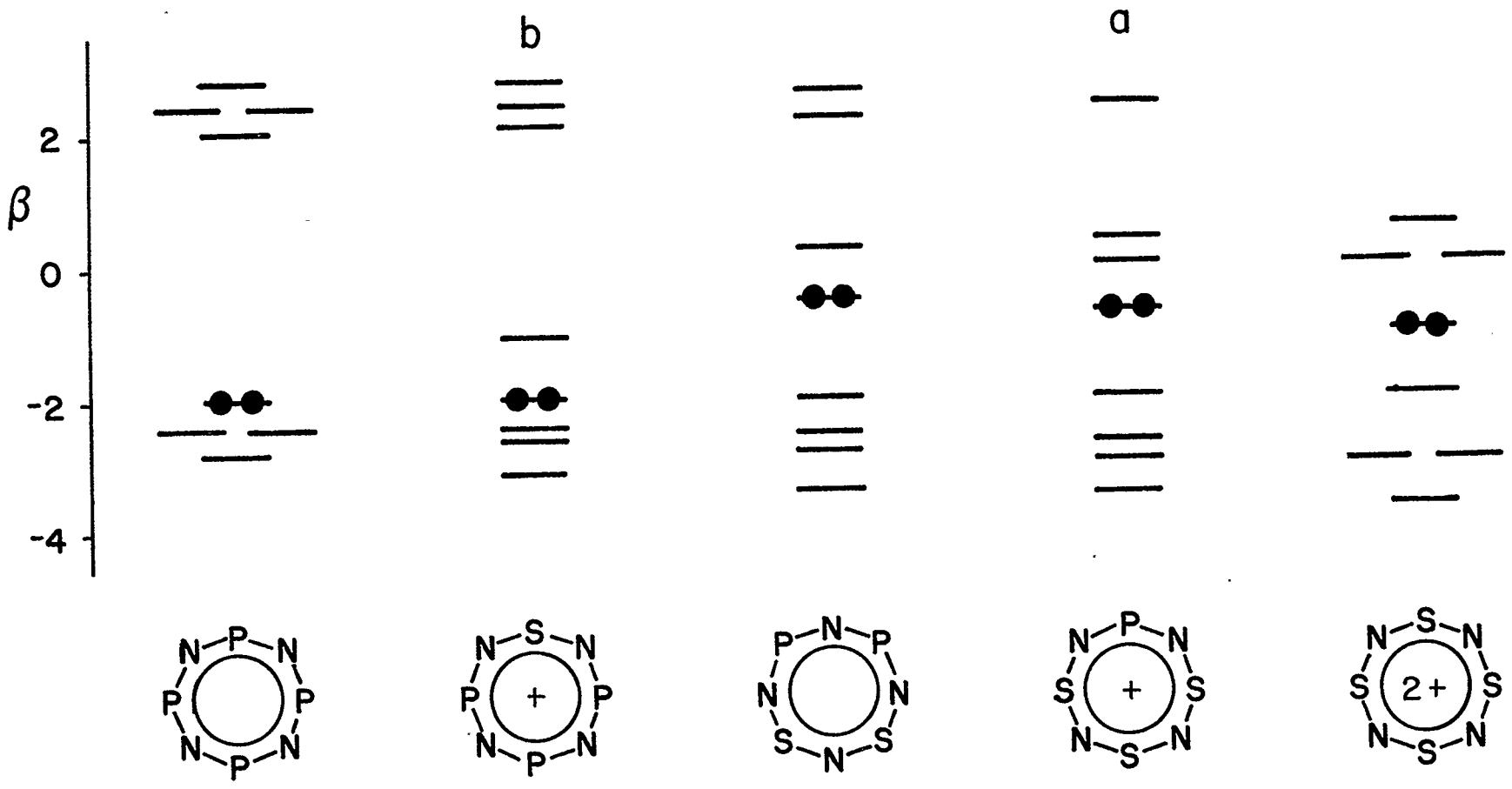

Figure 3.6 Qualitative comparison of the π-levels of eight membered $P_xN_4S_y$ systems. The HOMO is indicated by the occupancy.

(cf. 1,5-$(R_2PN)_2(SN)_2$) the electronic significance of which will be discussed in Section 3.3.3.3.

$(R_2PN)_3(NS)^+$ (Figure 3.6(b)) can be viewed as a single atom adjustment of a tetrameric phosphazene. The substitution does not affect the π-electron count, however, it is important to point out that the LUMO is significantly stabilized in comparison to the phosphazene. As was seen for the six-membered analog (see Section 3.3.2.3), this orbital is mainly based on the sulfur center and is strongly antibonding in character. On this basis one might expect this compound to exhibit many of the physical and chemical features already discussed for $(R_2PN)_2(NS)^+$.

Figure 3.6 shows a qualitative picture of the π-energy levels of the two compounds in comparison to those of the parent systems and the intermediate species 1,3-$(R_2PN)_2(SN)_2$, which will be examined in more detail in Section 3.3.3.2. This series of systems demonstrates how the high electronegativity of sulfur and nitrogen compared to phosphorus, stabilize the lower antibonding π-levels. This factor along with the effective π-electron delocalization achieved in the S-N containing systems, facilitates occupation of these antibonding MOs.

1,3-$(R_2PN)_2(SN)_2$

In accordance with all the P-N-S systems discussed so far, the calculations on the 1,3-$(R_2PN)_2(SN)_2$ system reveal a polarization of the π-structure into the P-N-P and S_2N_3 units of the molecule. The lower MOs are once again based on the S-N section and in this respect are very similar to the same orbitals of the six-membered $(R_2PN)(SN)_2$. In view of the structural similarities discussed in Section 2.3.3.3, these two systems

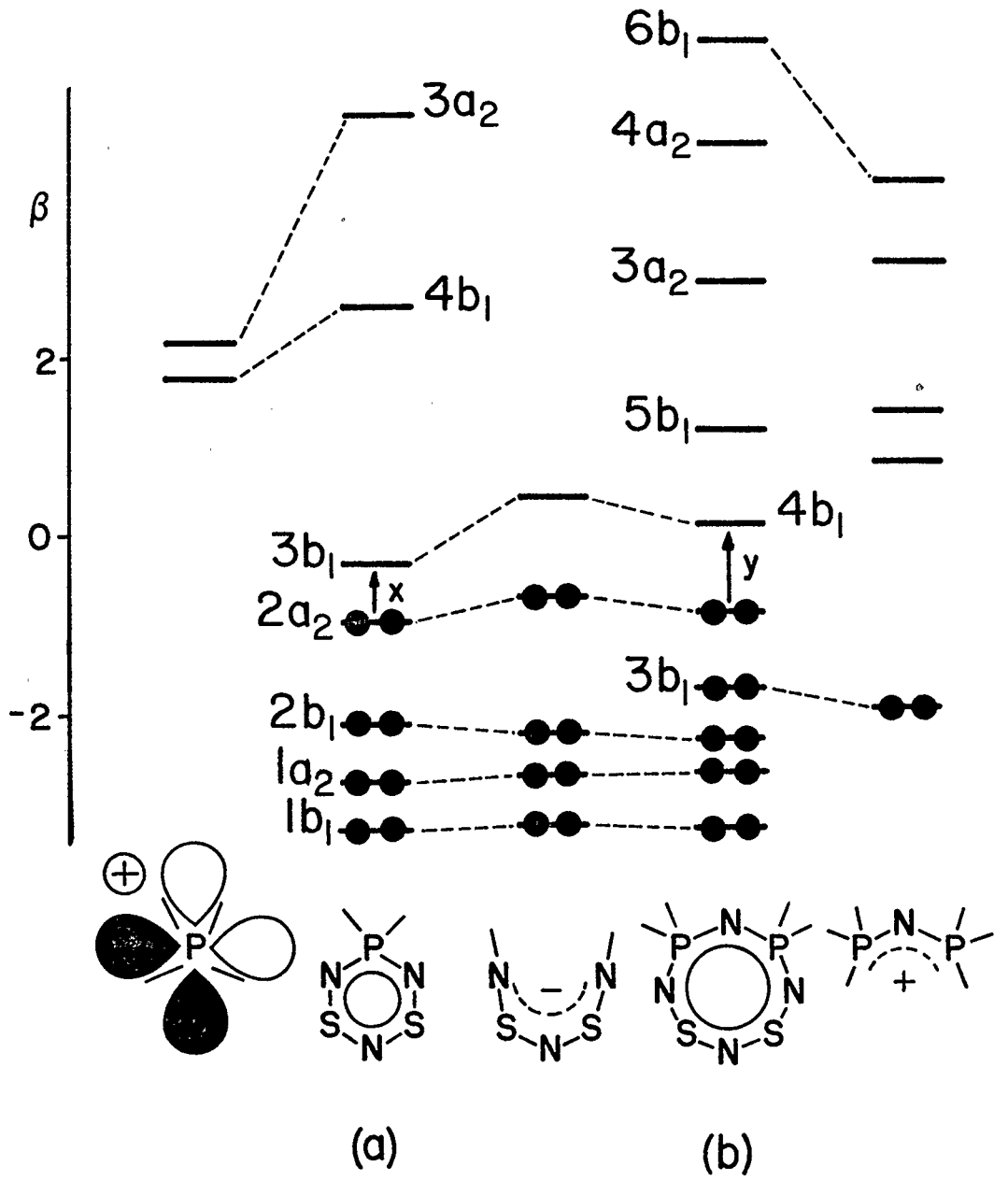

Figure 3.7 Interaction of the π-structure of $S_2N_3^-$ with the d orbitals of R_2P^+ to give $(R_2PN)(SN)_2$ (a) and with the π-structure of $(R_2PNPR_2)^+$ to give 1,3-$(R_2PN)_2(SN)_2$ (b). X corresponds to a visible absorption at 560 nm and Y corresponds to an absorption at 460 nm.

appear to contain an interchangeable S_2N_3 unit.

In Section 3.3.2.3, $(R_2PN)(SN)_2$ was viewed as an "Internal salt" made up of a phosphonium cation interacting with an $S_2N_3^-$ anion. This eight-membered ring can be discussed in a similar fashion, consisting of an $H_2\overset{+}{P}=N=PH_2$ cation and the same $S_2N_3^-$ anion. The molecule contains 10π-electrons (see Section 1.3.5.1), eight are accommodated by the anion and two by the cation. Calculations have been carried out on these two fragments for comparison. The results of these calculations are all illustrated in Figure 3.7. The interaction between the π-type d orbitals (d_{xz}, d_{yz}) of a monoatomic cation and the π-MOs of an open chain $S_2N_3^-$ anion are shown in (a). The most prominent effect of this interaction is the lowering in energy of the HOMO ($2a_2$) and particularly the LUMO ($3b_1$) of $S_2N_3^-$, as discussed in Section 3.3.2.2. In a similar manner, the interaction of the π-MOs of $H_2P=N=PH_2$ with the π-MOs of $S_2N_3^-$ also leads to a stabilization of the HOMO ($2a_2$) and LUMO ($4b_1$) of $S_2N_3^-$ (b). By comparison with the transitions identified for the six-membered ring using a rigorous calculation (x), it seems reasonable to correlate the strong visible absorption band observed at 460 nm for 1,3-$(R_2PN)_2(SN)_2$, with a π^*(HOMO $2a_2$) $\rightarrow\pi^*$(LUMO $4b_1$) electronic transition (y). In the same context, the second absorption band observed for 1,3-$(Me_2PN)_2(SN)_2$ at 300 nm is tentatively assigned to a π ($3b_1$)$\rightarrow\pi^*$(LUMO $4b_1$) electronic transition.

1,5-$(R_2PN)_2(SN)_2$

The electronic structure of 1,5-$(R_2PN)_2(SN)_2$ is very different to that of its structural isomer. Although they are both formally 10π-electron systems, the positions of the sulfur centers in the 1,5-isomer allows

the possibility of a cross-ring S-S σ-bond. A planar conformation (45) requires that two electrons are contained in a π*-MO, whilst formation of the cross-ring bond (46) accommodates these electrons in a σ-MO with bonding character. Both types of structure have been observed for

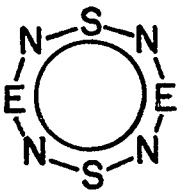

45

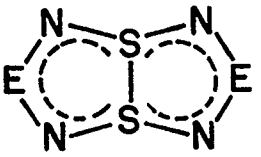

46

thiazenes of this nature. $S_4N_4^{2+}$ (E = S^+)[65,66] and 1,5-$(PhCN)_2(SN)_2$ (E = Ph-C)[171] have planar structures, and folded conformations are reported for 1,5-$Cl_2S_4N_4$ (E = Cl-S)[64], 1,5-$(Ph_3P{=}N)_2S_4N_4$ (E = Ph_3P=N-S)[87] and 1,5-$(Me_2NCN)_2(SN)_2$ (E = Me_2N-C)[171].

In $S_4N_4^{2+}$, the two extra electrons are contained in a π-type non-bonding orbital (43) and the high electron density is accommodated by

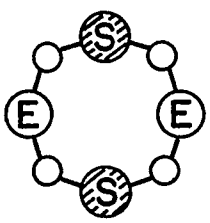

47

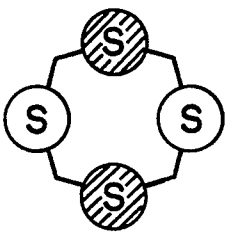

43

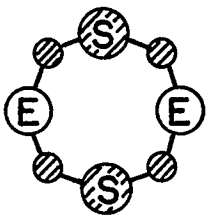

48

effective π-electron circumannular delocalization (see Section 1.3.5.5). However, an electropositive perturbation of the system in the 1,5-positions lowers the molecular symmetry and the π-HOMO (47) possesses a degree

of antibonding character with respect to the N-S-N region. In order to relieve the antibonding nature, the two electrons are placed into a cross-ring S-S σ-bond and the ring folds. Such is the case with 1,5-$(R_2PN)_2(SN)_2$ and many of the compounds listed. Presumably, an electronegative perturbation will enhance π-bonding in the S-N region (48) and the open structure will be more favorable. The atoms in the 1,5-positions may be removed from the molecular plane to relieve the antibonding interaction (see Section 3.3.3.1).

These simple conclusions are supported by calculations carried out by Oakley on these models[152]. Results indicated that the relative stability of 45 and 46 was dependent on the effective electronegativity of the atoms at the 1,5-positions. Electropositive groups at these positions are expected to destabilize the π-structure and enforce the folded conformation. Conversely, electronegative ligands will stabilize the π-structure and accommodate the antibonding character imposed by the two extra electrons. It would appear that carbon has the characteristics necessary for both structures (cf. 1,5-$(PhCN)_2(SN)_2$, planar and 1,5-$(Me_2NCN)_2(SN)_2$, folded), and the exocyclic ligands provide the determining factor.

CHAPTER 4

SOME CHEMICAL PROPERTIES OF THE UNSATURATED PHOSPHORUS, NITROGEN AND SULFUR HETEROCYCLES CONTAINING TWO COORDINATE SULFUR

4.1 INTRODUCTION

It was evident in Chapter 1 that the electron richness of the cyclothiazenes renders them far more reactive than the cyclophosphazenes. Much of the oxidative and reductive chemistry of the thiazenes results in rupture of the unsaturated ring framework. Conversely, there are few examples of ring cleavage reactions of the robust cyclophosphazenes. The three unsaturated P-N-S systems introduced in Chapter 2 exhibit a blend of spectroscopic and structural characteristics between those of the pure P-N and S-N heterocycles, from which they are derived. The low oxidation states of the sulfur centers in these compounds gives them the electron abundance observed in the pure thiazenes. Consequently, the HOMO and LUMO of the phosphathiazenes are sulfur-based and for this reason much of their chemistry is directed towards the sulfur centers. The chemistry of $(Ph_2PN)_2$-(NSCl) has already been extensively investigated and found to be very complex[149,154,181,182,183]. All of the studies indicate involvement of the monofunctional sulfur center. For example, reduction results in cleavage of a ring S-N bond, as discussed in Section 3.3.2.2.

This Chapter deals with a brief examination of some of the chemical properties of the P-N-S systems containing dicoordinate sulfur. Due to the thermal instability of many of the derivatives, the phenyl derivatives have been employed, in most cases, for chemical studies. Investigations

include: oxidation reactions, metathesis reactions of oxidation products, and cycloaddition reactions (see experimental Sections 5.4, 5.5, 5.6 and 5.7).

4.2 OXIDATION REACTIONS OF UNSATURATED P-N-S HETEROCYCLES

4.2.1 OXIDATIVE ADDITION AND CATION FORMATION

The reactions of the unsaturated P-N-S heterocycles with halogens and halogenating agents were employed to examine their oxidative chemistry. Various results are possible including, an oxidative addition to the inorganic ring, electron transfer from the ring to form a cation, and oxidation of the exocyclic ligands attached to the phosphorus centers. Due to the high electron density of the inorganic ring, the latter feature is not observed. All the P-N-S systems containing dicoordinate sulfur are readily oxidized by attack of the sulfur centers resulting in the formation of cationic or neutral products, depending on the heterocycle.

4.2.2 REACTIONS OF $(Ph_2PN)(SN)_2$ WITH HALOGENS

$(Ph_2PN)(SN)_2$ reacts instantly with many halogenating agents and the reactions can be easily monitored by the color changes. Chlorination (SO_2Cl_2) turns the deep purple solution to a yellow color, from which a yellow crystalline solid was isolated and characterized by chemical analysis and infrared spectroscopy. Bromination and iodination give orange and black solutions, respectively. However, the products could only be obtained as oils and useful spectroscopic or analytical data were unobtainable. The system appears to retain the heterocyclic framework of the starting material upon chlorination, with chlorine atoms bound

covalently to the two sulfur centers (49). Such a structure is consistent with related thiazyl halides[42]. As would be expected, the two electrons contained in a sulfur based antibonding π*-MO ($2a_2$) are readily released.

The infrared spectrum of 49 is very complex. However, the prominent P-N (1125 cm^{-1}) and S-N (899 cm^{-1}) stretches can be recognised. The P-N stretch is at lower wavelength than that of $(Ph_2PN)_3$ (1190 cm^{-1})[161]. Although the P-N bond appears weakened in comparison to the phosphazene, it is considerably stronger than in the reduced compound $(Ph_2PN)(SN)_2$ (1070 cm^{-1}). This is a result of a general strengthening of the π-structure of the ring upon removal of the antibonding character. The S-N stretch is significantly lower in energy than the same stretch in $S_3N_3Cl_3$ (1015-cm^{-1})[78], but the reason for this is not clear. The spectrum is too complex to confidently assign any S-Cl modes.

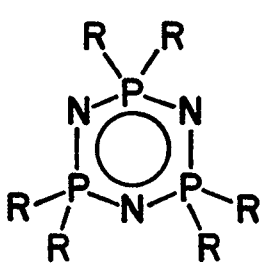

2

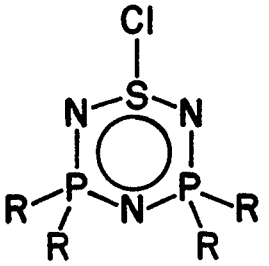

35

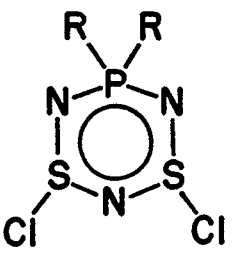

49

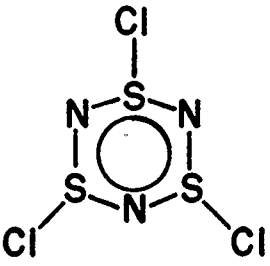

9

$(Ph_2PN)(NSCl)_2$ is the second cyclophosphathiazyl halide and is a member of the series of known compounds having the general formula $(R_2PN)_x(NSCl)_y$ (2, 35, 49, 9). The P-N-P section of 35 has been shown to retain many of the spectroscopic and structural characteristics of the pure phosphazene (2)[149]. Therefore, one may expect the Cl-S-N-S-Cl unit of 49 to resemble the same unit in $S_3N_3Cl_3$ (9)[22,78,79,81]. There are two geometrical possibilities for 49. The chlorine atoms may adopt either a cis (50)

or trans (51) configuration with respect to the PS_2N_3 ring. Unfortunately, it has not been possible to obtain a suitable crystal of 49 for a structural analysis, however, an X-ray structural determination of a

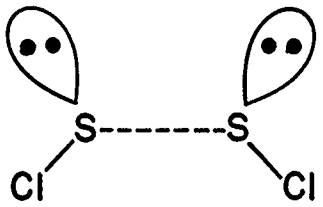

50

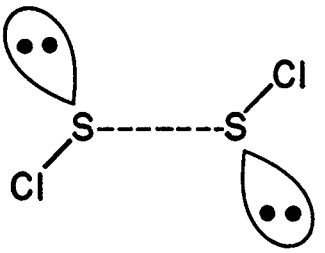

51

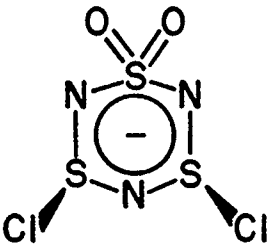

52

related anionic system, $(NSCl)_2(NSO_2)^-$ (52), has shown it to have the chlorine atoms in a cis configuration[189]. In view of the cis configuration in $S_3N_3Cl_3$[22,81] and 52, one may expect a similar structure for 49. Although the reason for the preference over the trans arrangement is not clear, simple electronic considerations allow a rationalization for the formation of the cis structure. As illustrated in Section 3.3.2.1, the sulfur based HOMO of $(R_2PN)(SN)_2$ is asymmetric with respect to the molecular C_2 axis. Assuming the oxidation mechanism involves a chloronium ion, attack must be directed to one of the two sulfur centers; the formation of a bridged intermediate (which would enforce a trans configuration) is forbidden. Therefore, secondary attack may occur on both sides of the P-N-S plane. Irrespective of the kinetic considerations, the cis configuration appears to be the thermodynamic sink for these molecules. There are no examples of six-membered trans thiazyl systems. In addition, $S_3N_3Cl_3$ is known to undergo a reversible monomerization in polar solvents to NSCl[190,191]. However, the cis form is the only observed isomer of $S_3N_3Cl_3$.

4.2.3 REACTIONS OF 1,3-$(Ph_2PN)_2(SN)_2$ WITH HALOGENS

CHLORINATION

In contrast to the oxidation properties of the six-membered ring $(Ph_2PN)(SN)_2$, the oxidation reactions of 1,3-$(Ph_2PN)_2(SN)_2$ are complex. Although all the halogens react instantaneously with 1,3-$(Ph_2PN)_2(SN)_2$, the isolable products vary considerably with the oxidant employed and the conditions of the experiment. The dichloride (53) could not be isolated from the chlorination reaction, instead, the yellow crystalline solid, obtained in high yield, was identified as $(Ph_2PN)_2(NSCl)$ (35) by infrared spectroscopy. The formation of this six-membered monochloride is independent of temperature, however, it can be explained as a decomposition

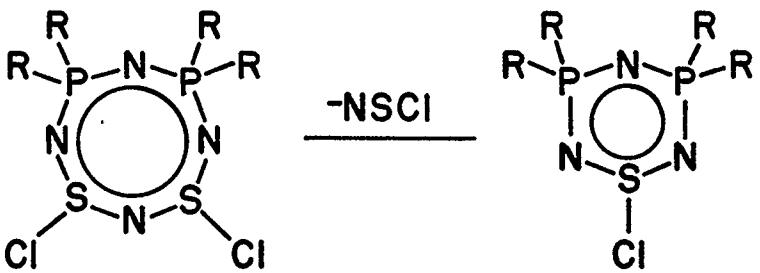

53 **35**

product of an unstable intermediate dichloride (53) via the release of an NSCl unit. The reason for the ring cleavage reaction is not clear, although, a similar process is exhibited by $S_4N_4Cl_4$ to form $S_3N_3Cl_3$[78,79].

BROMINATION AND IODINATION

Bromination proceeds rapidly to give a brown solution which fades to

an orange color. An orange crystalline compound was isolated from the solution, the nature of which could not be determined using spectroscopic methods and chemical analysis. Therefore X-ray diffraction techniques were employed and the species was found to be a twelve-membered cationic heterocycle, containing four phosphorus units, six nitrogen atoms and two sulfur atoms with two tribromide counter ions (54) (see Section 4.2.3.3). At higher temperatures 54 cannot be isolated, instead a monocationic six-membered $(Ph_2PN)_2(NS)^+$ is obtained (previously prepared from $(Ph_2PN)_2(NSCl)$)[180]. Continued heating results in the release of bromine from the tribromide anion to yield the bromide derivative of 35[180]; $S_4N_3^+Br_3^-$

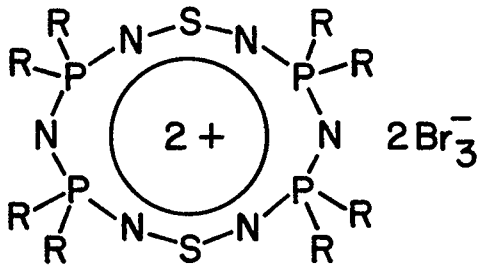

54

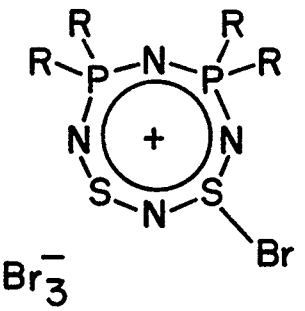

55

is formed as a by-product.

A black solution is produced upon addition of iodine to a solution of 1,3-$(Ph_2PN)_2(SN)_2$, from which a black crystalline material has been isolated. By comparison with the bromine reaction and from infrared spectroscopic data and chemical analysis, the solid was characterized as the triiodide salt of the twelve-membered dication (54).

In conjunction with the reaction of S_4N_4 with liquid Br_2 to give $S_4N_3^+Br_3^-$ (for which NSBr has been identified as an intermediate)[82,192,193], the formation of 54 can be rationalized using the unstable dihalide intermediate introduced in Section 4.2.3.1. Further bromination of a

dibromide allows the possibility of tribromide anion formation to leave a cationic ring (55). The elimination of NSBr from this cation (cf. 1,3-$(Ph_2PN)_2(NSCl)_2$) and dimerization accounts for the formation of both 54 and $S_4N_3^+Br_3^-$. A similar discussion can be used for the iodine reaction. The twelve-membered heterocycle is unstable with respect to the six-membered ring, the reason for which is not clear. The anomalous chlorination reaction can be understood with reference to the relative stabilities of the trihalide anions. In contrast to the well known tribromide and triiodide anions, the trichloride ion is very rare and poorly characterized. It is unstable with respect to an S-Cl bond and consequently, the cationic eight-membered species (55) is not formed by chlorination (see Section 4.2.3.1).

SPECTROSCOPIC AND STRUCTURAL CHARACTERIZATION OF $(Ph_2PN)_4(NS)_2^{2+}(Br_3^-)_2$

$(Ph_2PN)_4(NS)_2^{2+}$ is one of three known twelve-membered unsaturated P-N-S heterocycles. Two neutral systems with the same ring framework as 54 have been prepared from the diverse reactions of the $(Ph_2PN)_2(NSX)$ system. One has a cross-ring S-S σ-bond (56)[183] and the other has exocyclic dimethylamino groups attached covalently to the sulfur centers (57)[181]. These three systems exhibit the ring size flexibility of the cyclophosphazenes and the chemical diversity of the thiazenes, and show spectroscopic and structural characteristics of both. As with 56 and 57, the infrared spectra of the tribromide and triodide derivatives of 54 are very complex and it is difficult to identify specific bands. The single resonance observed in the ^{31}P NMR spectra of the tribromide

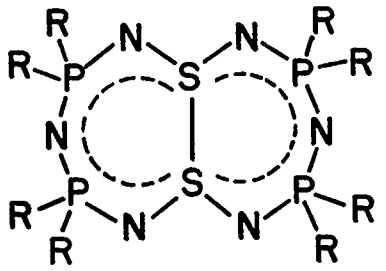

56

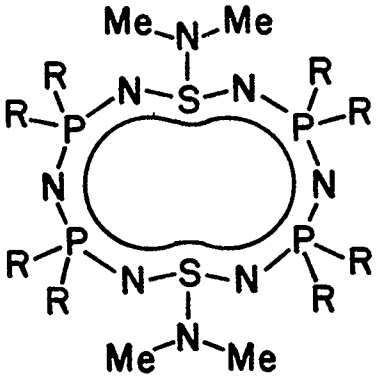

57

(12.0 ppm) and triodide (18.8 ppm) indicates four equivalent phosphorus centers. However the large chemical shift difference between the two salts suggests that the twelve-membered dication may not be present in solution.

The crystal and molecular structure of $(Ph_2PN)_4(NS)_2^{2+}(Br_3^-)$ was determined by X-ray crystallographic methods[†]. The crystal structure consists of discrete cationic and anionic units with no unusual intermolecular contacts. Selected bond lengths and angles for the structure are given in Table 4.1, and the atomic numbering scheme of the heterocycle and the α-carbon atoms of the phenyl groups is shown in the ORTEP drawing of the cation in Figure 4.1. A molecule of acetonitrile solvent was found in the crystal lattice, the bond lengths and angles of which are also given in Table 4.1.

The heterocycle is severely puckered, reminiscent of the distorted conformations observed for the larger cyclophosphazenes[38 40 41]. However, the presence of the sulfur centers results in some important differences. Although the two P-N-P units have structural characteristics

---

[†] The assistance of Dr. J. F. Richardson is gratefully acknowledged.

Table 4.1. Selected bond lengths (Å) and angles (Deg) for $(Ph_2PN)_4(NS)_2^{2+}(Br_3^-)_2.CH_3CN$

Atoms	Distance	Atoms	Angle
Br1-Br2	2.751(3)	Br1-Br2-Br3	178.6(1)
Br2-Br3	2.384(3)	Br4-Br5-Br6	176.5(1)
Br4-Br5	2.513(3)	S1-N1-P1	128.8(7)
Br5-Br6	2.543(3)	N1-P1-N2	113.7(5)
S1-N1	1.515(10)	N1-P1-C11	108.1(6)
N1-P1	1.663(10)	C11-P1-C21	107.5(7)
P1-N2	1.599(10)	N2-P1-C21	116.8(6)
N2-P2	1.556(10)	P1-N2-P2	140.0(7)
P2-N3	1.658(10)	N2-P2-C31	108.2(7)
N3-S2	1.516(10)	C31-P2-C41	108.7(7)
S2-N4	1.535(10)	N3-P2-C41	104.6(6)
N4-P3	1.649(10)	N2-P2-N3	115.9(6)
P3-N5	1.567(12)	P2-N3-S2	128.5(7)
N5-P4	1.589(12)	N3-S2-N4	112.2(6)
P4-N6	1.657(10)	S2-N4-P3	124.8(6)
N6-S1	1.521(10)	N4-P3-C51	101.8(7)
P1-C11	1.786(15)	C51-P3-C61	108.0(7)
P1-C21	1.774(15)	N5-P3-C61	109.2(7)
P2-C31	1.778(16)	N4-P3-N5	113.5(6)
P2-C41	1.784(14)	P3-N5-P4	134.3(7)
P3-C51	1.803(16)	N5-P4-C71	114.1(7)
P3-C61	1.721(15)	C71-P4-C81	108.6(8)
P4-C71	1.802(16)	N6-P4-C81	113.6(6)
P4-C81	1.769(16)	N5-P4-N6	111.6(6)
N7-C1	1.131(27)	P4-N6-S1	124.6(6)
C1-C2	1.423(30)	N6-S1-N1	111.8(6)
		C2-C1-N7	175.8(22)

See Appendix A4.3 for bond lengths and angles of phenyl groups.

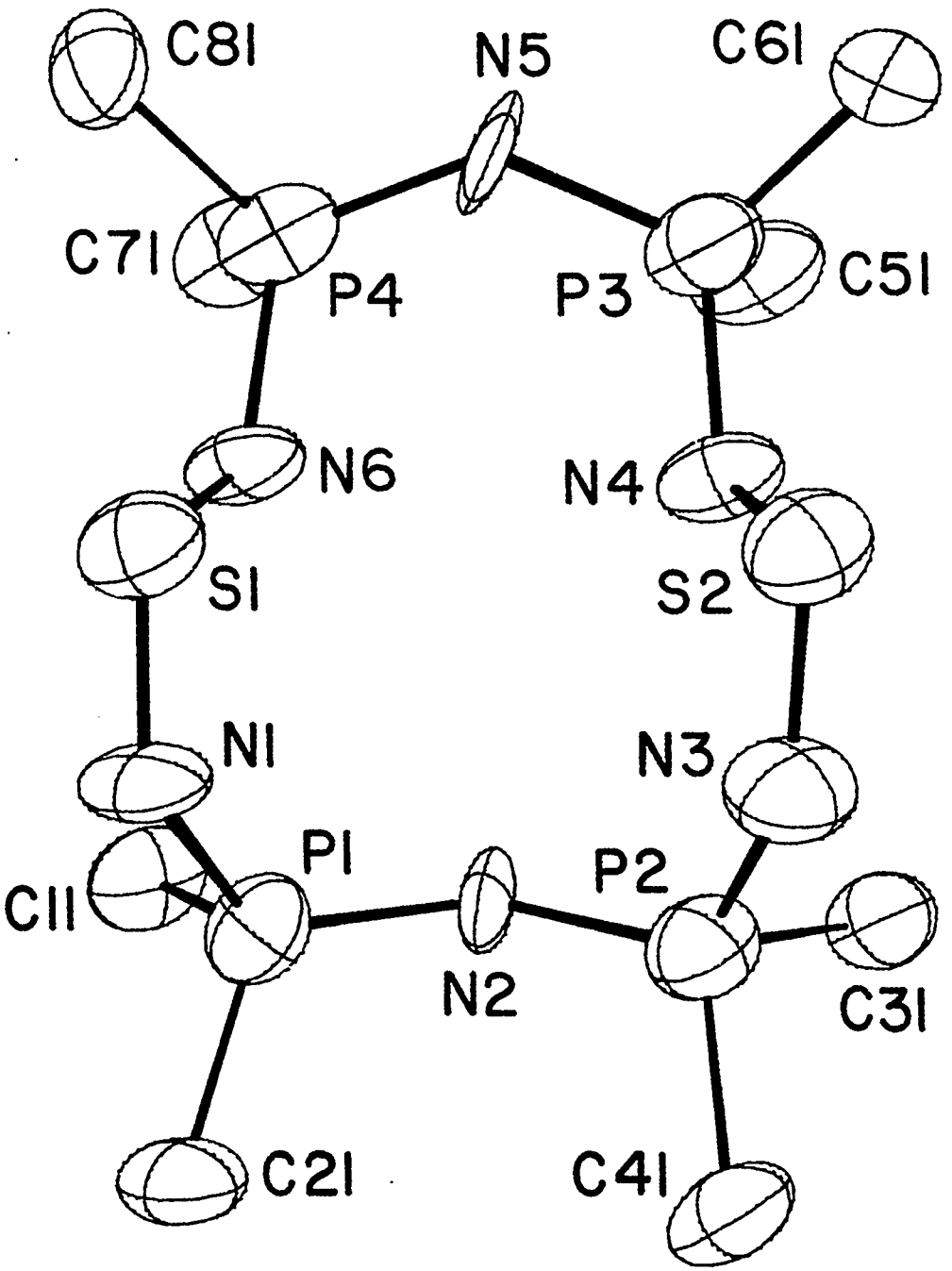

Figure 4.1 ORTEP view (50% probability ellipsoids) of $(Ph_2PN)_4(NS)_2^{2+}$ (phenyl groups represented by α-carbon atoms) showing the atomic numbering scheme.

which are very similar to those observed in phenylphosphazenes, the P-N bonds of the P-N-S units (average d(P-N(S)) = 1.657 Å) are significantly longer than the pure P-N bonds. In addition, the S-N bonds are shorter (average d(S-N) = 1.522 Å) than in most S-N heterocycles containing di-coordinate sulfur ($S_4N_4^{2+}$ average d(S-N) = 1.55 Å)[65,66]. Such features are comparable with the structural parameters observed in the six-membered $(R_2PN)_2(NSX)$ systems (see Section 3.3.2.2), but more pronounced. The phenyl groups have no unusual attributes. Although both tribromide ions are nearly linear, one is symmetric as observed in $(Me_3NH^+)_2\ Br^-Br_3^-$ and the other asymmetric as observed in $Cs^+Br_3^-$[194].

The basic structural features of the heterocycle can be more clearly examined in terms of the local geometries[195]. The possible geometries of a phosphazene unit are illustrated in Figure 4.2(a) with the terminology employed to describe conformational details of methylcyclophosphazenes. Unlike $(Me_2PN)_6$, which contains a mixture of GG, GT and CT geometries[196], all of the phosphorus centers in $(Ph_2PN)_4(NS)_2^{2+}$ have the more energetically favorable GG arrangement (The less restricted $(Me_2PN)_7$[197] and $(Me_2PN)_8$[198] adopt GG and GT configurations at phosphorus) facilitated by the CT geometry at sulfur. The dication has pseudo symmetry through N2 and N5, so that the opposite S-N bonds are eclipsed (E) (viewed down S-S vector), as illustrated in Figure 4.2 (b). Although the NSN units are also in a CT configuration in the reduced S-S bonded system (56), the CT arrangements are in opposite directions. Due to the close proximity of the NSN units enforced by the cross-ring S-S contact, the opposite nitrogen atoms are staggered (S) about the S-S bond. Two opposite phosphorus centers adopt a GG' conformation to accommodate the twisted structure[183].

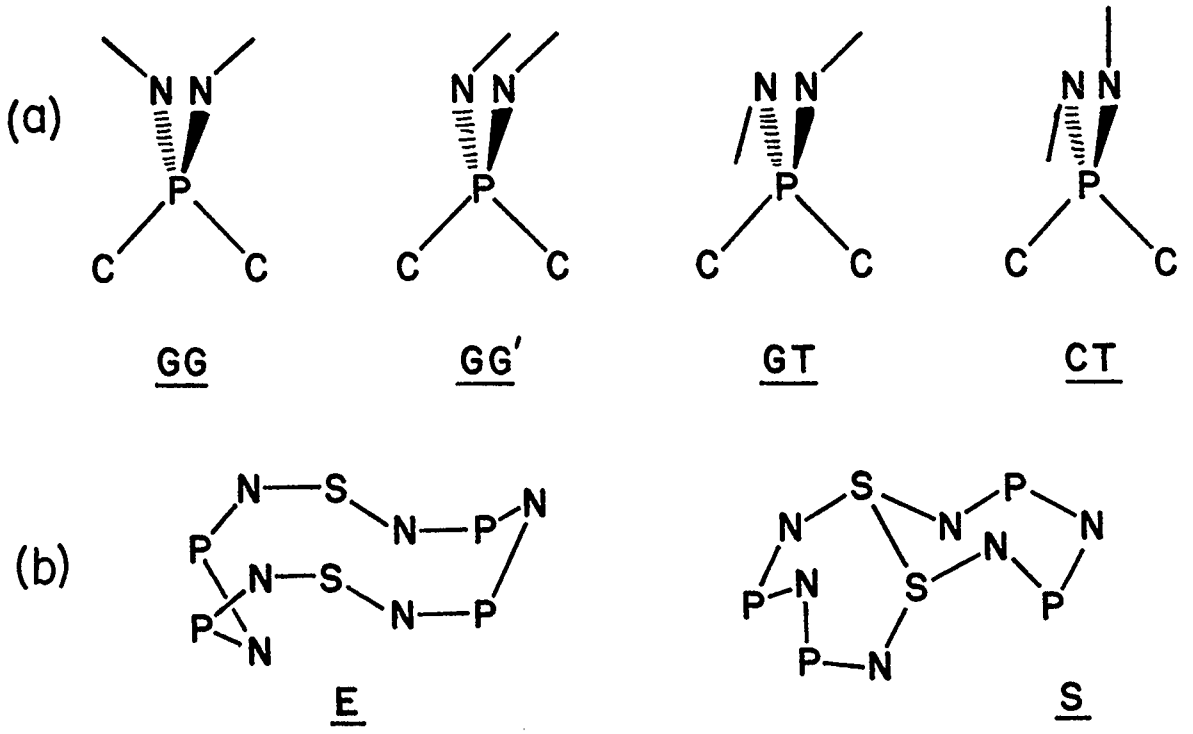

Figure 4.2 (a) Possible local geometries at phosphorus, G = gauche C = Cis T = trans. (b) Arrangements about the S-S vector, E = eclipsed, S = staggered.

4.2.4 REACTIONS OF 1,5-$(Ph_2PN)_2(SN)_2$ WITH HALOGENS

CHLORINATION AND BROMINATION

Reactions of 1,5-$(Ph_2PN)_2(SN)_2$ (17) with chlorinating agents and bromine are rapid and the crystalline products are easily obtained in high yield. Two electrons contained in the cross-ring S-S σ-bond of 17 are removed and a dihalide is formed in which the halogens are bound covalently to the sulfur centers (58). An analogous reaction with iodine is not observed, indicating that a relatively strong oxidant is required to remove the electrons from the bonding orbital (cf. $(Ph_2PN)(SN)_2$ and

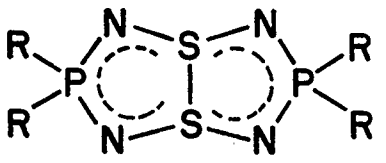

17

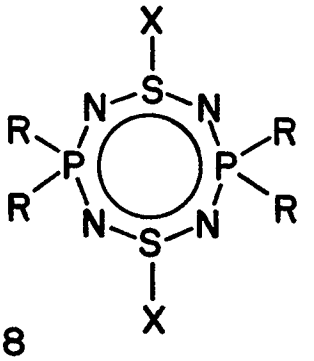

58

$1,3\text{-}(Ph_2PN)_2(SN)_2$. The smooth oxidative addition across the S-S bond is very different to the oxidation chemistry of the 1,3-isomer. While the chlorination reaction is reminiscent of the formation of $S_4N_4Cl_2$ from S_4N_4[62,63,64], the dibromide is the first example of a stable S-N heterocycle with a thiazyl bromide unit. The numerous studies of the bromination of S_4N_4 have shown it to be a complex reaction producing either polymers of the type $(NSBr_{0.4})_x$[199,200,201] (where bromine is present as Br_3^- and intercalated Br_2 molecules[202,203]) or the salt $S_4N_3^+$-Br_3^-[82], and in CS_2 a cationic carbon-bonded heterocycle, $(BrS)CS_2N_2^+$ (containing an exocyclic S-Br bond) is formed[204]. The thermal instability of sulfur-nitrogen heterocycles containing S-Br bonds can be attributed to the ease with which elimination of the monomeric NSBr unit occurs. Such a process requires cleavage of S-N bonds in cyclothiazenes. However, expulsion of NSBr from this P-N-S ring would involve breaking a relatively strong P-N bond.

The infrared spectra of the chloride and bromide derivatives of $1,5\text{-}(Ph_2PN)_2(NSX)_2$ are very similar, except for minor differences at lower energy, corresponding to S-X modes. The P-N stretches (1245 cm^{-1} X = Cl; 1240 cm^{-1}, X = Br) are shifted to high frequency in comparison to the reduced system, indicating a general stabilization caused by relief

of the angle strain imposed by the cross-ring contact in 17. The ^{31}P NMR spectrum of the dibromide shows a singlet at -7.34 ppm indicating equivalent phosphorus centers.

As discussed for the six-membered species $(Ph_2PN)(NSX)_2$ (see Section 4.2.2.) two structural possibilities are available for 1.5-$(Ph_2PN)_2(NSX)_2$ (58), with the halogen atoms in either cis or trans configurations with respect to the heterocycle. It is not possible to determine the actual configuration from the spectroscopic data, therefore an X-ray crystallographic study was carried out on the dibromide derivative†.

MOLECULAR STRUCTURE OF 1,5-$(Ph_2PN)_2(NSBr)_2$

The crystal structure consists of discrete molecular units with no unusual intermolecular contacts. Bond lengths and angles of the molecular structure are given in Table 4.2, and the atomic numbering scheme of the heterocycle and the α-carbon atoms is shown in the ORTEP drawing of the molecule in figure 4.3.

Cleavage of the cross-ring S-S bond allows the heterocycle to flatten (cf. 1,5-$(Ph_2PN)_2(SN)_2$ and 1,5-$(Me_2PN)_2(SN)_2$). The two phosphorus and four nitrogen atoms are planar to within 0.07 Å, and the two sulfur atoms are displaced on either side of this plane by 0.54 and 0.58 Å, respectively. The result is a chair conformation. The P-N bond lengths are slightly shorter than those of the reduced ring (1.623(3) and 1.620(3) Å) and are only slightly longer than those typically found in cyclophenylphosphazenes (≃ 1.59 Å). However, the S-N

† The assistance of Dr. J. F. Richardson is gratefully acknowledged.

Table 4.2 Bond lengths (Å) and angles (deg) for 1,5-$(Ph_2PN)_2(NSBr)_2$

Atoms	Distance	Atoms	Angle	Atoms	Angle
Br1-S1	2.454(7)	Br1-S1-N1	100.8(10)	C11-C12-C13	118.5(17)
Br2-S2	2.440(8)	Br1-S1-N4	105.3(7)	C12-C13-C14	122.0(17)
S1-N1	1.51(2)	S1-N1-P1	136.5(13)	C13-C14-C15	119.1(19)
N1-P1	1.61(2)	N1-P1-N2	118.0(11)	C14-C15-C16	114.9(20)
P1-N2	1.68(2)	N1-P1-C11	105.7(11)	C15-C16-C11	121.6(21)
N2-S2	1.47(2)	N1-P1-C21	106.8(12)	C16-C11-C12	121.4(19)
S2-N3	1.57(2)	C11-P1-C21	109.7(11)	C21-C22-C23	126.8(21)
N3-P2	1.65(2)	N2-P1-C11	105.5(10)	C22-C23-C24	118.0(18)
P2-N4	1.54(2)	N2-P1-C21	110.9(12)	C23-C24-C25	123.3(17)
N4-S1	1.57(2)	P1-N2-S2	144.5(16)	C24-C25-C26	120.1(17)
P1-C11	1.82(2)	Br2-S2-N2	104.5(8)	C25-C26-C21	113.5(21)
P1-C21	1.80(2)	Br2-S2-N3	105.2(9)	C26-C21-C22	116.2(22)
P2-C31	1.79(3)	N2-S2-N3	112.3(12)	C31-C32-C33	115.7(21)
P2-C41	1.73(3)	S2-N3-P2	132.2(12)	C32-C33-C34	115.1(20)
C11-C12	1.43(2)	N3-P2-N4	120.6(11)	C33-C34-C35	118.9(15)
C12-C13	1.35(3)	N3-P2-C31	102.5(12)	C34-C35-C36	115.2(22)
C13-C14	1.34(3)	N3-P2-C41	111.6(12)	C35-C36-C31	127.9(27)
C14-C15	1.59(3)	C31-P2-C41	106.7(12)	C36-C31-C32	124.4(23)
C15-C16	1.32(4)	N4-P2-C31	111.0(12)	C41-C42-C43	118.9(24)
C16-C11	1.37(3)	N4-P2-C41	103.8(11)	C42-C43-C44	123.8(24)
C21-C22	1.30(3)	P2-N4-S1	143.9(14)	C43-C44-C45	120.2(23)
C22-C23	1.37(2)	N4-S1-N1	115.7(12)	C44-C45-C46	119.8(16)
C23-C24	1.12(3)	P1-C11-C12	115.9(14)	C45-C46-C41	122.6(17)
C24-C25	1.39(2)	P1-C11-C16	119.9(16)	C46-C41-C42	112.1(23)
C25-C26	1.44(3)	P1-C21-C22	125.5(21)		
C26-C21	1.38(4)	P1-C21-C26	118.0(18)		
C31-C32	1.44(3)	P2-C31-C32	117.1(20)		
C32-C33	1.39(3)	P2-C31-C36	118.3(21)		
C33-C34	1.79(3)	P2-C41-C42	118.8(19)		
C34-C35	1.36(3)	P2-C41-C46	127.3(17)		
C35-C36	1.39(3)				
C36-C31	1.37(5)				
C41-C42	1.41(4)				
C42-C43	1.47(4)				
C43-C44	1.15(3)				
C44-C45	1.38(3)				
C45-C46	1.40(3)				
C46-C41	1.38(3)				

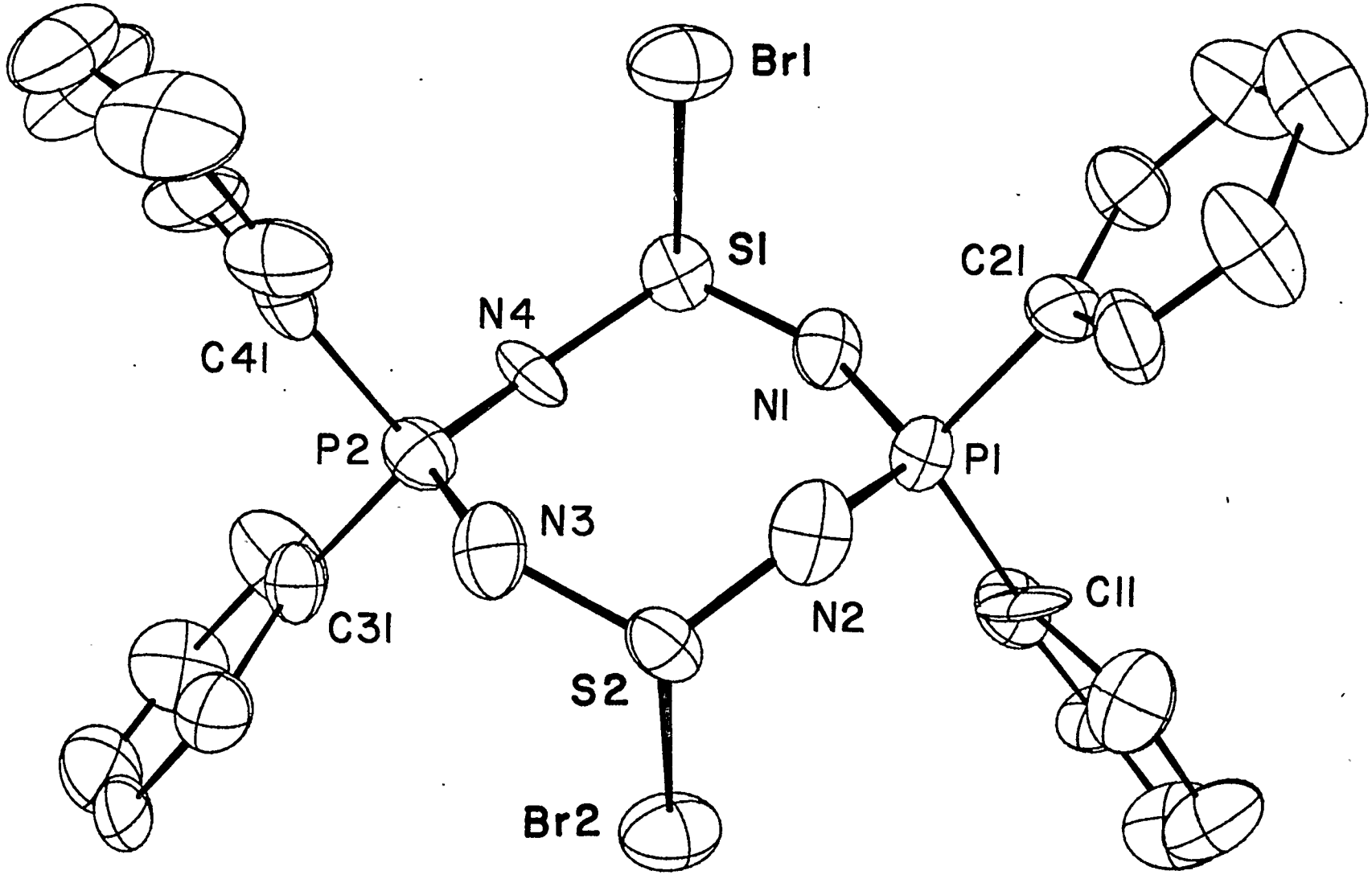

Figure 4.3 ORTEP view (50% probability ellipsoids) of 1,5-$(Ph_2PN)_2(NSBr)_2$ showing atomic numbering scheme.

bond lengths are considerably shorter than those of 17 (1.596(2) and 1.584(2) Å), indicating a localization of π-bonding in the N-S-N units. With reference to the six-membered $(R_2PN)_2(NSX)$ and twelve-membered $(R_2PN)_4(NS)_2^{2+}$ systems, the short S-N bond lengths in all of these structures may provide a rationalization for their thermodynamic stability over the systems possessing adjacent NSX or NS^+ moieties. Release of the cross-ring constriction results in larger endocyclic NP̂N and PN̂P angles than in 17, comparable to those in $(Ph_2PN)_4$ (NP̂N = 119.9(1), PN̂P = 127.9(2)°)[170].

The exocyclic bromine substituents adopt a trans configuration. There are few structurally characterized compounds containing S-Br bonds with which to compare the S-Br bond length values. However, the fact that these values are longer than the sum of the covalent radii of sulfur and bromine (2.28 Å)[205] and the bond length of the exocyclic S-Br unit in $(BrS)CS_2N_2^+$[204], suggests some ionic character. Indeed, the only other structurally characterized phosphathiazyl halides $(Ph_2PN)_2(NSX)$ show long S-X bonds (S-Cl = 2.357(2) Å[149], S-I = 2.713(3) Å[182]).

The trans addition of the halogen atoms to the P-N-S ring (59) is consistent with the related structure of $S_4N_4Cl_2$ (19)[64]. A folded structure is imposed on the latter by the remaining cross-ring S-S bond, which

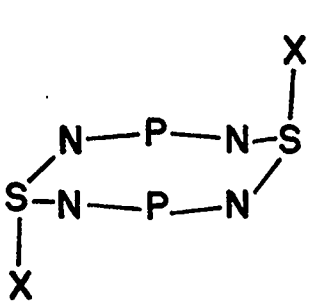

59

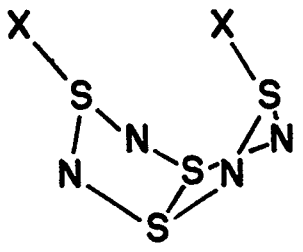

19

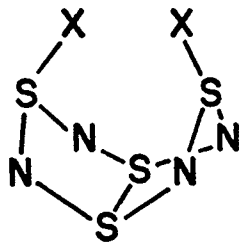

60

is absent in 59. The thermodynamic preference for the trans configuration in $S_4N_4Cl_2$ is clear on steric grounds (cf. 60). However, simple kinetic considerations also favor the trans structure for both compounds. Assuming a chloronium (or bromonium) ion is involved in the initial oxidative attack of the cross-ring bond, the symmetric nature of the S-S σ-MO facilitates the formation of a bridged intermediate. Consequently, secondary attack of the chloride ion would be restricted to the other side of the ring, hence the trans addition.

4.3 METATHESIS REACTIONS OF P-N-S CHLORIDES: FORMATION AND DECOMPOSITION OF $R_2PS_3N_5$

4.3.1 INTRODUCTION

The chemical reactivity of S-Cl bonds provides important synthetic pathways to various S-N compounds from simple thiazyl chlorides. A number of metathetical reactions have been employed to prepare new systems without disrupting the heterocyclic framework of the starting thiazyl compound. $Me_3SiNSNSiMe_3$ is a common metathetical reagent in S-N chemistry. Although it has been found to undergo a number of interesting reactions, the reactions with $S_3N_3Cl_3$ and $S_4N_4Cl_2$ to produce $S_4N_5^+$(61)[126] (cf. $S_4N_5^-$) and S_5N_6 (7)[19], respectively, demonstrate its synthetic use in cleanly adding an N_2S unit across two S-Cl centers. The driving force of these reactions is the formation of Me_3SiCl. On the basis of these reactions, the same bifunctionality of $(Ph_2PN)(NSCl)_2$ and 1,5-$(Ph_2PN)_2(NSCl)_2$ offers the possibility for the preparation of bicyclic and cage P-N-S systems.

4.3.2 PREPARATION OF $R_2PS_3N_5$

$(R_2PN)(NSCl)_2$ (R = Me, Ph) reacts rapidly with $Me_3SiNSNSiMe_3$ to give a brown crystalline solid in high yield. The compound was characterized as a bicyclic system, $R_2PS_3N_5$ (62), from spectroscopic data and chemical analysis and by comparison with the previously reported fluoro derivative[206]. $F_2PS_3N_5$ was isolated from the complex reaction between PF_5 and $Me_3SiNSNSiMe_3$ in ether. An X-ray structural analysis of the yellow crystalline solid confirmed the bicyclic structure[207], showing an N_2S unit attached to one side of a six-membered ring at the sulfur centers to give a cage-like conformation. The most outstanding feature of the structure is the unusually long S-N bond lengths (1.69 Å) connecting the

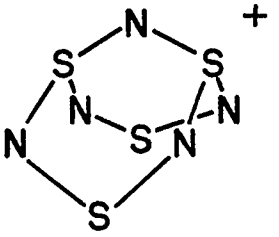

61

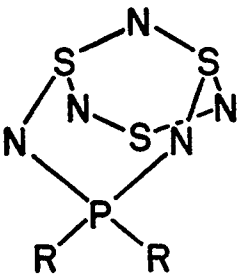

62

N_2S unit to the P-N-S ring. This suggests some instability within the molecule, the reason for which is unclear.

The bicyclic phosphathiazene is isoelectronic with $S_4N_5^+$[126], formally an S_4N_4 structure with one of the cross-ring S-S bonds bridged by a nitrogen atom and one of the opposite sulfur centers replaced by an R_2P unit. Consequently, like $S_4N_5^+$, the molecule has no cross-ring interactions and should not be considered a cage.

4.3.3 THERMAL DEGRADATION OF $R_2PS_3N_5$: PREPARATION OF $(F_2PN)(SN)_2$

Like many unsaturated S-N compounds (see Section 1.3.4), these bicyclic species have a low kinetic barrier to decomposition. In solution the slow decomposition of $Me_2PS_3N_5$ and $Ph_2PS_3N_5$ is evident from the color change to deep purple. All the reactions were monitored using ^{31}P NMR spectroscopy. During a controlled thermolysis, spectra were obtained for samples of the reaction mixture at regular intervals. The results for the methyl derivative are shown in Figure 4.4. The signal in the initial spectrum (0 minutes) corresponds to the bicyclic species. As expected, its intensity decreases during the reaction in favor of one new signal, corresponding to the six-membered ring $(Me_2PN)(SN)_2$. After 90 minutes, the latter is the only signal in the spectrum indicating a quantitative decomposition process involving release of an N_2S unit. The crystalline $(Ph_2PN)(SN)_2$ was recovered in high yield from the thermal decomposition of $Ph_2PS_3N_5$.

Although an N_2S unit has been postulated in the decomposition mechanisms of a number of S-N systems[96,97,98,99], the species has never been isolated (see Section 1.3.4). An *ab initio* study of the hypothetical species has indicated a very low energy barrier (9-15 kcal mol^{-1}) between N_2S and its constituent elements[208], explaining the difficulty in detection. An anion radical, $N_2S^{\bullet-}$, was reported as a thermolysis product of $F_2PS_3N_5$[206] on the basis of an e.s.r. spectrum. The blue color of the reaction mixture was assigned to a six-membered radical cation, $(F_2PN)(SN)_2^{\bullet+}$. However, the thermolysis was reinvestigated in this work and the blue product was isolated and characterized as the neutral species, $(F_2PN)(SN)_2$ (see Section 2.3.2).

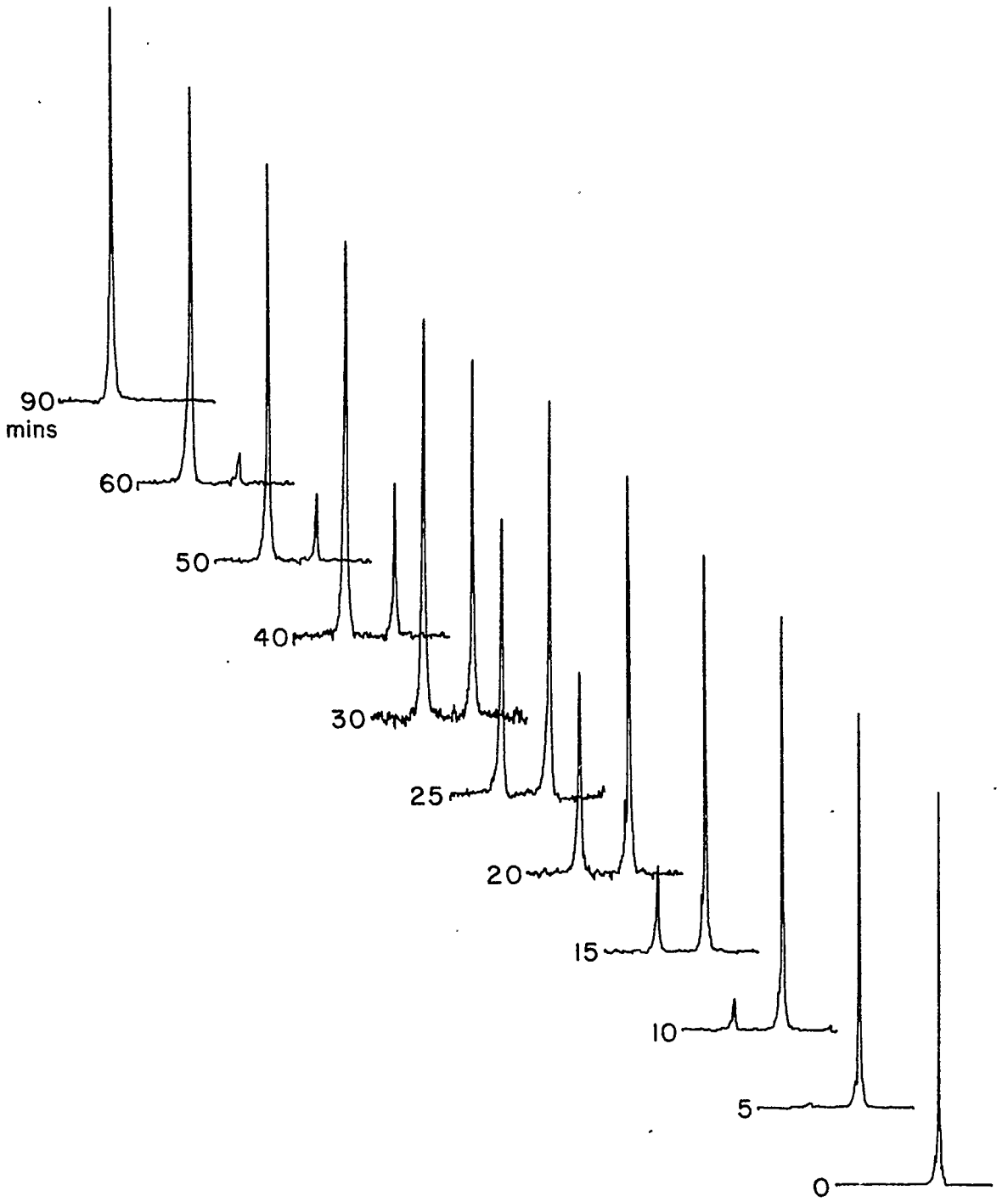

Figure 4.4 ^{31}P NMR study of the thermal decomposition of $Me_2PS_3N_5$ in toluene at 98-100°C. Right signal corresponds to $Me_2PS_3N_5$ and left signal to $(Me_2PN)(SN)_2$.

The initial oxidative addition to the $(R_2PN)(SN)_2$ heterocycle is indirectly reversible. Metathetical addition of an N_2S unit followed by thermal release of this unit regenerates the six-membered ring (Figure 4.5). The latter is formally a reductive elimination from the ring, resulting in repopulation of the antibonding π^*-MO. The reversibility of the oxidation demonstrates the relatively low energy of the π-system, a function of the high electronegativity of sulfur and nitrogen and the general stabilization of the S-N based orbitals by interaction with the phosphorus center (see Section 3.3.2.3).

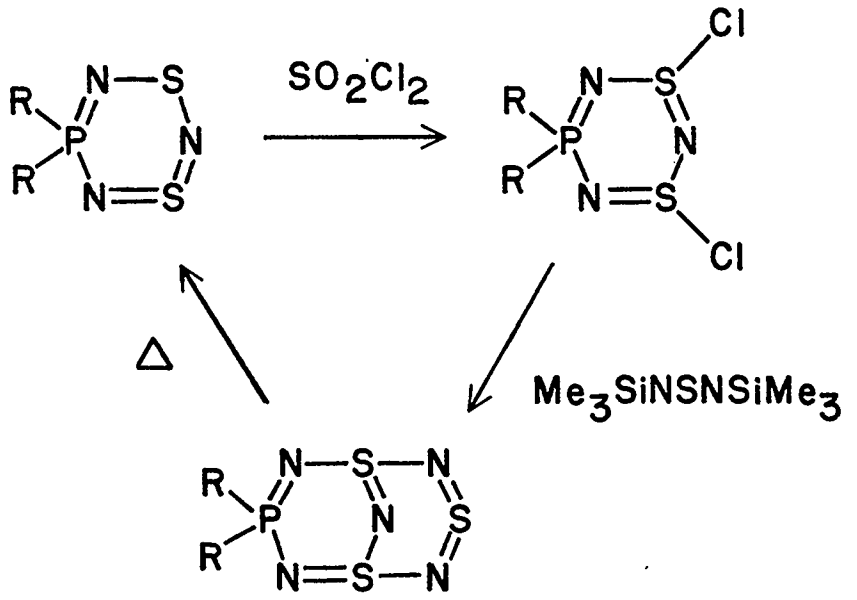

Figure 4.5 Reversible oxidative addition and reductive elimination to $(R_2PN)(SN)_2$.

4.3.4 PREPARATION OF $1,5\text{-}(Ph_2PN)_2(NS)_2N_2S$

$1,5\text{-}(Ph_2PN)_2(NSCl)_2$ reacts with $Me_3SiNSNSiMe_3$ to give a red crystalline solid. The thermally unstable product was characterized, by infrared spectroscopy and chemical analysis, as a metathesis product, $1,5\text{-}(Ph_2PN)_2$

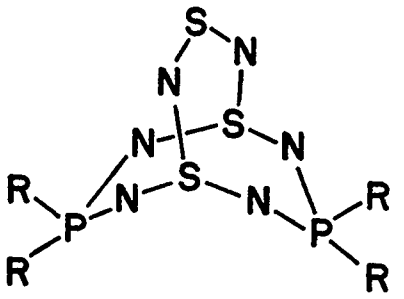

63

$(NS)_2N_2S$. Assuming the reaction is analogous to the formation of S_5N_6 from $S_4N_4Cl_2$[19], a bicyclic structure is predicted in which an N_2S unit bridges the opposite sulfur centers of the eight-membered ring (63). Such a compound is isoelectronic with the as yet unknown $S_5N_6^{2+}$. In order to confirm the structure of $1,5\text{-}(Ph_2PN)_2(NS)_2N_2S$ an X-ray diffraction study will be attempted.

4.4 CYCLOADDITION REACTIONS OF UNSATURATED P-N-S HETEROCYCLES

4.4.1 INTRODUCTION

The majority of the chemistry of unsaturated S-N heterocycles involves oxidation or reduction of the system resulting in ring cleavage. However, S_4N_4 has been found to react with a variety of unsaturated organic systems, without disruption of the ring, to form adducts. Becke-Goehring and Schläfer reported S_4N_4 adducts with cyclopentadiene, norbornadiene and cycloheptadiene, which they suggested were analogous to the Diels-Alder products, the thiazene acting as a diene[209]. More recent studies have shown that the variable oxidation states of sulfur allow the formation of slightly different products than those observed in the common organic cyclization reaction. An X-ray structural determination of the S_4N_4. bis (norbornadiene) adduct (64) has shown that the carbon units are bound at the opposite ends of a relatively planar eight-membered S_4N_4 heterocycle, by connection to the sulfur centers only[210]. Therefore, the cyclization

reaction with the S-N system results in the formation of five-membered C_2S_2N rings, in contrast to the six-membered rings commonly formed between an organic diene and dienophile. Although S_4N_2 also reacts with many olefins, the products are not straightforward adducts[211,212].

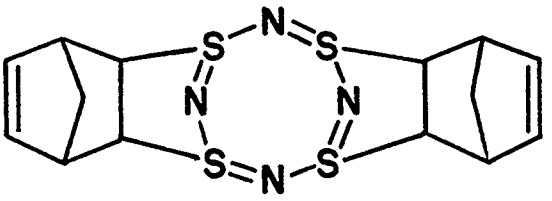

64

4.4.2 PREPARATION OF NORBORNADIENE ADDUCTS OF UNSATURATED P-N-S HETEROCYCLES

$(R_2PN)(SN)_2$ and 1,3-$(R_2PN)_2(SN)_2$ both undergo rapid cycloaddition reactions with norbornadiene to produce 1:1 adducts[151] 65 and 66, respectively. In contrast, the 1,5-isomer of the eight-membered ring does not

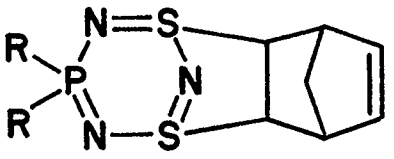

65

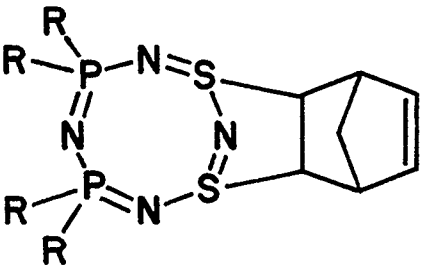

66

react with norbornadiene. The cycloadditions can be visually monitored by the loss of color and the solution produces a white precipitate in Et_2O. However, when the adducts are dissolved in methylene chloride or acetonitrile, the characteristic intense colors of the six-membered rings are regenerated indicating that the additions are reversible. The color

can be removed by addition of excess norbornadiene to the solution. The ease of dissociation of the adducts is also observed in the mass spectra, which show no parent ion. Instead, the fragmentation patterns resemble a superposition of those found for the free olefin and heterocycle. Nevertheless, the norbornadiene adducts are all stable in the solid state. Ease of formation and recrystallization of the adducts allowed analytical characterization of the unstable phosphathiazenes.

4.4.3 MOLECULAR STRUCTURE OF P-N-S NORBORNADIENE ADDUCTS

The ^{1}H and ^{13}C NMR spectra of the norbornadiene adducts unambiguously establish the positions of the addition. In all cases, one olefinic bond of the norbornadiene molecule is bound across the two sulfur centers, 3,5-positions in $(R_2PN)(SN)_2$ and 5,7-positions in 1,3-$(R_2PN)_2(SN)_2$. The ^{13}C NMR spectrum of $(Me_2PN)(NS)_2.C_7H_8$ is shown in Figure 4.6, a representative of all of the ^{1}H and ^{13}C NMR spectra of these species. The mirror symmetry of the molecule is illustrated by the chemical equivalence of the 2 and 3, 5 and 6 and 1 and 4 positions in the norbornene residue. This can only be attained by S, S rather than S, N or N, N addition of the olefin to the heterocycle. In addition, the inequivalence of the two

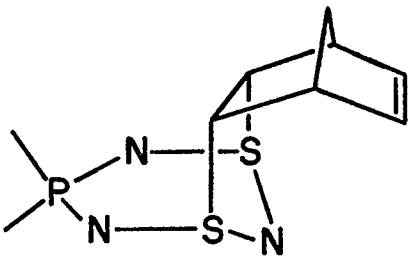

endo

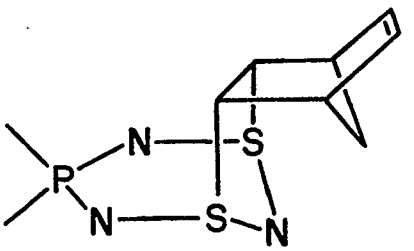

exo

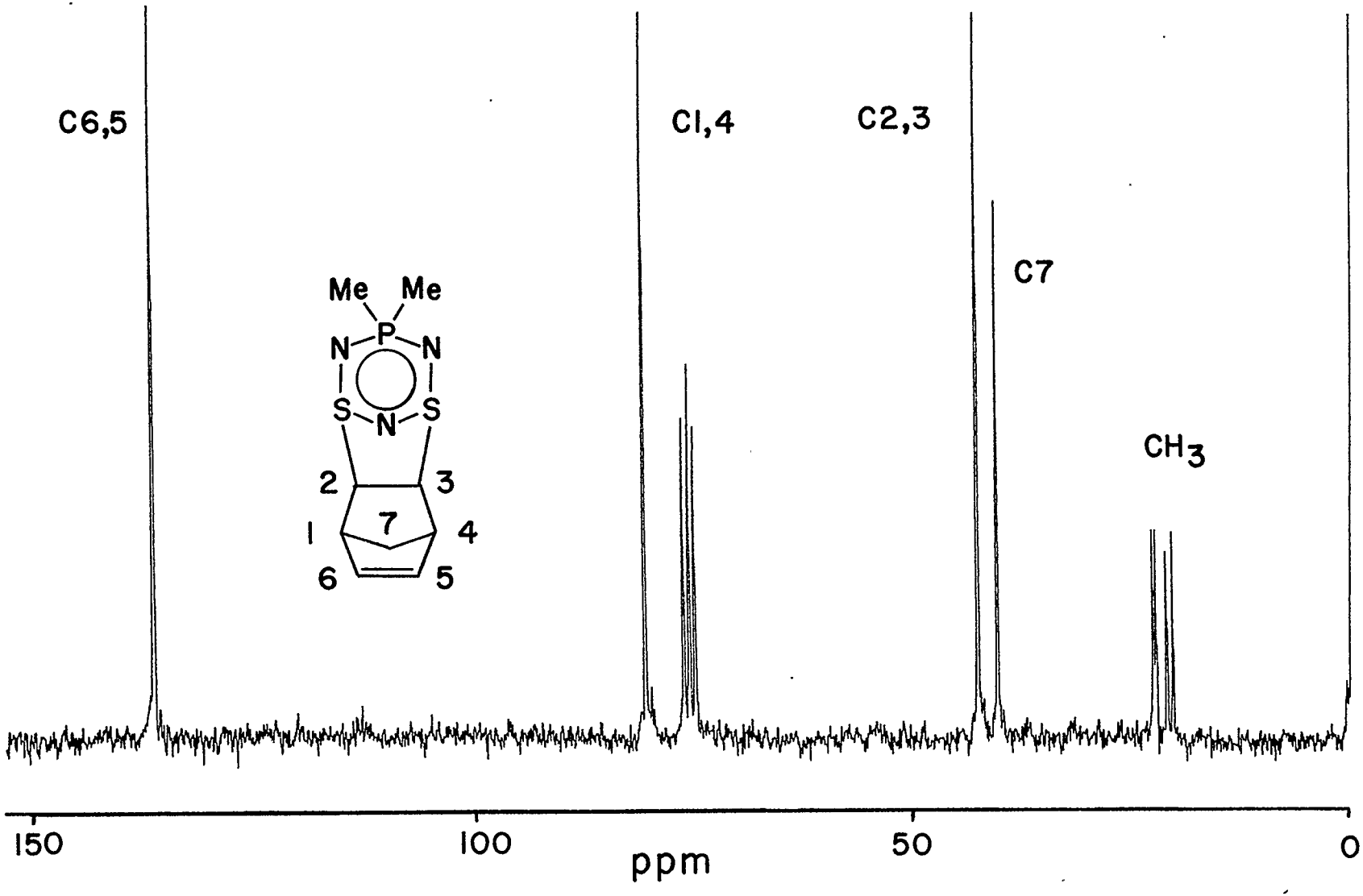

Figure 4.6 ^{13}C NMR spectrum of $(Me_2PN)(NS)_2.C_7H_8$.

methyl groups attached to the phosphorus center indicates the symmetrical addition of the olefin to one side of the heterocycle. As well as being regiospecific, the addition appears to be stereospecific, there is no evidence for more than one stereoisomer in solution or in the solid state. Many of the possible conformations for the addition can be rejected on steric grounds. However, X-ray crystallography was required to assign the endo or exo structure†.

A schematic representation of the molecular structure of $(Ph_2PN)(NS)_2 \cdot C_7H_8$ is shown in Figure 4.7. The structure confirms the addition of norbornadiene to the P-N-S ring in a 3,5-fashion across the two sulfur atoms. Moreover, it establishes the exo stereochemistry of the addition.

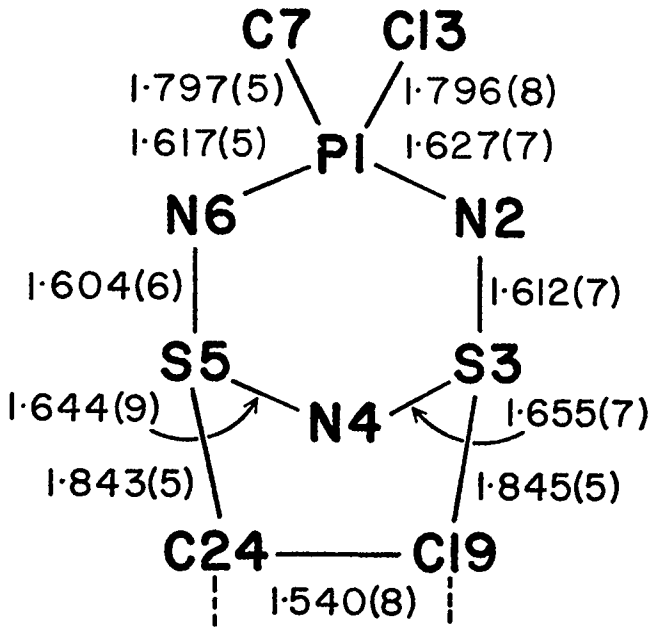

Atoms	Angle
N2-P1-C7	107.4(3)
N6-P1-C7	109.2(3)
N2-P1-C13	108.7(3)
N6-P1-C13	108.8(3)
C7-P1-C13	104.6(3)
N6-P1-N2	117.4(3)
P1-N2-S3	116.8(4)
N2-S3-N4	112.2(3)
S3-N4-S5	106.4(4)
N4-S5-N6	111.0(3)
S5-N6-P1	119.4(4)

Figure 4.7 Pertinent bond lengths (Å) and angles (Deg) of $(Ph_2PN)(NS)_2 \cdot C_7H_8$.

† An X-ray crystallographic study was performed by Dr. P. N. Swepston, Mr. M. C. Noble and Dr. A. W. Cordes.[151]

The adduct exhibits the expected conformational changes in comparison to the free heterocycle. The N4 atom is now displaced from the plane of the central N_2S_2 unit (which is planar to within 0.01 Å) by 0.817(6) Å, producing a dihedral angle of 55.8(4)°. The phosphorus atom is rotated towards the C_7H_8 group rather than away from it and is displaced by 0.195(2) Å away from the central N_2S_2 plane, producing a dihedral angle of 13.4(4)° (cf. 19.8(2)° in the free heterocycle). Thus the $(PN)(SN)_2$ ring adopts a somewhat flattened chair conformation. There is little change in the geometry at phosphorus, but the sulfur centers are now close to tetrahedral (cf. average NŜN in free ring of 116.6(2)°). The lengthening of all the S-N bonds can be attributed to the rupture of the π-system. The S-C distance is similar to that found in $S_4N_4.2C_7H_8$ (62) (1.851(5) Å)[210].

4.4.4. SYMMETRY ASPECTS OF THE FORMATION OF NORBORNADIENE ADDUCTS OF UNSATURATED P-N-S HETEROCYCLES

It is possible to rationalize the formation of the olefinic adducts of $(R_2PN)(SN)_2$ and 1,3-$(R_2PN)_2(SN)_2$ by reference to the electronic structures of these heterocycles. It was evident in Chapter 3 that, although the conjugation between the S-N π-structure and the phosphorus π-type orbitals is important in these molecules, the ordering and constitution of the π-MOs of a free $S_2N_3^-$ fragment are essentially unchanged by the interaction with the phosphorus orbitals. Indeed, the six and eight-membered system were both treated as internal salts containing an $S_2N_3^-$ unit (see Section 3.3.3.2). Because the cycloaddition reactions have been found to occur at the sulfur centers, for symmetry purposes both

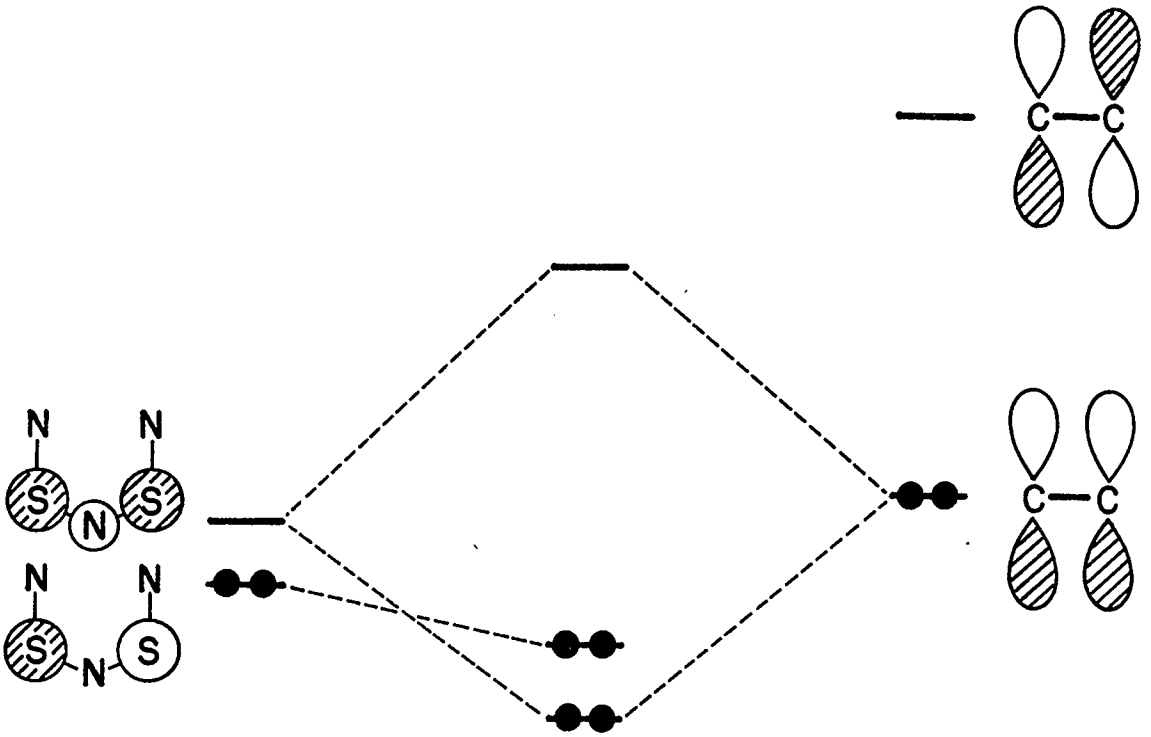

Figure 4.8 Symmetry correlation diagram for the π-HOMO and LUMO of $S_2N_3^-$ interacting with the HOMO and LUMO of an electron-rich olefin.

systems can be considered in terms of an $S_2N_3^-$ unit with 8π-electrons. Oakley has shown that a concerted reaction between the olefin and the sulfur centers of the heterocycle can then be regarded as a symmetry allowed ($8_s + 2_s$) cycloaddition. Figure 4.8 illustrates the orbital symmetry correlation diagram for the process. The preference for S, S over N, N addition is obvious in terms of the eigenvector coefficients of the HOMO and LUMO[213]. As discussed in Chapter 3, both orbitals are primarily sulfur-based, so that efficient overlap in the transition state is best achieved via addition at the sulfur as opposed to nitrogen. The stereospecificity of the reaction has no ready explanation on symmetry grounds.

More recently Oakley has found a similar reaction between norborna-

diene and $Ph_3P{=}N{-}S_3N_3$, which can also be treated in the same fashion[214]. In the report he also explains how the high energy of the olefinic HOMO and the low energy of the S-N LUMO results in an orbital interaction which is opposite to the common organic cycloaddition, involving a donation from the diene to the olefinic π^*-orbital. In order that the S-N cycloadditions are kinetically favorable, electron-rich olefins must be employed (cyclohexene does not react with $(R_2PN)(SN)_2$) and the LUMO of the S-N heterocycle must be low in energy, so that an effective interaction can take place.

CHAPTER 5

EXPERIMENTAL PROCEDURES AND SPECTROSCOPIC AND STRUCTURAL CHARACTERIZATION

5.1 GENERAL PROCEDURES

5.1.1 REAGENTS

All the solvents employed for reactions and recrystallizations were of reagent grade and most were dried before use. Toluene, pentane and heptane were set to reflux overnight with sodium and freshly distilled before use. Acetonitrile was set to reflux over calcium hydride and then phosphorus pentoxide, and was freshly distilled from CaH_2. Methylene chloride was distilled from phosphorus pentoxide and diethyl ether (Malinckrodt) from lithium aluminium hydride, which was also used as received in certain cases. All solvent distillations and all reactions were carried out under an atmosphere of nitrogen (99.98% purity passed through Ridox and silica gel).

S_4N_4 was prepared by the literature method[215] and recrystallized twice from hot toluene. Tetramethyldiphosphine was prepared by reduction of tetramethyldiphosphine disulfide (Alfa) with iron powder (Ventron), which were both used as received. In contrast to the reported procedure[216], we discovered that an excess of iron produced a mixture of trimethylphosphine and $Me_2P\text{-}PMe_2$. When a stoichiometric quantity of iron was used, the $Me_2P\text{-}PMe_2$ obtained was not contaminated. Tetraphenyldiphosphine[217], diphenylphosphine[218], bis-(trimethylsilyl)sulfur diimide[219], dimethylphosphorane trichloride[220] and diphenylphosphorane trichloride[220] were all

prepared by the literature methods. Chlorodiphenylphosphine (Alfa), triphenylphosphite (Aldrich), iodine (Shawinigan), norbornadiene (Aldrich), bromine (Fisher) and phosphorus pentafluoride (Penwalt) were commercial products and were used as received. Sulfuryl chloride (Aldrich) was freshly distilled prior to use.

5.1.2 INSTRUMENTATION

Infrared spectra (4000 - 250 cm^{-1}) were recorded as Nujol mulls (CsI windows) on a Perkin-Elmer 467 grating spectrophotometer. UV-visible spectra were obtained using a Cary 15 or a Unicam SP1800 spectrophotometer. ^{1}H, ^{13}C, ^{15}N and ^{31}P NMR spectra were recorded with a Varian XL-200 spectrometer. Raman spectra were measured on samples in glass capillaries with a Jarrel-Ash model 25-100 double grating spectrometer equipped with a photon counting detection system, using a coherent radiation Dye Laser pumped by a CR-4 argon ion laser. Mass spectra were recorded on a Varian CH5 instrument operating at 70 eV. X-ray diffraction data were collected on an Enraf Nonius CAD4F automated diffractometer fitted with a low temperature attachment. Chemical analyses were performed by the Analytical services of the Department of Chemistry, University of Calgary, and by M.H.W. Laboratories, Phoenix, Arizona.

5.1.3. X-RAY DATA COLLECTION

The experimental conditions of each of the five X-ray data collections differ considerably, however, the general procedures were constant. Unless otherwise stated the procedure described below was used for all the crystallographic experiments.

The crystal was mounted in an arbitrary orientation on the diffractometer. After optically centering the crystal, a polaroid photograph was obtained (X=0, rotation about ϕ). The horizontal and vertical coordinates of 25 of the reflections observed on the photograph were entered into the Enraf-Nonius centering program PHOTO. The 25 reflections were then accurately centered by the program SETANG and these data were used with the program INDEX to calculate the initial cell constants and orientation matrix. The program TRANS was then used to transform the triclinic cell parameters into those of the correct higher symmetry cell. The crystal was then accurately aligned using the program ALIGN. The 25 reflections were then recentered using SETANG and the data collection cell parameters were obtained by the least-squares program LS. In cases where the diffraction data was collected at low temperature (-100(5)^{o}C), after cooling alignment and centering procedures were repeated. Data were collected using the program DATCOL. Final cell parameters were obtained with 25 accurately centered, high angle reflections using the constrained least-squares program CELDIM. Intensities were measured using the ω-2θ scan mode, with the first and last 16 steps of a 96 step scan considered to be background. The intensity was calculated as I=(P-2(B1+B2))Q, where P is the sum of the central 64 steps, Q is the scan rate and B1 and B2 are the backgrounds. The standard deviation of the intensity σ(I)=(P+4(B1+B2))1/2Q.

5.1.4 SOLUTION AND REFINEMENT

Data were processed using the X-Ray 76 package of programs[222] and all the solutions were obtained using MULTAN 78[223]. The data were corrected for background, Lorentz and polarization effects and E values were calcu-

lated using a K curve[223]. Atomic scattering factors were those of Cromer and Waber[224]. Real and anomalous dispersion corrections were applied to all non-hydrogen atoms[225]. Agreement factors are of the form $R = \Sigma(||F_o|-|F_c||)/\Sigma|F_o|$ and $R_w = (\Sigma w(|F_o|-|F_c|)^2/\Sigma wF_o^2)^{1/2}$. The crystals were measured and the boundary faces identified manually under a microscope.

5.2 PREPARATION OF $(R_2PN)(SN)_2$, 1,3-$(R_2PN)_2(SN)_2$ AND 1,5-$(R_2PN)_2(SN)_2$ COMPOUNDS

5.2.1 REACTION OF Ph_2P-PPh_2 WITH S_4N_4

S_4N_4 (1.32 g, 7.2 mmol) was added to a solution of Ph_2P-PPh_2 (2.65 g, 7.2 mmol) in 50 ml of toluene and the mixture was stirred and heated to reflux. After 16 hours the mixture was cooled to room temperature and reduced in volume to about 20 ml by removal of the solvent *in vacuo*. The solution was then filtered, to remove any precipitated $(Ph_2PS)_2$, and eluted down a 30 x 500 mm Bio-Beads S-X8 chromatography column. Five fractions were collected, distinguished by their colors; pink, yellow, orange, purple and yellow, respectively. The ^{31}P NMR spectrum of the first fraction showed it to consist of a complex mixture of phosphorus-containing compounds, but no pure compounds could be isolated. Fractional crystallization of the next three fractions from warm acetonitrile resulted in isolation of $(Ph_2PN)_3$ and $(Ph_2PN)_4$ (0.15 g, combined weight) from fraction two, 1,5-$(Ph_2PN)_2(SN)_2$, d.p 210-5°C (0.07 g, 0.15 mmol, 2% based on nitrogen), 1,3-$(Ph_2PN)_2(SN)_2$, m.p 135-6°C (0.28 g, 0.60 mmol, 8% based on nitrogen) and $(Ph_2PS)_2$ from fraction three and $(Ph_2PN)(SN)_2$, m.p 93-4°C (0.35 g, 1.2 mmol, 14% based on nitrogen), $(Ph_2PS)_2$ and S_8 from fraction

four. S_4N_4 (0.36 g, 1.9 mmol) was recovered from the fifth fraction. Due to the difficulties encountered in separation, the weights of the products should be regarded as isolation rather than optimum yields. A ^{31}P NMR spectrum of an identical reaction mixture (Figure 2.1) shows a number of intense signals most of which can be attributed to the compounds described above.

5.2.2 REACTION OF Me_2P-PMe_2 WITH S_4N_4

S_4N_4 (1.66 g, 9.0 mmol) was added to a frozen solution of Me_2P-PMe_2 (1.10 g, 9.0 mmol) in 40 ml of toluene and the mixture was allowed to warm, with care, to room temperature over a period of 30 minutes (CAUTION: The reaction between Me_2P-PMe_2 and S_4N_4 is very vigorous in the initial stages. If the temperature is allowed to increase too quickly, there is a possibility of an explosion). The mixture was then set to reflux and after two hours was cooled to room temperature. The volume was reduced to about 20 ml by removal of the solvent *in vacuo* and then the mixture was filtered, to remove any precipitated $(Me_2PS)_2$, and eluted down a 30 x 500 mm Bio-Beads S-X8 chromatography column. Four fractions were collected; pink, yellow, orange and purple. The first fraction was shown by ^{31}P NMR spectroscopy to contain a complex mixture of products but no pure compounds could be isolated. Fractional crystallization of the other fractions resulted in the isolation of $(Me_2PN)_3$ and $(Me_2PN)_4$ from fraction two and 1,3-$(Me_2PN)_2(SN)_2$, m.p 81-2^oC, 1,5-$(Me_2PN)_2(SN)_2$, d.p 175-80^oC and $(Me_2PS)_2$ from fraction three. Removal of the solvent from the purple fraction, left a deep purple oil which was fractionally sublimed *in vacuo* onto an ice-water (0^oC) cooled finger to give deep purple crystals (with a green

lustre) of $(Me_2PN)(SN)_2$, m.p 16-17°C. Due to the difficulty in separating the products and the relative instability of the methylphosphathiazenes, no yields were recorded. The ^{31}P NMR spectrum of the reaction mixture showed the isolated compounds to be the major components.

5.2.3 REACTION OF Ph_2PH with S_4N_4

S_4N_4 (1.42 g, 7.7 mmol) was added to a solution of Ph_2PH (2.87 g, 15.4 mmol) in 50 ml of toluene and the mixture was stirred and heated to reflux. After 16 hours the mixture was cooled to room temperature and reduced in volume to about 20 ml by removal of the solvent *in vacuo*. The solution was filtered and eluted down a 30 x 500 mm Bio-Beads S-X8 chromatography column. Three fractions were collected; yellow, orange and purple, and fractional crystallization of each of these from acetonitrile resulted in the isolation of $(Ph_2PN)_3$ from fraction one, 1,3-$(Ph_2PN)_2(SN)_2$ (1.09 g, 2.2 mmol, 30% based on nitrogen) and 1,5-$(Ph_2PN)_2(SN)_2$ (0.02 g, 0.05 mmol, 1% based on nitrogen) from fraction two, and $(Ph_2PN)(SN)_2$ (0.51 g, 1.8 mmol, 20% based on nitrogen) and S_8 from fraction three. The ^{31}P NMR spectrum of an identical reaction mixture showed these to be the major components in addition to $Ph_2P(S)H$.

5.2.4 REACTION OF $(PhO)_3P$ WITH S_4N_4

S_4N_4 (1.13 g, 6.1 mmol) was added to a solution of $(PhO)_3P$ (3.80 g, 12.26 mmol) in 20 ml of toluene, and the mixture was set to reflux for one hour. The resulting black mixture was eluted down a 20 x 200 mm Fluorisil chromatography column and the green-blue fraction was collected

and reduced in volume by removal of the solvent *in vacuo*. This was then eluted down a 30 x 500 mm Bio-Beads S-X8 chromatography column. The blue fraction was collected and removal of the solvent *in vacuo* gave impure $((PhO)_2PN)(SN)_2$ (0.31 g, 0.96 mmol) as a deep blue oil.

5.3 CHARACTERIZATION OF THE P-N-S HETEROCYCLES

5.3.1 $(R_2PN)(SN)_2$

SPECTROSCOPIC DATA

Infrared, UV-visible and NMR (^1H, ^{15}N and ^{31}P) spectra are presented in Tables 5.1, 5.2 and 5.3, respectively, for all four derivatives (R = Ph, Me, PhO, F) of $(R_2PN)(SN)_2$. Due to the instability of the methyl, phenoxy and fluoro derivatives, chemical analysis was only possible for $(Ph_2PN)(SN)_2$ (Table 5.4), and an infrared spectrum of $(F_2PN)(SN)_2$ was not obtainable. (see section 5.6.3.2).

X-RAY DIFFRACTION STUDIES ON $(Ph_2PN)(SN)_2$

A crystal suitable for X-ray diffraction studies was obtained by recrystallization from acetonitrile and the X-ray data were collected and the structure solved by Dr. P. N. Swepston under the supervision of Dr. A. W. Cordes at the University of Arkansas, Fayetteville, Arkansas[150,151]

5.3.2 1,3-$(R_2PN)_2(SN)_2$

SPECTROSCOPIC DATA

Infrared, UV-visible and NMR (^1H and ^{31}P) spectra and chemical analysis data for the methyl and phenyl derivatives are presented in Tables 5.5, 5.2, 5.3 and 5.4, respectively.

X-RAY DIFFRACTION DATA COLLECTION FOR 1,3-$(Ph_2PN)_2(SN)_2$

Crystals suitable for X-ray diffraction studies were obtained by recrystallization from acetonitrile. A block shaped crystal fragment was cut from a large orange crystal and was mounted on the end of a glass fiber with epoxy resin. The crystal was then coated with epoxy resin. The procedure for data collection preparation and data collection was identical to that given in section 5.1.3. Crystal data and experimental conditions for the data collection are given in Table 5.6.

SOLUTION AND REFINEMENT OF THE STRUCTURE OF 1,3-$(Ph_2PN)_2(SN)_2$

Initial coordinates for all the non-hydrogen atoms of the asymmetric unit (half of the molecule)[226] were obtained from the solution and refined by full-matrix least-squares techniques. A series of isotropic and anisotropic refinement cycles resulted in agreement factors of $R = 0.087$ and $R_w = 0.090$. The weighting scheme used was $w = (\sigma^2(F) + nF^2)^{-1}$ $(n = 0.0003)$ where $\sigma(F)$ was derived from counting statistics. The ten unique hydrogen

atoms were located in a difference Fourier synthesis and were included in idealized positions (C-H = 0.95 Å) with thermal parameters 10% greater than the carbon atom to which they are attached, but were not refined. After two cycles of refinement including hydrogen atom contributions, the model converged with agreement factors of R = 0.054 and R_w = 0.063. On the final cycle of refinement the maximum shift/error = 0.02, and the error in an observation of unit weight was 2.30. Atomic coordinates of the asymmetric unit are presented in Table 5.7.

5.3.3 1,5-$(R_2PN)_2(SN)_2$

SPECTROSCOPIC DATA

Infrared and NMR (^1H and ^{31}P) spectra and chemical analysis data for the methyl and phenyl derivatives are presented in Tables 5.8, 5.3 and 5.4 respectively.

X-RAY DIFFRACTION DATA COLLECTION FOR 1,5-$(Ph_2PN)_2(SN)_2$

A rectangularly-shaped pale yellow crystal, suitable for X-ray diffraction studies was obtained by recrystallization from acetonitrile/methylene chloride. The crystal was coated in epoxy resin and mounted on the end of a glass fiber. The procedure for data collection preparation and data collection was identical to that given in section 5.1.3. Crystal data and experimental conditions for data collection are given in Table 5.9.

SOLUTION AND REFINEMENT OF THE STRUCTURE OF $1,5\text{-}(Ph_2PN)_2(SN)_2$

Crystallographic two-fold symmetry is imposed on the molecular structure and therefore only half of the atomic positions are unique.[226]. All of the non-hydrogen atomic coordinates were obtained from the solution and were refined by full-matrix least-squares techniques. The agreement factors following isotropic and anisotropic refinement of the positions were, $R = 0.054$ and $R_w = 0.063$, and the weighting scheme used was $w = (\sigma^2(F) + nF^2)^{-1}$ ($n = 0.0006$). The ten unique hydrogen atoms were included in idealized positions (C-H = 0.95 Å) following determination of their positions in a difference Fourier synthesis. They were given thermal parameters 10% greater than the carbon atom to which they were attached, but were not refined. The final agreement factors of the converged model after two cycles of refinement including hydrogen atom contributions, were $R = 0.045$ and $R_w = 0.059$. On the final cycle of refinement the maximum shift/error = 0.08, and the error in observation of unit weight was 4.36. Atomic coordinates of the asymmetric unit are presented in Table 5.10.

X-RAY DIFFRACTION DATA COLLECTION FOR $1,5\text{-}(Me_2PN)_2(SN)_2$

A yellow diamond-shaped crystal suitable for X-ray diffraction studies was obtained by recrystallization from a methylene chloride/acetonitrile mixture. The crystal was coated in epoxy resin and mounted on the end of a glass fiber. Preliminary Weisenberg photographs were obtained and the systematic extinctions indicated the space group was either Pnma or $Pna2_1$. The crystal was mounted on the diffractometer and the program SEARCH was

employed to obtain the 25 reflections to be used for calculation of the cell constants and orientation matrix. The remaining data collection preparation and data collection procedure were the same as those described in Section 5.1.3. Crystal data and experimental conditions for the data collection are given in Table 5.11.

SOLUTION AND REFINEMENT OF THE STRUCTURE OF $1,5\text{-}(Me_2PN)_2(SN)_2$

Pnma was the final choice of space group, on the basis of the centric distribution of E values. The solution gave the coordinates of the two phosphorus atoms, the two unique nitrogen atoms, the one unique sulfur atom and three of the four carbon atoms[226]. The fourth carbon atom was located in a difference Fourier synthesis. Two cycles of isotropic refinement gave agreement factors of $R = 0.047$ and $R_w = 0.059$. A difference Fourier following three anisotropic refinement cycles revealed the positions of the eight unique hydrogen atoms, which were included in the model with the thermal parameter of the carbon atom to which they were attached, but were not refined. Subsequent anisotropic refinement of the non-hydrogen atoms resulted in final agreement factors of $R = 0.033$ and $R_w = 0.036$. On the final cycle of refinement the maximum shift/error = 0.01 and the error in observation of unit weight was 2.76. Atomic coordinates of the asymmetric unit are presented in Table 5.12.

5.4 REACTIONS OF P-N-S HETEROCYCLES WITH HALOGENS

5.4.1 $(Ph_2PN)(SN)_2$

CHLORINATION

SO_2Cl_2 (0.06 ml, 0.7 mmol) was added dropwise, by syringe, to a stirred solution of $(Ph_2PN)(SN)_2$ (0.20 g, 0.7 mmol) in 20 ml of CH_3CN. The purple solution turned yellow immediately. The volume of the mixture was reduced to 10 ml by removal of the solvent *in vacuo*. A few yellow-orange crystals of $(Ph_2PN)(NSCl)_2$ were obtained from the solution by cooling in the freezer (-20^oC). Infrared spectral data is presented in Table 5.13 and chemical analysis data in Table 5.4.

BROMINATION

Br_2 (0.04 ml, 0.7 mmol) was added dropwise, by syringe to a stirred solution of $(Ph_2PN)(SN)_2$ (0.20 g, 0.7 mmol) in 20 ml of CH_3CN. The purple solution turned red-orange immediately. The volume of the mixture was reduced to 10 ml by removal of the solvent *in vacuo*. Various attempts to obtain a solid from the solution were unsuccessful. Subsequent solvent removal *in vacuo* resulted in a red oil which could not be characterized.

IODINATION

A solution of I_2 (0.18 g, 0.7 mmol) in 20 ml of CH_3CN was added dropwise to a stirred solution of $(Ph_2PN)(SN)_2$ (0.20 g, 0.7 mmol) in 20 ml of

CH_3CN. The purple solution turned black immediately. The volume of the mixture was reduced to 10 ml by removal of the solvent *in vacuo*. Various attempts to obtain a solid from the solution were unsuccessful. Subsequent removal of the solvent *in vacuo* resulted in a black oil which could not be characterized.

5.4.2 1,3-$(Ph_2PN)_2(SN)_2$

CHLORINATION

SO_2Cl_2 (0.04 ml, 0.4 mmol) was added dropwise, by syringe, to a stirred solution of 1,3-$(Ph_2PN)_2(SN)_2$ (0.20 g, 0.4 mmol) in 20 ml of CH_3CN. The deep orange solution turned yellow immediately. The volume of the mixture was reduced to 10 ml by removal of the solvent *in vacuo*. Yellow crystals were obtained from the cooled solution (-20°C). An infrared spectrum of the crystals identified them as $(Ph_2PN)_2(NSCl)$[149] (0.15 g, 0.3 mmol, 75%).

BROMINATION

Br_2 (0.025 ml, 0.4 mmol) was added dropwise, by syringe, to a stirred solution of 1,3-$(Ph_2PN)_2(SN)_2$ (0.20 g, 0.4 mmol) in 20 ml of CH_3CN. The deep orange solution turned deep red-brown immediately. The mixture was stirred for 30 minutes after which time the color became pale orange. The volume was reduced to 10 ml by removal of the solvent *in vacuo*. Orange crystals of $(Ph_2PN)_4(NS)_2^{2+}(Br_3^-)_2$ (0.11 g, 0.1 mmol 40%) were obtained from the cooled solution (-20°C). Infrared and ^{31}P NMR spectroscopic

data and chemical analysis data for $(Ph_2PN)_4(NS)_2^{2+}(Br_3^-)_2$ are given in Tables 5.14 and 5.4 respectively. When the solution of $(Ph_2PN)_4(NS)_2^{+}(Br_3^-)_2$ was warmed the only isolable crystalline products were $(Ph_2PN)_2(NS)^+Br_3^-$ and $(Ph_2PN)_2(NSBr)$, identified by their infrared spectra.[183]

IODINATION

A solution of I_2 (0.10 g, 0.4 mmol) in 20 ml of CH_3CN was added to a stirred solution of 1,3-$(Ph_2PN)_2(SN)_2$ (0.20 g, 0.4 mmol) in 20 ml of CH_3CN. The deep orange solution turned black immediately and was stirred for 30 minutes. The volume of the solution was reduced to 10 ml by removal of the solvent *in vacuo*. On cooling (-20°C) a black crystalline solid was obtained which was recrystallized from CH_3CN and gave black shiny crystals of $(Ph_2PN)_4(NS)_2^{2+}(I_3^-)_2$ (0.16 g, 0.1 mmol, 45%). Infrared and ^{31}P NMR data and chemical analysis data for $(Ph_2PN)_4(NS)_2^{2+}(I_3^-)_2$ are given in Tables 5.14 and 5.4, respectively.

X-RAY DIFFRACTION DATA COLLECTION FOR $(Ph_2PN)_4(NS)_2^{2+}(Br_3^-)_2$

A crystal suitable for X-ray diffraction studies was obtained by recrystallization from acetonitrile. Due to the moisture sensitivity of $(Ph_2PN)_4(NS)_2^{2+}(Br_3^-)_2$, it was necessary to carry out all the manipulations of the crystal under an atmosphere of nitrogen in a glove bag. A rectangularly-shaped crystal fragment was cut from a needle-like bright orange crystal and mounted in a quartz capillary and was held in place by silicon grease. The capillary was flame sealed. The preparation for

data collection and data collection procedure were identical to those given in Section 5.1.3. Crystal data and experimental conditions for data collection are given in Table 5.15.

SOLUTION AND REFINEMENT OF THE STRUCTURE OF $(Ph_2PN)_4(NS)_2^{2+}(Br_3^-)_2$

The initial atomic coordinates of all the phosphorus, nitrogen, sulfur and bromine atoms were obtained from the solution. Following isotropic refinement the carbon atoms of the eight phenyl groups were located in a difference Fourier synthesis. The two tribromide anions and the inorganic atoms of the heterocycle were refined anisotropically and the phenyl groups were refined isotropically as groups. The atomic positions of a solvent molecule (CH_3CN) were obtained in a difference Fourier synthesis and refined isotropically and anisotropically. The carbon atoms of the phenyl groups were refined separately, isotropically and the initial agreement factors were R = 0.078 and R_w = 0.089. The data was corrected for absorption using the Gaussian method with a 12x10x18 grid[227]. Hydrogen atoms were added in idealized positions (C-H = 0.95 Å) to the phenyl groups, with thermal parameters 10% greater than the carbon atom to which they are attached, but were not refined. After two more cycles of anisotropic refinement the model converged with agreement factors of R = 0.048 and R_w = 0.045. The weighting scheme used was $W = (\sigma^2(F) + nF^2)^{-1}$ (n = 0.0002). On the final cycle the maximum shift/error = 1.54, and the error in an observation of unit weight was 0.87. Atomic coordinates of the cation and two anions in the asymmetric unit are given in Table 5.16†.

† Structure factors can be obtained from Dr. T. Chivers.

5.4.3 1,5-$(Ph_2PN)_2(SN)_2$

CHLORINATION

SO_2Cl_2 (0.05 ml, 0.6 mmol) was added dropwise, by syringe, to a stirred solution of 1,5-$(Ph_2PN)_2(SN)_2$ (0.30 g, 0.6 mmol) in 15 ml of CH_2Cl_2. Within seconds a white precipitate appeared. The solid was redissolved upon addition of 50 ml of CH_2Cl_2 with warming. The pale green solution was cooled in the freezer and produced shiny pale green (almost white) crystals of 1,5-$(Ph_2PN)_2(NSCl)_2$ (0.27 g, 0.5 mmol, 80%) d.p 156-8^oC.

BROMINATION

Br_2 (0.03 ml, 0.6 mmol) was added dropwise, by syringe, to a stirred solution of 1,5-$(Ph_2PN)_2(SN)_2$ (0.30 g, 0.6 mmol) in 15 ml of CH_2Cl_2. The solution became yellow and cooling (-20^oC) produced shiny yellow crystals of 1,5-$(Ph_2PN)_2(NSBr)_2$ (0.33 g, 0.5 mmol, 80%) d.p 163-5^oC.

SPECTROSCOPIC DATA FOR 1,5-$(Ph_2PN)_2(NSX)_2$ COMPOUNDS

Infrared and ^{31}P NMR spectroscopic data and chemical analysis data are presented in Tables 5.13 and 5.4, respectively.

X-RAY DIFFRACTION DATA COLLECTION FOR 1,5-$(Ph_2PN)_2(NSBr)_2$

Crystals suitable for X-ray diffraction studies were obtained by recrystallization from CH_2Cl_2. The moisture and air sensitivity of this compound required that the crystals be handled under a nitrogen atmosphere

in a glove bag. A yellow block-shaped crystal was chosen and placed in a quartz capillary, and was secured by silicon grease. The capillary was flame sealed. The procedure for data collection preparation and data collection were identical to those described in Section 5.1.3 and the crystal data and experimental conditions for data collection are presented in Table 5.17.

SOLUTION AND REFINEMENT OF THE STRUCTURE OF $1,5\text{-}(Ph_2PN)_2(NSBr)_2$

The solution gave the coordinates of the inorganic ring atoms and the two bromine atoms. The carbon atoms of the four phenyl groups were located in a difference Fourier synthesis following an isotropic refinement of the ring atoms. After two cycles of isotropic refinement of all the atoms, the twenty hydrogen atoms of the phenyl groups were located in a difference Fourier synthesis and were included in idealized positions (C-H = 0.95 Å) and given a thermal parameter 10% of that of the carbon to which they are attached, but were not refined. Initial agreement factors were R = 0.046 and R_w = 0.054. The data was corrected for absorption using the Gaussian method with a 12x8x16 grid[227] and after two more cycles of anisotropic refinement, the final agreement factors of the converged model were R = 0.043 and R_w = 0.047. On the final cycle of refinement the maximum shift/error = 1.63, and the error in observation of unit weight was 1.34. Atomic coordinates for the asymmetric unit are given in Table 5.18†.

† Structure factors can be obtained from Dr. T. Chivers.

5.5 PREPARATION AND CHARACTERIZATION OF BICYCLIC P-N-S HETEROCYCLES

5.5.1 $Ph_2PS_3N_5$

PREPARATION FROM $(Ph_2PN)(SN)_2$

SO_2Cl_2 (0.10 ml, 1.0 mmol) was added dropwise, by syringe, into a stirred solution of $(Ph_2PN)(SN)_2$ (0.30 g, 1.0 mmol) in 20 ml of CH_3CN. Following the addition a solution of $Me_3SiNSNSiMe_3$ (0.21 g, 1.0 mmol) in 10 ml of CH_3CN was added to the yellow solution, which turned brown. The volume of the solution was reduced to 10 ml by removal of the solvent *in vacuo*, and on cooling (-30^oC) clusters of orange needle-like crystals were obtained and filtered immediately. These were then recrystallized from CH_3CN to give brown-orange crystals of $Ph_2PS_3N_5$ (0.25 g, 0.7 mmol, 72%).

PREPARATION FROM Ph_2PCl_3 and $Me_3SiNSNSiMe_3$

$Me_3SiNSNSiMe_3$ (0.35 g, 1.69 mmol) was dissolved in 8 ml of CH_3CN and added dropwise to a stirred slurry of Ph_2PCl_3 (0.33 g, 1.12 mmol) in 40 ml of CH_3CN. The mixture became clear yellow at first, but soon turned deep orange. After three hours there was no further visible change and a ^{31}P NMR spectrum of the reaction mixture showed it to contain a large number of phosphorus containing compounds, one of which was $Ph_2PS_3N_5$. The solvent was removed from the reaction mixture *in vacuo* to leave a red-brown oil. An infrared spectrum of the oil showed bands corresponding mainly to $Ph_2PS_3N_5$, however, it was not possible to isolate any pure material.

5.5.2 $Me_2PS_3N_5$

PREPARATION FROM $(Me_2PN)(SN)_2$

Freshly sublimed $(Me_2PN)(SN)_2$ (0.24 g, 1.44 mmol) was dissolved in 20 ml of CH_3CN and SO_2Cl_2 (0.12 ml, 1.5 mmol) was added dropwise, by syringe. The resulting yellow-green slurry was filtered to remove a pale brown precipitate and the yellow filtrate was collected. A solution of $Me_3SiNSNSiMe_3$ in 15 ml of CH_3CN was added dropwise giving an instantaneous color change from yellow to red-brown. The solvent was removed *in vacuo* and the red-brown oily solid was recrystallized from CH_3CN to give brown crystals of $Me_2PS_3N_5$ (0.13 g, 0.6 mmol). Due to the thermal and chemical instability of this compound it was not possible to obtain a chemical analysis.

PREPARATION FROM Me_2PCl_3 AND $Me_3SiNSNSiMe_3$

$Me_3SiNSNSiMe_3$ (1.04 g, 5.1 mmol) was dissolved in 8 ml of CH_2Cl_2 and added dropwise to a stirred slurry of Me_2PCl_3 (0.61 g, 3.5 mmol) in 40 ml of CH_2Cl_2. The mixture became a clear yellow solution but very quickly turned deep orange-red. After three hours there was no further visible change and a ^{31}P NMR spectrum of the reaction mixture indicated a variety of species, none of which could be isolated. The solution was gently warmed and within minutes the color changed to a deep purple.

5.5.3 $F_2PS_3N_5$

$F_2PS_3N_5$ was prepared from the reaction between PF_5 and $Me_3SiNSNSiMe_3$

in diethyl ether, using the procedure described in the Ph.D thesis of I. Ruppert. The yellow crystalline solid was purified by sublimation onto an ice-water ($0^{o}C$) cooled finger *in vacuo*.

5.5.4 SPECTROSCOPIC DATA FOR $R_2PS_3N_5$

Infrared and ^{31}P NMR spectra of methyl, phenyl and fluoro derivatives and chemical analysis data of the phenyl derivative are presented in Tables 5.19 and 5.4, respectively.

5.5.5 PREPARATION OF $1,5\text{-}(Ph_2PN)_2(NS)_2N_2S$

A solution of $Me_3SiNSNSiMe_3$ (0.04 g, 0.2 mmol) in 10 ml of CH_2Cl_2 was added dropwise to a solution of $1,5\text{-}(Ph_2PN)_2(NSCl)_2$ (0.10 g, 0.2 mmol) in 20 ml of CH_2Cl_2. The solution quickly became orange in color. The volume of the solution was reduced by removal of the solvent *in vacuo* and the solution was cooled ($-20^{o}C$). Red crystals of $1,5(Ph_2PN)_2(NS)_2N_2S$ (0.03 g, 0.05 mmol, 27%) were obtained, and the infrared and ^{31}P NMR spectra and chemical analysis data are presented in Tables 5.19 and 5.4 respectively.

5.6 THERMAL DECOMPOSITION OF BICYCLIC P-N-S HETEROCYCLES

5.6.1 $Ph_2PS_3N_5$

^{31}P NMR STUDY OF THERMAL DECOMPOSITION

$Ph_2PS_3N_5$ (0.30 g, 0.8 mmol) in 20 ml of toluene was warmed in an oil

bath which had been previously heated to 95-100°C. After allowing 5 minutes for the solution temperature to equilibrate, samples were removed from the vessel at 0, 5, 10, 15, 25, 40, 55, 75 and 100 minutes, and ^{31}P NMR spectra of these samples were obtained at -60°C.

REGENERATION OF $(Ph_2PN)(SN)_2$

$Ph_2PS_3N_5$ (0.20 g, 0.57 mmol) in 25 ml of toluene was warmed to reflux for three hours. The resulting purple solution was reduced in volume, by removal of the solvent *in vacuo*, to about 10 ml, and was eluted down a 30 x 500 mm Bio Beads S-X8 chromatography column. Two bands were observed, purple and yellow. S_4N_4 was isolated from the latter, and the purple fraction contained $(Ph_2PN)(SN)_2$ (0.12 g, 0.40 mmol, 70%).

5.6.2 $Me_2PS_3N_5$

^{31}P NMR STUDY OF THERMAL DECOMPOSITION

$Me_2PS_3N_5$ (0.25 g, 1.0 mmol) in 30 ml of toluene was warmed in an oil bath which had been previously heated to 95-100°C. After allowing 5 minutes for the solution temperature to equilibrate, samples were removed from the vessel at 0, 5, 10, 15, 20, 25, 30, 40, 50, 60 and 90 minutes, and ^{31}P NMR spectra of the samples were obtained at -60°C. An array of these spectra is displayed in Figure 4.4.

REGENERATION OF $(Me_2PN)(SN)_2$

$Me_2PS_3N_5$ (0.25 g, 1.0 mmol) in 25 ml of toluene was set to reflux

for two hours. The resulting red-purple solution was reduced in volume, by removal of the solvent *in vacuo*, to about 10 ml and was eluted down a 30 x 500 mm Bio-Beads S-X8 chromatography column. Two bands were observed; purple and yellow. S_4N_4 was isolated from the latter. The purple material was identified as $(Me_2PN)(SN)_2$, by infrared spectroscopy. However, due to the thermal instability of $(Me_2PN)(SN)_2$, an accurate yield could not be obtained.

5.6.3 $F_2PS_3N_5$

^{31}P NMR STUDY OF THERMAL DECOMPOSITION

$F_2PS_3N_5$ (0.65 g, 2.8 mmol) in 20 ml of toluene was warmed in an oil bath which had been previously heated to 85-95°C. After allowing 5 minutes for the solution temperature to equilibrate, samples were removed from the solution every 5 minutes and ^{31}P NMR spectra of the samples were obtained. The spectra obtained after 10 minutes were very complex and the only signals that could be definitely assigned were those of the starting bicyclic compound.

PREPARATION AND ISOLATION OF $(F_2PN)(SN)_2$

$F_2PS_3N_5$ (0.1 g, 0.4 mmol) was dissolved in 5 ml of Nujol. The flask containing the solution was connected in series to another flask which led to a vacuum line. The system was evacuated and the empty flask was cooled in liquid nitrogen. The solution was warmed with an oil bath to 85-95°C. The yellow color changed very quickly to a blue-green and a volatile blue material appeared in the cooled flask. After three hours

the blue green color in the reaction flask subsided and the reaction was terminated. The cooled collection flask was allowed to warm to room temperature causing the blue material to melt and form an oil, characterized as $(F_2PN)(SN)_2$ (see Section 5.3.1 and 5.7.3). This compound is very thermally unstable in the pure form and decomposes over a period of an hour to give a yellow-green liquid, at room temperature.

SPECTROSCOPIC DATA OF $(F_2PN)(SN)_2$

UV-visible and NMR (^{19}F and ^{31}P) spectra are presented in Tables 5.2 and 5.3 respectively.

5.7 CYCLOADDITION REACTIONS OF P-N-S HETEROCYCLES

5.7.1 PREPARATION OF NORBORNADIENE ADDUCTS OF $(R_2PN)(SN)_2$

The following procedure was carried out for all the derivatives (R = Ph, Me, PhO, F) of $(R_2PN)(SN)_2$. A slight excess of norbornadiene was added dropwise to a blue/purple solution of $(R_2PN)(SN)_2$ in diethyl ether. The loss of color was immediate and a white precipitate was observed. The crude material was filtered off and recrystallized from a mixture of CH_3CN, CH_2Cl_2 and norbornadiene. Yields were almost quantitative. The crystals do not melt, instead all decompose above 100^oC initially exhibiting the intense color of the free heterocycle.

5.7.2 PREPARATION OF NORBORNADIENE ADDUCTS OF 1,3-$(Ph_2PN)_2(SN)_2$

Norbornadiene (0.04 g, 0.4 mmol) was added dropwise to a solution of

1,3-$(Ph_2PN)_2(SN)_2$ in 20 ml of diethyl ether. The mixture was stirred for one hour after which time the color had changed from orange to very pale yellow and a heavy precipitate was observed. The crude solid was filtered off and recrystallized from a mixture of CH_3CN and CH_2Cl_2 to give colorless crystals of 1,3-$(Ph_2PN)_2(SN)_2.C_7H_8$ (0.14 g, 0.24 mmol, 60%).

5.7.3 SPECTROSCOPIC DATA OF NORBORNADIENE ADDUCTS OF P-N-S HETEROCYCLES

Infrared and NMR (^1H, ^{13}C, ^{19}F and ^{31}P) spectra and chemical analysis data are presented in Tables 5.20, 5.21 and 5.4, respectively.

5.7.4 X-RAY DIFFRACTION STUDIES ON $(Ph_2PN)(NS)_2C_7H_8$

A crystal suitable for X-ray diffraction studies was obtained by recrystallization from CH_3CN/CH_2Cl_2. The X-ray diffraction data were collected and the structure solved by Dr. P. N. Swepston and Mr. M. C. Noble under the supervision of Dr. A. W. Cordes at the University of Arkansas, Fayetteville, Arkansas[151].

Table 5.1 Infrared Spectra of $(R_2PN)(SN)_2$ compounds (cm^{-1})

R = Ph		R = Me		R = PhO	
1587(w)	840(vw)		863(m)	1594(s)	826(vw)
1564(w)				1489(vs)	802(m)
1480(m)	765(m)			1470(s)	773(m)
1437(s)	759(m)	1414(w)	750(vw)	1456(s)	757(s)
1336(w)	741(vs)			1335(vw)	
1315(w)	727(vs)		727(w)	1308(vw)	717(w)
1276(w)	692(vs)	1299(w)	688(vs)	1290(vw)	689(s)
	621(w)	1289(m)			656(vw)
	619(w)	1224(w)		1215(m)	646(vw)
1161(w)				1190(vs)	618(vw)
1123(vs)			597(w)	1161(s)	572(w)
1115(vs)	526(s)				557(w)
1070(vs)	507(s)	1083(vs)		1095(s)	500(m)
1029(s)	447(vw)			1035(s)	
1026(m)	437(vw)	1019(w)		1010(m)	
997(m)	350(vw)	942(m)	390(w)	945(vs)	380(vw)
937(vw)	319(vw)	927(m)	360(w)	902(m)	306(vw)
	282(vw)				

Table 5.2 UV-visible spectra of $(R_2PN)(SN)_2$ and $1,3\text{-}(R_2PN)_2(SN)_2$ compounds

$(R_2PN)(SN)_2$	λmax[a]	ε[b]	λmax	ε	λmax	ε
R = Ph	550	5×10^3	301	1×10^3[d]		
R = Me	543	4×10^3	295	sh[e]	270	2×10^3
R = PhO	583	C	sh[d e]			
R = F	573	C	410			

$1,3\text{-}(R_2PN)_2(SN)_2$	λmax[a]	ε[b]	λmax	ε	λmax	ε
R = Ph	460	8×10^3	342	d		
R = Me	455	6×10^3	350			

a λmax values measured in nm. All CH_2Cl_2 solutions

b Extinction coefficients measured in $M^{-1}cm^{-1}$

c Not measured

d Obscured by $\pi\rightarrow\pi^*$ transitions of phenyl groups

e Sh = shoulder

Table 5.3 NMR spectra of $(R_2PN)(SN)_2$, 1,3-$(R_2PN)_2(SN)_2$ and 1,5-$(R_2PN)_2(SN)_2$ compounds[a]

	X	^{15}N[b]	$^{31}P\{^1H\}$[c]
$(R_2PN)(SN)_2$			
R = Ph	-	dd 116.2 ($^1J_{PN}$ = 51.7)	-21.2
		dt 336.2 ($^3J_{PN}$ = 17.2)	
		($^2J_{NN}$ = 2.8)	
R = Me	d 1.71 ($^2J_{PH}$ = 14.4)[d]	dd 123.2 ($^1J_{PN}$ = 51.1)	6.2
		dt 338.9 ($^3J_{PN}$ = 16.6)	
		($^2J_{NN}$ = 3.0)	
R = PhO	-	dd 135.8 ($^1J_{PN}$ = 38.9)	-3.4
		dt 407.4 ($^3J_{PN}$ = 20.8)	
		($^2J_{NN}$ = 2.7)	
R = F	d -22.2 ($^1J_{PF}$ = 1054.7)[e]	-	d -7.6 ($^1J_{PF}$ = 1055.3)
1,3-$(R_2PN)_2(SN)_2$			
R = Ph	-	-	18.7
R = Me	d 1.85 ($^2J_{PH}$ = 13.3)[d]	-	28.3
1,5-$(R_2PN)_2(SN)_2$			
R = Ph	-	-	113.9
R = Me	1.46[f]	-	110.0
	1.51[f]		
	dd 19.6 ($^1J_{CP}$ = 92)[g]		
	dd 18.9 ($^1J_{CP}$ = 75)[g]		

[a] in $CDCl_3$, chemical shifts in ppm, coupling constants in Hz

[b] reference $NH_{3(l)}$ at 25°C

[c] reference external 85% H_3PO_4

[d] X = ^1H reference Me_4Si

[e] X = ^{19}F reference F_3CCOOH

[f] X = $^1H\{^{31}P\}$

[g] X = ^{13}C reference Me_4Si

d = doublet t = triplet

Table 5.4 Chemical Analyses

T = % Theoretical F = % Found experimentally

Element		H	C	N	P	S	X
$(Ph_2PN)(SN)_2$	T:	3.46	49.47	14.42	10.63	22.01	
	F:	3.67	49.26	14.18	10.79	21.84	
$1,3\text{-}(Ph_2PN)_2(SN)_2$	T:	4.11	58.76	11.42			
	F:	4.01	58.95	11.31			
$1,3\text{-}(Me_2PN)_2(SN)_2$	T:	4.99	19.83	23.13			
	F:	5.12	19.88	22.89			
$1,5\text{-}(Ph_2PN)_2(SN)_2$	T:	4.11	58.76	11.42			
	F:	4.05	58.83	11.75			
$1,5\text{-}(Me_2PN)_2(SN)_2$	T:	4.99	19.83	23.13	25.57	26.47	
	F:	4.69	19.98	22.91	25.44	26.39	
$(Ph_2PN)(NSCl)_2$	T:	2.78	39.79	11.60			19.57
	F:	3.32	40.39	11.78			19.89 [a]
$(Ph_2PN)_4(NS)_2^{2+}(Br_3^-)_2$	T:	2.96	40.22	6.71			32.80
	F:	3.30	42.27	6.18			26.13 [b]
$(Ph_2PN)_4(NS)_2^{2+}(I_3^-)_2$	T:	2.44	34.93	5.09	7.51	3.88	46.14
	F:	2.67	35.61	5.00	8.32	4.35	43.79 [c]
$1,5(Ph_2PN)_2(NSCl)_2$	T:	3.59	51.34	9.98			12.63
	F:	3.80	51.35	9.98			12.89 [a]

Table 5.4 (continued)

Element		H	C	N	P	S	X
$1,5\text{-}(Ph_2PN)_2(NSBr)_2$	T:	3.13	44.48	8.85			24.80[b]
	F:	3.10	44.33	8.61			24.57
$Ph_2PS_3N_5$	T:	2.87	41.00	19.92		27.36	
	F:	3.35	40.93	20.09		26.73	
$1,5\text{-}(Ph_2PN)_2(NS)_2N_2S$	T:	3.66	52.35	15.26			
	F:	3.77	52.56	12.80			
$(Ph_2PN)(SN)_2.C_7H_8$	T:	4.73	59.51	10.96			
	F:	4.59	59.46	10.89			
$(Me_2PN)(SN)_2.C_7H_8$	T:	5.44	41.68	16.20	11.94	24.73	
	F:	5.67	40.85	16.20	11.81	24.95	
$((PhO)_2PN)(SN)_2.C_7H_8$	T:	4.37	54.93	10.11	7.45	15.43	
	F:	4.23	54.64	10.09	7.41	15.61	
$(F_2PN)(SN)_2.C_7H_8$	T:	3.02	31.46	15.72			
	F:	3.11	31.02	15.07			
$1,3\text{-}(Ph_2PN)_2(SN)_2.C_7H_8$	T:	4.84	63.90	9.62			
	F:	4.70	63.72	9.68			

a,X = Cl; *b*,X = Br; *c*,X = I

Table 5.5 Infrared Spectra of 1,3-$(R_2PN)_2(SN)_2$ compounds (cm^{-1})

R = Ph		R = Me	
1585(vw)			870(m)
1479(w)		1418(m)	857(m)
1440(s)	782(vw)	1409(m)	778(vw)
1332(vw)	762(vw)		755(m)
1309(vw)	755(vw)	1302(s)	730(vw)
	741(m)	1292(m)	
	732(s)	1284(s)	
	725(s)	1219(vs)	
1196(vs)	702(s)		
1179(vs)	696(s)		
1161(s)	672(vw)		
1127(m)	623(vw)	1116(vs)	637(m)
1108(m)	597(vw)		590(w)
1070(vw)	544(vs)		
1034(vw)	534(s)		
1030(vw)	513(vs)	1032(m)	
1002(vw)	435(vw)		464(w)
976(vw)		972(m)	434(m)
928(m)		952(s)	425(m)
	395(vw)	942(vs)	373(vw)
	348(vw)	932(s)	
849(vw)	337(vw)	881(s)	

Table 5.6 Crystal data and experimental conditions of the X-ray diffraction data collection for 1,3-$(Ph_2PN)_2(SN)_2$

$C_{24}H_{20}N_4P_2S_2$	Mol. Wt. = 490.53	Space group = C2/c
a = 15.200(11) Å	b = 9.307(3) Å	c = 17.675(13) Å β = 113.24(3)°
V = 2298(3) Å^3	D_c = 1.45 gcm^{-3}	Z = 4

Radiation: Mo Kα (graphite monochromator), λ = 0.71069 Å.

Temperature: -100(5)°C.

Maximum Θ: 30°

Scan mode: ω-2Θ

Scan range: $\Delta\omega^\circ = 1.5(0.8 + 0.347 \tan\Theta)^\circ$.

Scan speed: 0.6 - 6.7° min^{-1}

2Θ range of 25 reflections used in determination of cell: $5^\circ \leqslant \Theta \leqslant 21^\circ$.

Standard reflections: (0 0 12), (10 2 2), (3 3 1).

Standard reflections measured every 1000 seconds of X-ray exposure time, and showed no significant intensity fluctuation.

Total number of reflections measured: 2042.

Number of reflections having $I>3\sigma(I)$: 1529

Number of reflections in the final cycle: 1529.

Number of variables in the final cycle: 146.

Highest peak in the final difference Fourier: 1.15 eÅ^{-3} at (0.0049, 0.1429, 0.3275). Of no chemical significance.

Absorption coefficient: μ(Mo Kα) = 3.91 cm^{-1}

Crystal dimensions: 0.40 x 0.32 x 0.15 mm.

Boundary planes: $(11\bar{1})$, $(\bar{1}\bar{1}1)$, $(\bar{1}11)$, $(1\bar{1}\bar{1})$, (001), $(00\bar{1})$, $(0\bar{1}0)$.

Table 5.7 Atomic coordinates ($X10^4$) for the non-hydrogen atoms in the asymmetric unit of 1,3-$(Ph_2PN)_2(SN)_2$

Atom	x/a	y/b	z/c
P1	84.9(7)	2271.3(12)	3324.8(7)
S1	599.2(9)	771.4(12)	3415.9(9)
N1	0*	3045(5)	2500*
N2	755(3)	868(4)	3614(2)
N3	0*	-1296(6)	2500*
C1	-1105(3)	1843(4)	3265(2)
C2	-1902(3)	2436(4)	2648(2)
C3	-2820(3)	2148(5)	2606(3)
C4	-2941(3)	1267(5)	3180(3)
C5	-2155(3)	666(5)	3800(3)
C6	-1231(3)	954(5)	3849(3)
C7	627(3)	3526(4)	4136(2)
C8	1354(3)	3128(5)	4873(3)
C9	1793(3)	4125(6)	5486(3)
C10	1513(3)	5540(5)	5364(3)
C11	785(3)	5957(5)	4646(3)
C12	337(3)	4975(5)	4026(2)

*Parameters are restricted by the symmetry of the crystal

Table 5.8 Infrared spectra of 1,5-$(R_2PN)_2(SN)_2$ compounds (cm^{-1})

R = Ph		R = Me	
1587(s)			887(m)
1574(vw)			871(w)
1437(s)	766(s)	1402(w)	796(vw)
1332(vw)	749(m)		753(w)
1308(w)	740(s)		723(vw)
	725(s)	1292(s)	
	691(s)	1287(w)	688(s)
1166(w)	676(m)		663(w)
1125(vs)		1112(s)	647(s)
1086(s)	535(vs)		512(vw)
1053(vs)		1050(vs)	504(vw)
1027(vs)	469(w)		450(m)
998(s)	445(w)	955(3)	426(w)
	407(w)		
	362(vw)		359(vw)
	270(vw)		

Table 5.9 Crystal data and experimental conditions of the X-ray diffraction data collection for $1,5(Ph_2PN)_2(SN)_2$

$C_{24}H_{20}N_4P_2S_2$	Mol. Wt. = 490.53	space group = C2/c
a = 10.045(3) Å	b = 15.930(2) Å c = 14.130(4) Å	β = 93.98(1) A
V = 2256(1) $Å^3$	Dc = 1.47 gcm^{-3}	Z = 4

Radiation: Cu Kα (Ni pre-filter), λ = 1.5418Å.

Temperature: -100(5)°C.

Maximum Θ: 75°.

Scan mode: ω-2Θ.

Scan range: $\Delta\omega^{o} = 1.5(0.9 + 0.142 \tan\Theta)^{o}$.

Scan speed: 0.7 - 6.7 min^{-1}.

2Θ range of 25 reflections used in determination of cell: $18^{o} \leqslant \Theta \leqslant 33^{o}$.

Standard reflections: (0 8 0), (0 8 7), (4 0 4).

Standard reflections measured every 1000 seconds of X-ray exposure time, and showed no significant intensity fluctuations.

Total number of reflections measured: 2323.

Number of reflections having $I>3\sigma(I)$: 1994.

Number of reflections in the final cycle: 1994.

Number of variables in the final cycle: 145.

Highest peak in the final difference Fourier: 0.7 $eÅ^{-3}$ at (-02124, -0.0576, 0.3075). Of no chemical significance.

Absorption coefficient: μ(Cu Kα) = 24.25.

Crystal dimensions: 0.28 x 0.20 0.19 mm.

Boundary Planes: (010, (0$\bar{1}$0), (001), (00$\bar{1}$), ($\bar{1}$10), (1$\bar{1}$0), (10$\bar{1}$), (111).

Table 5.10 Atomic coordinates ($X10^4$) for the non-hydrogen atoms in the asymmetric unit of 1,5-$(Ph_2PN)_2(SN)_2$

Atom	x/a	y/b	z/c
P1	-1646.1(7)	722.9(4)	1620.2(5)
S1	-708.6(6)	1658.3(4)	3205.2(5)
N1	-1856(2)	1116(2)	2659(2)
N2	-376(2)	1150(2)	1162(2)
C1	-3095(3)	952(2)	851(2)
C2	-4363(3)	741(2)	1133(2)
C3	-5492(3)	923(2)	548(2)
C4	-5365(3)	1302(2)	-316(3)
C5	-4118(3)	1506(2)	-612(2)
C6	-2976(3)	1335(2)	-23(3)
C7	-1531(2)	-402(2)	1663(2)
C8	-1856(3)	852(2)	2465(2)
C9	-1778(3)	1720(2)	2465(3)
C10	-1378(3)	-214(2)	1670(3)
C11	-1047(3)	-1700(2)	878(2)
C12	-1120(3)	-829(2)	866(2)

Table 5.11 Crystal data and experimental conditions of the X-ray diffraction data collection for $1,5\text{-}(Me_2PN)_2(SN)_2$

$C_4H_{12}N_4P_2S_2$	Mol. Wt. = 242.24	Space group = Pnma
a = 11.081(5) Å	b = 8.216(5) Å	c = 11.837(6) Å
V = 1078(1) $Å^3$	D_c = 1.49 gcm^{-1}	Z = 4

Radiation: Mo $K\alpha$ (graphite monochromator), λ = 0.71069 Å.

Temperature: $-100(5)^oC$.

Maximum Θ: 30^o

Scan mode: ω-2Θ

Scan range: $\Delta\omega^o = 1.5(0.6 + 0.347 \tan\Theta)^o$.

Scan speed: 0.4 - 6.7^o min^{-1}

2Θ range of 16 reflections used in determination of cell: $11^o \leqslant \Theta \leqslant 14^o$.

Standard reflections (-1 -2 6), (-4 -3 3), (-7 0 2).

Standard reflections measured every 1000 seconds of X-ray exposure time, and showed no significant intensity fluctuations.

Total number of reflections: 1818.

Number of reflections having $I>3\sigma(I)$: 692.

Number of reflections in the final cycle: 1143 (including those for which $Ic>3\sigma(Io)$).

Number of variables in the final cycle: 64.

Highest peak in the final difference Fourier: 0.23 $Å^{-3}$ (0.09192, 1.1241, 0.1667). Of no chemical significance.

Absorption coefficient: μ(Mo $K\alpha$) = 7.309 cm^{-1}.

Crystal dimensions: 0.22 x 0.25 x 0.27 mm.

Boundary Planes: (100), (0$\bar{1}$0), (00$\bar{1}$), (001), (110), ($\bar{1}\bar{1}$0), (111), ($\bar{1}\bar{1}\bar{1}$), ($\bar{1}$1), (11$\bar{1}$).

Table 5.12 Atomic coordinates ($X10^4$) for the non-hydrogen atoms in the asymmetric unit of 1,5-$(Me_2PN)_2(SN)_2$

Atom	x/a	y/b	z/c
P1	4195(1)	7500*	310(1)
P2	538(1)	7500*	469(1)
N1	1080(3)	9110(4)	1115(2)
N2	3469(3)	9125(4)	713(3)
S1	2411(1)	9052(1)	1627(1)
C1	817(5)	7500*	-1026(4)
C2	-1069(5)	7500*	647(4)
C3	4420(5)	7500*	-1192(5)
C4	685(5)	7500*	4104(5)

*Parameters are restricted by the symmetry of the crystal.

Table 5.13 Infrared[a] and ^{31}P NMR spectra of $(Ph_2PN)(NSCl)_2$ and $1,5\text{-}(Ph_2PN)_2(NSX)_2$ compounds

$(Ph_2PN)(NSCl)_2$		$1,5\text{-}(Ph_2PN)_2(NSCl)_2$		$1,5\text{-}(Ph_2PN)_2(NSBr)_2$	
1586(w)	737(vs)	1580(w)	735(vs)	1585(w)	730(s)
1484(w)		1475(m)	724(vs)	1475(w)	722(s)
1440(VS)	692(s)	1437(vs)	696(vs)	1439(s)	690(s)
1335(vw)	690(w)				
1312(w)	637(m)	1312(m)	645(w)	1310(w)	
	619(vw)	1245(vs)		1240(vs)	
1190(w)	543(vs)	1190(vs)	546(s)	1183(s)	545(s)
		1177(vs)	527(m)	1170(vs)	519(m)
	499(s)	1164(vs)	480(w)	1156(vs)	479(w)
1125(vs)	472(w)	1125(vs)		1120(s)	
1074(vs)	448(w)		438(w)	1112(s)	440(w)
1028(m)	416(s)	1030(m)	421(w)	1029(w)	420(w)
1000(m)	369(w)	1000(m)	383(m)	1000(m)	376(w)
898(vs)	358(w)				
847(w)	337(w)	851(vw)	331(w)		
768(vw)	311(m)				
756(m)	299(m)	750(m)	290(m)	741(w)	265(w)
$^{31}P\{^1H\}$	[b]		[b]		7.3[c]

[a] cm^{-1}

[b] not measured

[c] in $CDCl_3$, δ measured in ppm, external 85% H_3PO_4 reference

Table 5.14 Infrared[a] and ^{31}P NMR[b] spectra of $(Ph_2PN)_4(NS)_2^{2+}(X^-_3)_2$ compounds

$(Ph_2PN)_4(NS)_2^{2+}(Br_3^-)$		$(Ph_2PN)_4(NS)_2^{2+}(I_3^-)_2$	
1583(m)	720(s)	1582(m)	
1578(vw)	760(m)	1574(vw)	750(s)
1478(m)	748(s)	1474(m)	741(m)
1438(vs)	737(vs)	1437(vs)	735(s)
		1330(w)	727(s)
1307(s)	696(vs)	1305(w)	694(vs)
1290(s)	632(w)		
1260(s)		1248(vs)	588(vw)
1200(vs)	560(vs)		
1177(vs)	547(s)	1168(vs)	545(vs)
1160(s)	535(s)		533(vs)
1127(vs)	506(vs)	1122(vs)	513(vs)
1117(vs)		1115(vs)	503(vs)
	465(w)	1068(vw)	465(w)
1027(w)		1024(w)	452(w)
1000(m)		999(m)	433(s)
	419(m)	889(s)	
840(m)	322(vw)	846(w)	
		826(m)	
^{31}P {H}	12.0		18.8

[a] cm^{-1}

[b] in $CDCl_3$, δ measured in ppm, external 85% H_3PO_4 reference

Table 5.15 Crystal data and experimental conditions of the X-ray diffraction data collection for $(Ph_2PN)_4(NS)_2^{2+}(Br_3^-)_2$

$C_{48}H_{40}N_6P_4S_2Br_6$	Mol. Wt. = 1461.54	Space group = $P2_1/n$
a = 16.956(3) Å	b = 13.978(1) Å	c = 23.796(4) Å β = 91.605(8)°
V = 5638(1) Å^3	D_c = 1.618 gcm^{-3}	Z = 4

Radiation: Mo Kα (graphite monochromator), λ = 0.71069 Å.

Temperature: 21(2)°C.

Maximum Θ: 22.5°.

Scan Mode: ω-2Θ.

Scan range: $\Delta\omega^\circ = 1.5(0.60 + 0.347 \tan\Theta)^\circ$.

Scan speed: 0.5° - 5° min^{-1}.

2Θ range of 25 reflections used in determination of cell: $8^\circ \leqslant \Theta \leqslant 17^\circ$.

Standard reflections: (-3 7 2), (0 3 9), (0 4 -6).

Standard reflections measured every 1500 seconds of X-ray exposure time, and showed no significant intensity fluctuations.

Total number of reflections measured: 8087.

Number of reflections having $I>3\sigma(I)$: 1394.

Number of reflections in the final cycle: 4157 (including those for which $Ic>3\sigma(Io)$).

Number of variables in the final cycle: 372.

Highest peak in the final difference Fourier: 1.0 eÅ^{-3} (0.9412, 0.3806, 0.4053). Of no chemical significance.

Absorption coefficient: μ(Mo Kα) = 28.01.

Crystal dimensions: 0.20 x 0.36 x 0.49 mm.

Boundary planes: $(\bar{1}0\bar{1})$, (101), $(10\bar{1})$, $(\bar{1}01)$, (010), $(0\bar{1}0)$, $(01\bar{1})$.

Table 5.16 Atomic Coordinates (x 10^4) for the non-hydrogen atoms of $(Ph_2PN)_4(NS)_2^{2+}(Br_3^-)_2.CH_3CN$

Atom	x/a	y/b	z/c	Atom	x/a	y/b	z/c
Br1	4915(1)	4921(1)	4065(1)	C33	8037(10)	7356(13)	2322(7)
Br2	4746(1)	3528(1)	3254(4)	C34	7929(9)	8232(12)	2055(6)
Br3	4588(1)	2349(2)	2535(1)	C35	7159(10)	8481(12)	1897(6)
Br4	5110(1)	7900(2)	0407(1)	C36	6562(9)	7800(12)	1986(6)
Br5	5544(1)	9373(1)	0936(1)	C41	5884(8)	5326(10)	1745(6)
Br6	6006(2)	10798(1)	1522(1)	C42	5778(9)	5678(11)	1202(6)
P1	4172(2)	6614(3)	2289(2)	C43	5732(9)	5055(12)	0762(6)
P2	5880(2)	6159(3)	2313(2)	C44	5773(11)	4089(14)	0857(8)
P3	6055(3)	7490(3)	4152(2)	C45	5868(10)	3720(12)	1384(7)
P4	4357(3)	7776(3)	4168(2)	C46	5904(10)	4371(12)	1823(7)
S1	3770(2)	6340(3)	3440(2)	C51	6397(9)	8664(11)	3959(7)
S2	6237(2)	5845(3)	3480(2)	C52	6759(11)	9214(16)	4375(7)
N1	3780(6)	6045(7)	2828(4)	C53	6943(12)	10146(18)	4244(9)
N2	5106(6)	6751(7)	2351(4)	C54	6779(14)	10498(17)	3742(11)
N3	6127(6)	5515(8)	2876(4)	C55	6378(15)	9988(20)	3323(9)
N4	6073(6)	6919(7)	3546(4)	C56	6207(11)	9005(14)	3447(8)
N5	5216(6)	7529(8)	4410(4)	C61	6715(9)	7025(10)	4642(6)
N6	4190(6)	7289(7)	3541(4)	C62	7505(11)	6869(12)	4518(7)
N7[a]	2010(9)	6849(10)	3502(5)	C63	8027(11)	6494(14)	4906(9)
C1[a]	1559(13)	6573(17)	3804(9)	C64	7811(13)	6263(14)	5421(9)
C2[a]	0961(12)	6197(14)	4149(8)	C65	7027(12)	6351(14)	5567(7)
C11	3736(9)	7775(11)	2241(5)	C66	6482(9)	6734(12)	5167(7)
C12	2897(10)	7834(12)	2264(6)	C71	4203(10)	9027(11)	4019(7)
C13	2558(9)	8768(13)	2199(6)	C72	4593(11)	9680(16)	4332(7)
C14	3004(12)	9482(13)	2118(7)	C73	4428(13)	10669(17)	4244(9)
C15	3823(13)	9477(14)	2137(7)	C74	3936(13)	10933(14)	3851(9)
C16	4182(9)	8569(14)	2172(6)	C75	3496(13)	10310(19)	3561(9)
C21	3816(8)	5941(11)	1703(6)	C76	3654(11)	9321(14)	3626(7)
C22	3684(9)	6337(11)	1203(7)	C81	3676(9)	7414(12)	4677(6)
C23	3451(10)	5839(14)	0704(7)	C82	3809(13)	6679(18)	5008(10)
C24	3452(10)	4861(13)	0771(7)	C83	3272(17)	6299(17)	5386(10)
C25	3641(11)	4358(13)	1238(8)	C84	2558(12)	6805(15)	5398(8)
C26	3818(9)	4929(12)	1718(6)	C85	2389(10)	7494(13)	5076(7)
C31	6679(9)	6969(11)	2238(5)	C86	2940(11)	7805(11)	4677(6)
C32	7454(10)	6682(11)	2413(6)				

[a] solvent molecule CH_3CN

Table 5.17 Crystal data and experimental conditions of the X-ray diffraction data collection for 1,5-$(Ph_2PN)_2(NSBr)_2$

$C_{24}H_{20}N_4P_2S_2Br_2$	Mol. Wt. = 650.35	Space group = Pn
a = 11.4758(26) Å	b = 7.2398(9) Å	c = 16.9139(41) Å β = 106.42(1)°
V = 1347.9(5) Å^3	D_c = 1.607 gcm^{-3}	Z = 2

Radiation: Mo Kα (graphite monochromator), λ = 0.71069 Å.

Temperature: 21(2)°C.

Maximum θ: 30°.

Scan mode: ω-2θ

Scan range: $\Delta\omega^\circ = 1.5(0.56 + 0.347 \tan\theta)^\circ$.

Scan speed: 0.6° - 5° min^{-1}

2θ range of 25 reflections used in determination of cell: $6^\circ \leqslant \theta \leqslant 15^\circ$.

Standard Reflections: $(\bar{1}34)$, $(\bar{4}\bar{1}7)$, $(\bar{1}2\bar{6})$.

Standard Reflections measured every 1500 seconds of X-ray exposure time, and showed no significant intensity fluctuations.

Total number of unique reflections: 3917.

Number of reflections having $I>3\sigma(I)$: 1199.

Number of reflections in the final cycle: 2588 (including those for which $Ic>3\sigma(Io)$).

Number of variables in the final cycle: 185.

Highest peak in the final difference Fourier: 1.36 eÅ^{-3} at (0.6809, 0.5025, 0.6916). Of no chemical significance.

Absorption coefficient: μ(Mo Kα) = 21.94.

Crystal dimensions: 0.22 x 0.33 x 0.5 mm.

Boundary Planes: $(\bar{1}01)$, (101), $(10\bar{1})$, $(0\bar{1}0)$, (010), $(\bar{1}0\bar{1})$.

Table 5.18 Atomic coordinates for the non-hydrogen atoms of $1,5\text{-}(Ph_2PN)_2(NSBr)_2$ (X 10^4 for Br, S, and P: x 10^3 for C and N)

Atom	x/a	y/b	z/c	Atom	x/a	y/b	z/c
Br1	6244*	-695(5)	7892*	C22	354(2)	404(3)	494(1)
Br2	6858(1)	5684(5)	5437(1)	C23	277(2)	491(3)	428(1)
S1	5917(1)	-143(11)	6414(4)	C24	259(2)	642(2)	433(1)
S2	7257(6)	5197(11)	6914(4)	C25	296(1)	739(2)	507(1)
P1	4809(7)	3384(11)	6567(5)	C26	359(2)	644(4)	582(1)
P2	8341(6)	1586(10)	6758(4)	C31	952(2)	35(4)	763(2)
N1	494(2)	131(3)	625(1)	C32	963(2)	134(3)	840(1)
N2	609(2)	656(3)	702(1)	C33	1022(3)	29(4)	909(2)
N3	826(2)	366(3)	714(1)	C34	1079(2)	-189(2)	886(1)
N4	718(1)	51(3)	633(1)	C35	1044(2)	-252(3)	807(1)
C11	402(1)	316(2)	736(1)	C36	960(3)	-142(5)	752(2)
C12	409(2)	472(3)	788(1)	C41	915(2)	161(3)	604(1)
C13	342(1)	470(2)	843(1)	C42	995(3)	309(4)	605(2)
C14	264(2)	334(3)	844(1)	C43	1068(2)	307(3)	546(2)
C15	253(2)	165(3)	783(1)	C44	1047(2)	216(2)	488(1)
C16	313(2)	184(3)	728(1)	C45	960(2)	78(2)	476(1)
C21	388(2)	463(4)	5-0(1)	C46	892(1)	59(2)	532(1)

* Restricted to define the origin.

Table 5.19 Infrared[a] and ^{31}P NMR[b] spectra of $Ph_2PS_3N_5$, $Me_2PS_3N_5$ and 1,5-$(Ph_2PN)_2(NS)_2N_2S$.

$Ph_2PS_3N_5$		$Me_2PS_3N_5$		1,5-$(Ph_2PN)_2(NS)_2N_2S$	
1587(w)	747(w)			1580(vw)	740(m)
1480(w)	724(s)		722(vs)		723(s)
1440(s)	714(w)	1410(m)	713(vs)	1433(s)	
1336(w)	697(m)			1380(w)	693(m)
	687(m)	1295(vs)	680(s)		665(vw)
1130(s)	650(w)		635(s)	1180(w)	
1116(s)	613(vw)			1115(vs)	
1091(vs)	567(5)	1090(vs)	580(vs)	1092(vs)	549(vs)
1076(s)	540(w)	1070(vs)	540(vs)		530(vs)
1031(w)	504(s)			1023(m)	501(s)
991(m)	468(m)	980(vs)	475(vs)	996(m)	478(m)
	436(w)	948(vs)			440(m)
	426(vw)	920(vs)	418(vs)		412(w)
809(s)		870(vs)	382(vs)	812(w)	368(w)
768(w)		797(s)	340(w)	760(w)	346(w)
		756(m)	270(m)		
$^{31}P\{^1H\}$ -21.3		-4.4		43.7	

[a] in cm^{-1}

[b] in $CDCl_3$, δ measured in ppm, external 85% H_3PO_4 reference

Table 5.20 Infrared spectra of norbornadiene adducts of P-N-S Heterocycles (Cm^{-1})

$(R_2PN)(NS)_2.C_7H_8$				
R = Ph	R = Me	R = PhO	R = F	1,3-$(Ph_2PN)_2(NS)_2.C_7H_8$
1588(vw)	1565(vw)	1595(m)		1589(vw)
1569(vw)	1560(vw)	1588(m)		
	1518(vw)			
	1511(w)			
	1498(vw)	1492(vs)		
1436(s)		1455(m)		1438(s)
1323(m)		1327(m)	1325(m)	1324(vw)
1314(w)	1299(s)		1294(w)	
	1289(s)	1287(w)		1291(vw)
1281(w)	1282(m)	1269(vw)	1264(w)	1280(vw)
	1268(w)	1261(vw)		1240(vs)
1258(w)	1258(w)	1225(m)	1206(vw)	
1189(vw)	1188(w)	1187(vs)	1194(s)	
1180(w)	1177(w)	1171(m)		1180(vw)
1159(w)		1156(w)		1164(w)
1120(s)		1125(w)		1130(vs)
1111(vs)		1116(w)	1105(vs)	1113(vs)
				1098(m)
	1055(vs)	1054(vs)	1082(vs)	1072(w)
		1041(vs)		1037(vw)
1036(vs)		1029(s)	1019(m)	1021(vw)
1023(vs)	1020(s)	1024(s)		
1013(vs)		1019(s)		1001(vw)
		1006(m)		
992(vs)	997(vs)	985(w)	981(w)	
	979(m)	961(s)		
	952(m)			
931(w)	933(vs)	934(vs)	919(m)	cont'd ...

Table 5.20 (continued)

907(vw)	907(m)	907(m)	907(m)	
867(vw)	864(vs)	899(m)	865(m)	885(vw)
	842(vw)	868(m)		
830(vw)	832(vw)	823(vw)	832(w)	835(vs)
		822(vw)		
		803(s)		
797(m)	787(m)	791(m)	799(m)	
777(vw)	773(vw)	769(m)	781(w)	779(vw)
767(w)				
756(s)		757(s)		750(s)
741(m)	745(s)	748(s)	744(m)	
725(s)	739(s)	735(s)	735(s)	729(vs)
718(vs)	721(vs)		720(w)	705(m)
699(s)	694(s)	693(m)	693(m)	
688(m)				
661(vw)	653(vw)	667(vw)	663(vw)	
629(w)		631(vw)		639(vw)
617(vw)		619(w)	616(w)	616(vw)
		610(vw)		606(vw)
	599(m)	573(m)		
550(s)	546(m)	551(m)		552(m)
536(m)		542(w)	537(w)	539(s)
518(m)		521(m)		
		506(vw)		512(s)
	501(w)	500(vw)		
495(w)		487(w)	497(w)	490(w)
457(vw)	450(w)	451(vw)	473(w)	465(vw)
447(vw)		441(vw)	435(vw)	453(w)
433(w)	425(w)		424(w)	438(vw)
				423(vw)
	377(w)			
355(vw)	369(w)	368(vw)	368(vw)	
335(vw)	325(vw)	359(vw)	332(vw)	
	273(vw)			

Table 5.21 NMR spectra of $(R_2PN)(NS)_2.C_7H_8$ compounds and $1,3\text{-}(Ph_2PN)_2(NS)_2.C_7H_8$[a]

	^1H[b]	$^{13}C\{^1H\}$[b]	$^{31}P\{^1H\}$[c]
$(R_2PN)(NS)_2.C_7H_8$			
R = Ph	m 1.18, 1.84 (AB, 10.0)	41.9	-17.7
	t 3.21 (2.0)	43.8	
	d 4.13 (1.6)	81.6	
	6.23	139.5	
R = Me	d 1.32 ($^2J_{PH}$ = 13.4)	d 21.9 ($^1J_{PC}$ = 99. 1)	1.8
	d 1.57 ($^2J_{PH}$ = 14.0)	d 22.4 ($^1J_{PC}$ - 78.6)	
	m 1.20, 1.80 (AB, 9.3)	41.4	
	3.26	43.7	
	d 4.31 (1.1)	82.2	
	6.39	139.6	
R = PhO	m 1.09, 1.68 (AB, 10.0)	41.2	-23.4
	3.08	43.5	
	d 3.93 (1.6)	84.0	
	6.12	139.0	
R = F	m 1.32, -.80 (AB, 10.0)	41.1	d -10.9 ($^1J_{PF}$ = 935.9)
	t 3.33 (1.8)	43.9	d -23.2 ($^1J_{PF}$ = 936.2)
	d 4.66 (1.6)	85.0	
	6.40	139.2	
	^{19}F:[d] dd 32.5 ($^1J_{PF}$ = 1000.4, $^2J_{FF}$ = 81.9)	dd -3.1 ($^1J_{PF}$ = 935.1, $^2J_{FF}$ = 80.5)	
$1,3\text{-}(Ph_2PN)_2(NS)_2.C_7H_8$			
	1.5 (AB)	44.2	6.2
	t 3.22 (1.6)	45.2	
	d 4.02 (1.9)	82.7	
	6.10	139.4	

[a] in $CDCl_3$, δ in ppm, J in Hz
[b] reference Me_4Si
[c] reference external 85% H_3PO_4
[d] reference F_3CCOOH
m = multiplet d = doublet t = triplet

CONCLUSIONS AND FUTURE RESEARCH DIRECTIONS

The preparation and characterization of the three P-N-S heterocycles fulfil the primary objective of this work. They are the beginning of a series of unsaturated systems which relate the well known phosphazene and thiazene series of compounds. In addition to providing a useful comparison between the P-N and S-N heterocyclic environment, the results emphasize many of the concepts already established for the parent systems. The strong visible spectra observed for the open, almost planar systems are a useful probe into the electronic environment of the P-N-S heterocycles and the studies support the basic conclusions concerning S-N and P-N bonding. Adjustment of exocyclic ligands on these compounds may provide further useful electronic information. Two of four possible eight-membered P-N-S heterocycles have been isolated. The unknown species both require a tri-coordinate sulfur center, and it is conceivable that these systems may be a minor product of the reaction between Ph_2PCl and S_4N_4.

The chemical properties of the P-N-S heterocycles are reminiscent of those of related cyclothiazenes. However, in certain cases the presence of the P-N units gives unique stability to the products. For all of the systems oxidation involves removal of two valence electrons resulting in a general stabilization of the electronic structure of the heterocycle, for one reason or another. Although the products are very different for each system, the initial steps appear to involve oxidative addition to the sulfur centers. A variety of phosphathiazyl halides have been isolated and characterized, including the first example of an S-N heterocycle containing a thiazyl bromide (NSBr) unit. However, an unusual ring-opening reaction is observed for the oxidation of $1,3\text{-}(Ph_2PN)_2(SN)_2$, in

which an NSX unit is thermally released from the heterocycle. The stability of the N-S-N unit appears to be the reason for processes of this nature. The twelve-membered dicationic P-N-S species produced in these reactions indicates the possibility of an extensive series of compounds with the ring size flexibility of the cyclophosphazenes and the cationic, neutral, and anionic chemistry of the cyclothiazenes. The phosphathiazyl halides provide a number of synthetic possibilities, some of which have already been explored, such as the metathetical formation of bicyclic P-N-S systems. Finally, the cycloaddition reactions of the P-N-S heterocycles are very similar to those of S_4N_4. One may expect much of the diverse chemistry of the cyclothiazenes to apply to these P-N-S systems resulting in a variety of interesting compounds.

REFERENCES

1. E. Hengge and D. Kovar, *Angew. Chem. Int. Ed. Engl.*, 16, 403 (1977).
2. R. Steudel and H. J. Mausle, *Angew. Chem. Int. Ed. Engl.*, 18, 152 (1979).
3. F. A. Cotton and G. Wilkinson, "*Advanced Inorganic Chemistry*", 4th Ed., 453, John Wiley, New York (1980).
4. F. A. Cotton and G. Wilkinson, "*Advanced Inorganic Chemistry*", 4th Ed., 386, John Wiley, New York (1980).
5. F. A. Cotton and G. Wilkinson, "*Advanced Inorganic Chemistry*", 4th Ed., 456, John Wiley, New York (1980).
6. A. Stock and E. Pohland, *Chem. Ber.*, 59, 2215 (1926).
7. J. von Liebig and F. Wöhler, *Annalen*, 11, 139 (1834).
8. H. Rose, *Annalen*, 11, 131 (1834).
9. M. Gregory, *J.Pharm.*, 21, 315 (1835).
10. J. Bojes and T. Chivers, *J. Chem. Soc. Chem. Commun.*, 1023 (1980).
11. J. Bojes, T. Chivers, W. G. Laidlaw and M. Trsic, *J. Am. Chem. Soc.*, 104, 4837 (1982).
12. C. M. Mikulski, P. J. Russo, M. S. Saran, A. G. MacDiarmid, A. F. Garito and A. J. Heeger, *J. Am. Chem. Soc.*, 97, 6358 (1975).
13. A. J. Banister, P. J. Dainty, A. C. Hazell, R. G. Hazell and J. G. Lomburg, *J. Chem. Soc. Chem. Commun.*, 1187 (1969).
14. A. C. Hazell and R. G. Hazell, *Acta Chem. Scand.*, 26, 1987 (1972).
15. A. J. Banister and H. G. Clarke, *J. Chem. Soc. Dalton Trans.*, 2661 (1972).
16. U. Thewalt, *Z. Anorg. Allg. Chem.*, in press.
17. T. Chivers and J. Proctor, *J. Chem. Soc. Chem. Commun.*, 642 (1978).

18. T. Chivers and J. Proctor, *Can. J. Chem.*, 57, 1286 (1979).

19. H. W. Roesky, M. N. S. Rao, T. Nakajima and W. S. Sheldrick, *Chem. Ber.*, 112, 3531 (1979).

20. J. Bojes and T. Chivers, *J. Chem. Soc. Chem. Commun.*, 391 (1978).

21. J. Bojes, T. Chivers, W. G. Laidlaw and M. Trsic, *J. Am. Chem. Soc.*, 101, 4517 (1979).

22. G. Weigers and A. Vos, *Acta Crystallogr.*, 20, 192 (1966).

23. H. Kluver and O. Glemser, *Z. Naturforsch. B*, 32b, 1209 (1977).

24. A. C. Hazell, G. A. Weigers and A. Vos, *Acta Crystallogr.*, 20, 186 (1966).

25. H. H. Baalman, H. P. Velius and J. C. van der Grampel, *Recl. Trav. Chim. Pay-Bas.*, 91, 935 (1972).

26. R. Clipsham, R. M. Hart and M. A. Whitehead, *Inorg. Chem.*, 8 2431 (1969).

27. J. C. van der Grampel, *Rev. Inorg. Chem.*, 3, 1 (1981).

28. R. Appel and M. Halstenberg, *Angew. Chem. Int. Ed. Engl.*, 15, 696 (1976).

29. J. Weiss, *Acta Crystallogr. Sect. B*, 33, 2272 (1977).

30. S. Pohl, O. Peterson and H. W. Roesky, *Chem. Ber.*, 112, 1545 (1979).

31. H. W. Roesky, *Angew. Chem. Int. Ed. Engl.*, 11, 642 (1972).

32. H. G. Heal and A. J. Banister, *Phosphorus and Sulfur*, 5, 95 (1978).

33. H. W. Roesky, *Adv. Inorg. Chem. Radiochem.*, 22, 239 (1979).

34. A. J. Banister, *Phosphorus and Sulfur*, 6, 421 (1979).

35. H. W. Roesky, *Angew. Chem. Int. Ed. Engl.*, 18, 91 (1979).

36. R. Gleiter, *Angew. Chem. Int. Ed. Engl.*, 20, 444 (1981).

37. T. Chivers and R. T. Oakley, *Top. Curr. Chem.*, 102, 119 (1982).

38. H. R. Allcock, *Chem. Rev.*, 72, 315 (1972).

39. R. Keat, "Phosphazenes", in *Organophosphorus Chemistry* (specialist Periodical Reports), The Chemical Society, London, 4 (1973).

40. D. P. Craig and N. L. Paddock in "*Nonbenzenoid Aromatics*", 2, 273 (1971).

41. S. S. Krishnamurthy, A. C. Sau and M. Woods, *Adv. Inorg. Chem. Radiochem.*, 21, 41 (1978).

42. H. G. Heal, "*The Inorganic Heterocyclic Chemistry of Sulfur, Nitrogen and Phosphorus*", Academic Press, London (1980).

43. M. Yoshifujii, I Shima, N. Inamoto, K. Hirotsu and T. Higuchi, *J. Am. Chem. Soc.*, 103, 4587 (1981).

44. W. Schafer, A. Schweig, K. Dimroth and H. Karter, *J. Am. Chem. Soc.*, 98, 4410 (1976).

45. L. Pauling, "*The Nature of the Chemical Bond*", 3rd Ed., Cornell University Press, Ithaca, New York (1960).

46. R. D. Harcourt and H. M. Hugel, *J. Inorg. Nucl. Chem.*, 43, 239 (1981).

47. M. J. S. Dewar, "*The Molecular Orbital Theory of Organic Chemistry*", McGraw-Hill, New York (1969).

48. K. A. R. Mitchell, *Chem. Rev.*, 69 157 (1969).

49. D. P. Craig, *J. Chem. Soc.*, 997 (1959).

50. D. P. Craig, in "*Theoretical Organic Chemistry*", Kekule Symposium Butterworth and Co., Ltd, London., 20 (1959).

51. A. Streitweiser, "*Molecular Orbital Theory for Organic Chemists*", John Wiley, New York (1961).

52. M. Trsic, W. L. Laidlaw and R. T. Oakley, *Can. J. Chem.*, 60, 2281 (1982).

53. M. Villena-Blanco and W. L. Jolly, *Inorg. Synth*,. 9 98 (1968).

54. *Gmelins Handbuch der Anorganischem Chemie, Part B, Section 3*, "Schwefel", Verlag Chemie, Weinheim (1963).

55. R. Adkins and A. G. Turner, *J. Chromatogr.*, 110, 202 (1975).

56. G. S. Lu and J. Donohue, *J. Am. Chem. Soc.*, 66, 818 (1944).

57. D. Clark, *J. Chem. Soc.*, 1615 (1952).

58. B. D. Sharma and J. Donohue, *Acta Crystallogr.* 16, 891 (1963).

59. M. L. DeLucia and P. Coppens, *Inorg. Chem.*, 17, 2336 (1978).

60. H. J. Emeleus, *Endeavour*, 32, 76 (1973).

61. I. Lindqvist, *J. Inorg. Nucl. Chem.*, 6, 159 (1958).

62. L. Zborilova and P. Gebauer, *Z. Anorg. Allg. Chem.*, 448, 5 (1979)

63. L. Zborilova and P. Gebauer, *Z. Chem.*, 19, 79 (1979).

64. Z. Zak, *Acta Crystallogr.*, B37, 23 (1981).

65. R. J. Gillespie, D. R. Slim and J. D. Tyrer, *J. Chem. Soc. Chem. Commum.*, 253 (1977).

66. R. J. Gillespie, J. P. Kent, J. F. Sawyer, D. R. Slim and J. D. Tyrer, *Inorg Chem.*, 20, 3799 (1981).

67. M. G. B. Drew, D. H. Templeton and A. Zalkin, *Inorg. Chem.*, 6, 1906 (1967).

68. A. Gieren and B. Dederer, *Z. Anorg. Allg. Chem.*, 440, 119 (1978).

69. U. Thewalt, *Z. Naturforsch.*, 835, 855 (1980).

70. R. J. Gillespie, J. P. Kent and J. F. Sawyer, *Acta Crystallogr.*, B36, 655 (1980).

71. R. J. Gillespie, J. P. Kent and J. F. Sawyer, *Inorg. Chem.*, 20, 3784 (1981).

72. B. Krebs, G. Henkel, S. Pohl and H. W. Roesky, *Chem. Ber.*, 113, 226 (1980).

73. M. Goehring, "*Ergebrisse und Probleme der Chemie der Schwefelstick-*

stoff verbindungen", Academie-Verlag, Berlin (1957).

74. I. Ruppert, *J. Fluorine Chem.*, 20, 241 (1982).

75. H. Vincent and Y. Monteil, *Synth. React. Inorg. Met-Org. Chem.*, 8, 51 (1978).

76. O. Glemser and R. Mews, *Angew. Chem. Int. Ed. Engl.*, 19, 883 (1980).

77. O. Glemser, *Prep. Inorg. Reactions*, 1, 227 (1964).

78. G. G. Alange, A. J. Banister and B. Bell, *J. Chem. Soc. Dalton. Trans.*, 2399 (1972).

79. J. Nelson and H. G. Heal, *Inorg. Nucl. Chem. Lett.*, 6, 429 (1970).

80. B. Krebs, S. Pohl and O. Glemser, *J. Chem. Soc. Chem. Commun.*, 548 (1978).

81. B. Krebs and S. Pohl, *Chem. Ber.*, 106, 1069 (1973).

82. G. Wolmershäuser and G. B. Street, *Inorg. Chem.*, 17, 2685 (1978).

83. J. Bojes and T. Chivers, *Inorg. Chem.*, 17, 318 (1978).

84. J. Bojes, P. M. Boorman and T. Chivers, *Inorg. Nucl. Chem. Lett.*, 12, 551 (1976).

85. J. Bojes and T. Chivers, *J. Chem. Soc. Chem. Commun.*, 453 (1977).

86. J. Bojes, T. Chivers, G. MacLean, R. T. Oakley and A. W. Cordes, *Can. J. Chem.*, 57, 3171 (1979).

87. J. Bojes, T. Chivers, A. W. Cordes, G. MacLean and R. T. Oakley, *Inorg. Chem.*, 20, 16 (1981).

88. J. Bojes, T. Chivers, I. Drummond and G. MacLean, *Inorg. Chem.*, 17, 3668 (1978).

89. E. Fluck, M. Becke-Goehring and G. Dehoust, *Chem. Ber.*, 312, 60 (1961).

90. E. Fluck and R. M. Reinisch, *Z. Anorg. Allg. Chem.*, 328, 165 (1964).

91. E. Fluck, *Z. Anorg. Allg. Chem.*, 312, 195 (1961).

92. H. G. Heal, *Adv. Inorg. Chem. Radiochem.*, 15, 375 (1972).

93. R. D. Smith, *Chem. Phys. Lett.*, 55, 590 (1978).

94. A. J. Banister and Z. V. Hauptmann, *J. Chem. Soc. Dalton. Trans.*, 731 (1980).

95. T. Chivers, A. W. Cordes, R. T. Oakley and P. N. Swepston, *Inorg. Chem.*, 20, 2376 (1981).

96. T. Chivers and R. T. Oakley, *J. Chem. Soc. Chem. Commun.*, 752 (1979).

97. T. Chivers, W. G. Laidlaw, R. T. Oakley and M. Trsic, *J. Am. Chem. Soc.*, 102, 5773 (1980).

98. T. Chivers, R. T. Oakley, A. W. Cordes and P. N. Swepston, *J. Chem. Soc. Chem. Commun.*, 35 (1980).

99. A. Golloch and M. Kuss, *Z. Naturforsch. B: Anorg. Chem. Org. Chem.*, 27B, 1280 (1972).

100. M. M. Labes, P. Love and L. F. Nichols, *Chem. Rev.*, 79, 1 (1979).

101. A. J. Banister, *Nature Phys. Sci.*, 237, 92 (1972).

102. A. J. Banister, *Nature Phys. Sci.*, 239, 69 (1972).

103. E. Hückel, *Z. Phys.*, 70, 204 (1931).

104. A. J. Banister, H. G. Clarke, I. Rayment and H. M. M. Shearer, *Inorg. Nucl. Chem. Lett.*, 10, 647 (1976).

105. U. Thewalt and M. Burger, *Z. Naturforsch. B*, 36, 293 (1981).

106. M. H. Palmer, J. R. Wheeler, R. H. Findlay, N. P. C. Westwood and W. M. Lau, *J. Mol. Structure.*, 86, 193 (1981).

107. B. M. Gimarc and N. Trinajstic, *Pure Appl. Chem.*, 52, 1443 (1980).

108. T. Chivers, *Acc. Chem. Res.*, in press.

109. T. Chivers, P. W. Codding and R. T. Oakley, *J. Chem. Soc. Chem. Commun.*, 584 (1981).

110. R. W. H. Small, A. J. Banister and Z. V. Hauptmann, *J. Chem. Soc.*

Dalton Trans., 2188 (1981).

111. T. Chivers, P. W. Codding, W. G. Laidlaw, S. W. Liblong. R. T. Oakley and M. Trsic, *J. Am. Chem. Soc.*, 105, 1186 (1983).

112. J. Donohue, A. Caron and E. Goldish, *J. Am. Chem. Soc.*, 83, 3748 (1961).

113. J. W. Waluk, T. Chivers, R. T. Oakley and J. Michl, *Inorg. Chem.*, 21, 832 (1982).

114. J. Michl, *J. Am. Chem. Soc.*, 100, 6901 (1978).

115. L. Zborilova, J. Touzin, D. Navratilova and J. Mrkosova, *Z. Chem.*, 12, 27 (1972).

116. L. Zborilova and P. Gebauer, *Z. Anorg. Allg. Chem.*, 483, 44 (1981).

117. Y. Monteil and H. Vincent, *Z. Naturforsch. B*, 31b, 673 (1978).

118. G. Wolmershäuser, G. B. Street and R. D. Smith, *Inorg. Chem.*, 18, 383 (1979).

119. Y. Monteil and H. Vincent, *Z. Naturforsch. B*, 31b, 673 (1976).

120. T. Chivers and M. N. S. Rao, *Can. J. Chem.*, in press.

121. R. Gleiter, *J. Chem. Soc. A*, 3174 (1970).

122. M. S. Gopinathan and M. A. Whithead, *Can. J. Chem.*, 53, 1343 (1975).

123. D. R. Salahub and R. P. Messmer, *J. Chem. Phys.*, 64, 2039 (1976).

124. K. Tanaka, T. Yamabe, A. Tachibana, H. Kato and K. Fukui, *J. Phys. Chem.*, 82, 2121 (1978).

125. S. Millefiori and A. Millefiori, *Inorg. Chim. Acta*, 45, L19 (1980).

126. T. Chivers, L. Fielding, W. G. Laidlaw and M. Trisic, *Inorg. Chem.*, 18, 3379 (1979).

127. B. Meyer, *Chem. Rev.*, 76, 367 (1976).

128. W. G. Laidlaw, M. Trsic and R. T. Oakley, unpublished results.

129. R. J. Sharma, F. Aubke and N. L. Paddock, *Can. J. Chem.*, 59,

3175 (1981).

130. H. T. Searle, *Proc. Chem. Soc.*, 7 (1959).

131. H. Bode, *Z. Anorg. Allg. Chem.*, 252, 113 (1943).

132. H. N. Stokes, *J. Am. Chem. Soc.*, 19, 782 (1897).

133. R. T. Oakley and N. L. Paddock, *Can. J. Chem.*, 53, 3038 (1975).

134. W. Lehr, *Z. Anorg. Allg. Chem.*, 371, 225 (1969).

135. M. Biddlestone and R. A. Shaw, *J. Chem. Soc. Chem. Commum.*, 407 (1968).

136. S. P. Mishra and M. C. R. Symons, *J. Chem. Soc. Chem. Commun.*, 313 (1973).

137. J. Emsley and P. B. Udy, *J. Chem. Soc. A.*, 768 (1971).

138. M. L. Neilsen and G. Cranford, *Inorg. Synth.*, 6, 94 (1960).

139. M. L. Neilsen and J. T. Morrow, *Inorg. Synth.*, 6, 99 (1960).

140. H. P. Calhoun, R. T. Oakley, N. L. Paddock and J. Trotter, *Can. J. Chem.*, 53, 2413 (1975).

141. G. E. Coxon and D. B. Sowerby, *J. Chem. Soc. A*, 3012 (1979).

142. A. Wilson and D. R. Carroll, *J. Chem. Soc.*, 2548 (1960).

143. E. Hobbs, D. E. C. Corbridge and B. Raistrick, *Acta Crystallogr.*, 6, 621 (1953).

144. D. W. J. Cruickshank, *Acta Crystallogr.*, 17, 671 (1964).

145. A. J. Wagner and A. Vos, *Acta Crystallogr. Sect. B*, 27, (1971).

146. H. D. McGeachin and F. R. Tromans, *J. Chem. Soc.*, 4777 (1961).

147. D. B. Sowerby, *J. Chem. Soc.*, 1396 (1965).

148. R. D. Sharma, S. J. Rettig, N. L. Paddock and J. Trotter, *Can. J. Chem.*, 60, 535 (1981).

149. T. Chivers, M. N. S. Rao and J. F. Richardson, *J. Chem. Soc. Chem. Commun.*, 982 (1982).

150. N. Burford, T. Chivers, R. T. Oakley, A. W. Cordes and P. N. Swepston, *J. Chem. Soc. Chem. Commun.*, 1204 (1980).

151. N. Burford, T. Chivers, A. W. Cordes, W. G. Laidlaw, M. C. Noble, R. T. Oakley and P. N. Swepston, *J. Am. Chem. Soc.* 104, 2182 (1982).

152. N. Burford, T. Chivers, P. W. Codding and R. T. Oakley, *Inorg. Chem.*, 21, 982 (1982).

153. N. Burford, T. Chivers and J. F. Richardson, *Inorg. Chem.*, in press.

154. N. Burford, T. Chivers, M. N. S. Rao and J. F. Richardson, *A. C. S. Symposium series*, in press.

155. H. L. Kraus and H. Jung, *Z. Naturforsch. B: Anorg. Chem. Org. Chem.*, 16B, 624 (1961).

156. G. Kresze, in "*Organic Sulfur Chemistry*", C. J. M. Stirling Ed., Butterworths, London, 65 (1975).

157. T. Chivers and R. T. Oakley, *J. Chem. Soc. Chem. Commun.*, 752 (1979).

158 T. Chivers, W. G. Laidlaw, R. T. Oakley and M. Trsic, *J. Am. Chem. Soc.*, 102, 5773 (1980).

159. N. Logan and W. L. Jolly, *Inorg. Chem.*, 4, 1508 (1965).

160. T. Chivers, R. T. Oakley, O. J. Scherer and G. Wolmershauser, *Inorg. Chem.*, 20, 914 (1981).

161. N. L. Paddock, *Quart. Rev. Chem. Soc.*, 18, 168 (1964).

162. R. T. Oakley and N. L. Paddock, *Can. J. Chem.*, 53, 3038 (1975).

163. R. Steudel, *Z. Naturforsch. 36a*, 850 (1981).

164. H. T. Searle, J. Dyson, T. N. Ranganathan and N. L. Paddock, *J. Chem. Soc. Dalton. Trans.*, 203 (1975).

165. A. W. Cordes, P. N. Swepston, R. T. Oakley, N. L. Paddock and T. N. Ranganathan, *Can. J. Chem.*, 59, 2364 (1981).

166. G. S. Reddy and C. D. Weis, *J. Org. Chem.*, 28, 1822 (1963).

167. B. Grushkin, M. G. Sanchèz, M. V. Ernst, J. L. McClanahan, G. Ashby and R. G. Rice, *Inorg Chem.*, 4, 1538 (1965).

168. V. Mark, C. Dungan, M. Crutchfield and J. R. Van Wazer, *Top. Phosphorus Chem.*, 5, 227 (1967).

169. C. W. Allen, J. B. Faught, T. Moeller and I. C. Paul, *Inorg. Chem.*, 8, 1719 (1969).

170. M. J. Begley, D. B. Sowerby and R. J. Tillot, *J. Chem. Soc. Dalton Trans.* 2527 (1974).

171. I. Ernest, W. Holick, G. Rhis, G. Schomberg, G. Shoham, D. Wenkert and R. B. Woodward, *J. Am. Chem. Soc.*, 103, 1540 (1981)

172. T. Chivers, C. Lau and R. T. Oakley, unpublished results.

173. W. Flues, O. J. Scherer, J. Weiss, G. Wolmershauser, *Angew. Chem. Int. Ed. Engl.*, 15, 379 (1976).

174. J. Bragin and M. V. Evans, *J. Chem. Phys.*, 51, 268 (1969).

175. F. R. Ahmed, P. Singh and W. H. Barnes, *Acta Crystallogr. Sect B*, 25, 316 (1969).

176. R. Bartetzko and R. Gleiter, *Chem. Ber.*, 113, 1138 (1980).

177. R. H. Findlay, M. H. Palmer, A. J. Downs, R. G. Egdell and R. Evans, *Inorg. Chem.*, 19, 1307 (1980).

178. R. Bartetzko and R. Gleiter, *Inorg. Chem.*, 17, 995 (1978).

179. R. Gleiter and R. Bartetzko, *Z. Naturforsch.*, 36b, 956 (1981).

180. T. Chivers, M.N.S. Rao and J. F. Richardson, unpublished results.

181. T. Chivers, M. N. S. Rao and J. F. Richardson, *J. Chem. Soc. Chem. Commun.*, 186 (1983).

182 T. Chivers, M. N. S. Rao and J. F. Richardson, *J. Chem. Soc. Chem. Commun.*, in press.

183. T. Chivers, M.N.S. Rao and J. F. Richardson, *J. Chem. Soc. Chem. Commun.*, in press.

184. W. C. Marsh, T. N. Ranganathan, J. Trotter and N. L. Paddock, *J. Chem. Soc. A*, 573 (1971).

185. T. N. Ranganathan, S. M. Todd and N. L. Paddock, *Inorg. Chem.*, 12, 316 (1973).

186. C. A. Coulson, H. C. Longuet-Higgins, *Proc. Roy. Soc.* (London) A191, 39 (1947); A192, 16 (1947); A193, 447 (1948); A193, 456 (1948); A195, 188 (1948).

187. H. W. Roesky, W. Schaper, O. Peterson and T. Muller, *Chem. Ber.*, 110, 2695 (1977).

188. A. W. Cordes, C. G. Marcellus, R. T. Oakley and W. L. Pennington, unpublished results.

189. R. T. Oakley, M. Shevalier, A. W. Cordes and W. L. Pennington, *184th A. C. S. Symposium*, abs. Inorg. 86 (1982).

190. M. P. Berthet, H. Vincent and Y. Monteil, *Z Naturforsch*, 35b, 329 (1980).

191. L. Patton and W. L. Jolly, *Inorg. Chem.*, 9, 1079 (1970).

192. S. C. Peake and A. J. Downs, *J. Chem. Soc. Dalton Trans.*, 859 (1974).

193. R. D. Smith and G. B. Street, *Inorg. Chem.*, 17, 938 (1978).

194. A. J. Downs and C. J. Adams, "*Comprehensive Inorganic Chemistry*", 2, 1545 (1973).

195. S. Mizushima "*Structure of Molecules and Internal Rotation*", Academic Press, New York (1954).

196. R. T. Oakley, N. L. Paddock, S. J. Rettig and J. Trotter, *Can J. Chem.*, 55, 3118 (1977).

197. K. D. Gallicano, R. T. Oakley, N. L. Paddock, S. J. Rettig and J. Trotter, *Can. J. Chem.*, 55, 304 (1977).

198. R. T. Oakley, N. L. Paddock, S. J. Rettig and J. Trotter, *Can. J. Chem.*, 55, 2530 (1977).

199. G. B. Street, R. L. Bingham, J. I. Crowley and J. Kuyper, *J. Chem. Soc. Chem. Commun.*, 464 (1977).

200. M. Akhtar, C. K. Chiang, A. J. Heeger and A. G. MacDiarmid, *J. Chem. Soc. Chem. Commun.* 846 (1977).

201. M. Akhtar, C. K. Chiang, A. J. Heeger, J. Milliken and A. G. MacDiarmid, *Inorg. Chem.*, 17, 1539 (1978).

202. H. Temkin and G. B. Street, *Solid State Comm.*, 25, 455 (1978).

203. Z. Iqbal, R. H. Baughman, J. Kleppinger and A. G. MacDiarmid, *Solid State Comm.*, 25, 409 (1978).

204. G. Wolmershäuser, C. Kruger and Y-H, Tsay, *Chem. Ber.*, 115, 1126 (1982).

205. K. F. Purcell and J. C. Kotz, "*An Introduction to Inorganic Chemistry*", Saunders College (1980).

206. R. Appel, I. Ruppert, R. Milker and V. Bastian, *Chem. Ber.*, 107, 380 (1974).

207. J. Weiss, I. Ruppert and R. Appel, *Z. Anorg. Allg. Chem.*, 406, 329 (1974).

208. W. G. Laidlaw and M. Trsic, *Inorg. Chem.*, 20, 1792 (1981).

209. M. Becke-Goehring and D. Schläfer, *Z. Anorg. Allg. Chem.*, 356, 234 (1968).

210. A. M. Griffin and G. M. Sheldrick, *Acta Crystallogr.*, B31, 895 (1975).

211. H. Koenig, R. T. Oakley, A. W. Cordes and M. C. Noble, *Can. J.*

Chem., in press.

212. H. Koenig, R. T. Oakley, A. W. Cordes and M. C. Noble, *Inorg. Chem.* in press.

213. For a similar treatment of S_4N_4.2NBD see: T. Yamabe, K. Tanaka, A. Tachibana and K. Fukui, *J. Phys. Chem.*, 83, 767 (1979).

214. S. W. Liblong, R. T. Oakley, A. W. Cordes and M. C. Noble, *Can. J. Chem.*, in press.

215. M. Villena-Blanco and W. L. Jolly, *Inorg. Synth.*, 9, 98 (1967).

216. S. A. Butler and J. Chatt, *Inorg. Synth.*, 15, 187 (1974).

217. W. Kuchen and H. Buchwald, *Chem. Ber.*, 91, 2871 (1958).

218. L. Maier, in "*Organic Phosphorus Compounds*", Ed. G. M. Kosolapoff and L. Maier, 1, 17, John Wiley, New York (1972).

219. O. J. Scherer and R. Weiss, *Z. Naturforsch., B*, 25, 1486 (1970).

220. D. Hellwinkel, in "*Organic Phosporus Compounds*", Ed. G. M. Kosolapoff and L. Maier, 3, 202, John Wiley, New York (1972).

221. X-RAY 76 package of crystallographic programs, Technical Report TR-446, ed. J. M. Stewart, Computer Science Center, University of Maryland. (1976).

222. P. Main, S. E. Hull, L. Lessinger, G. Germain, J. P. Declercq and M. M. Woolfson, MULTAN 78 - a system of computer programs for the automatic solution of crystal structures from X-ray diffraction data, University of York, England, and University of Louvain, Belgium (1978).

223. Computing was performed at the University of Calgary.

224. P. T. Cromer and J. B. Mann, *Acta Crystallogr.*, A24, 321 (1968).

225. "*International Tables for X-ray Crystallography*", Kynoch Press, Birmingham, England, IV, 149 (1974).

226. "*International Tables for X-ray Crystallography*", Kynoch Press, Birmingham, England, I (1974).

227. CADABS: A local modification of a computer program by P. Coppens and coworkers designed to calculate absorption factors by a numerical integration method[228]; State University of New York at Buffalo Crystallographic programs, Buffalo, New York, U.S.A. (1974).

228. P. Coppens, L. Leiseroweitz and D. Rubinovich, *Acta Crystallogr.*, 18, 1035 (1965).

APPENDICES

A1 Thermal parameters and hydrogen atom positions for 1,3-$(Ph_2PN)_2(SN)_2$.

A2 Thermal parameters and hydrogen atom positions for 1,5-$(Ph_2PN)_2(SN)_2$.

A3 Thermal parameters, hydrogen atom positions, and C-H bond lengths for 1,5-$(Me_2PN)_2(SN)_2$.

A4 Thermal parameters, hydrogen atom positions, and bond lengths and angles of the phenyl groups for $(Ph_2PN)_4(NS)_2^{2+}(Br_3^-)_2$.

A5 Thermal parameters and hydrogen atom positions for 1,5-$(Ph_2PN)_2(NSBr)_2$.

The anisotropic thermal parameter was of the form

$$T = \exp(-2\pi^2(U_{11}h^2a^{*2} + \ldots U_{12}hka^*b^* + \ldots)).$$

The hydrogen atoms are numbered according to the carbon atom to which they are attached.

APPENDIX 1

A1.1 Thermal parameters (x 10^4) for non-hydrogen atoms of $1,3\text{-}(Ph_2PN)_2(SN)_2$

Atom	U_{11}	U_{22}	U_{33}	U_{12}	U_{13}	U_{23}
P1	200(5)	284(5)	340(6)	57(5)	162(5)	57(5)
S1	374(7)	248(6)	794(10)	121(5)	327(7)	167(6)
N1	312(28)	279(28)	289(28)	0*	190(23)	0*
N2	296(21)	346(22)	528(26)	49(17)	213(19)	49(19)
N3	363(32)	250(28)	761(43)	0*	282(31)	0*
C1	243(21)	239(21)	295(23)	71(17)	177(19)	51(18)
C2	239(21)	241(22)	274(22)	2(18)	126(18)	14(18)
C3	200(21)	389(25)	360(25)	23(19)	120(19)	-63(22)
C4	298(24)	288(23)	576(31)	-64(20)	301(23)	-114(24)
C5	476(31)	289(25)	577(32)	4(22)	389(27)	92(23)
C6	331(26)	345(27)	456(28)	129(20)	231(23)	165(22)
C7	187(20)	331(25)	274(23)	35(18)	140(18)	68(19)
C8	260(23)	438(27)	327(25)	127(21)	154(20)	141(22)
C9	223(24)	647(35)	309(26)	61(23)	114(21)	57(25)
C10	294(25)	525(31)	299(26)	-54(22)	187(22)	-61(23)
C11	403(27)	309(26)	322(25)	-29(20)	230(22)	-9(20)
C12	235(22)	408(27)	245(24)	69(20)	135(19)	98(20)

* Parameters are restricted by the symmetry of the crystal.

A1.2 Positional and thermal parameters (x 10^4) for hydrogen atoms of $1,3\text{-}(Ph_2PN)_2(SN)_2$

Atom	x/a	y/b	z/c	U
H2	-1845	3017	2239	276
H3	-3399	2592	2166	350
H4	-3538	1070	3155	426
H5	-2231	218	4251	492
H6	-634	622	4327	414
H8	1522	2153	4978	377
H9	2341	3872	5999	434
H10	1839	6184	5796	413
H11	581	6983	4568	380
H12	-162	5242	3511	325

APPENDIX 2

A2.1 Thermal parameters (x 10^4) for non-hydrogen atoms of $1,5\text{-}(Ph_2PN)_2(SN)_2$

Atom	U_{11}	U_{22}	U_{33}	U_{12}	U_{13}	U_{23}
P1	92(3)	154(3)	252(4)	-32(2)	71(3)	-98(3)
S1	97(3)	101(3)	239(3)	-21(2)	-8(2)	-45(3)
N1	126(11)	267(13)	300(13)	-46(10)	75(9)	-152(10)
N2	109(10)	239(12)	280(13)	-54(9)	65(9)	-84(10)
C1	127(12)	157(12)	291(14)	-4(10)	57(10)	-105(11)
C2	145(13)	272(14)	271(14)	-19(11)	84(11)	-85(12)
C3	104(12)	261(14)	347(16)	-23(11)	68(11)	-126(12)
C4	124(12)	198(13)	371(16)	11(10)	20(11)	-53(12)
C5	163(14)	248(15)	406(18)	14(12)	50(12)	56(13)
C6	140(12)	180(13)	414(18)	-34(10)	75(12)	-1(12)
C7	93(11)	172(12)	267(14)	-30(10)	39(10)	-79(11)
C8	139(12)	225(14)	363(16)	-26(11)	62(11)	-18(12)
C9	145(13)	207(14)	310(14)	-4(11)	63(11)	-69(12)
C10	142(13)	177(13)	400(17)	-28(10)	82(12)	-50(12)
C11	141(12)	222(14)	347(16)	-20(11)	104(11)	-118(12)
C12	137(12)	218(14)	274(14)	-18(11)	78(11)	-68(11)

A2.2 Positional and thermal parameters (x 10^4) for hydrogen atoms of $1,5\text{-}(Ph_2PN)_2(SN)_2$

Atom	x/a	y/b	z/c	U
H2	-4445	473	1728	250
H3	-6351	788	748	258
H4	-6144	1423	-720	257
H5	-4036	1762	-1212	303
H6	-2123	1477	-221	262
H8	-1802	-2299	2631	262
H9	-1979	-281	2626	236
H10	-1409	-2720	1828	256
H11	-761	-1990	342	252
H12	-898	-526	321	218

APPENDIX 3

A3.1 Thermal parameters ($\times 10^4$) for non-hydrogen atoms of 1,5-$(Me_2PN)_2(SN)_2$

Atom	U_{11}	U_{22}	U_{33}	U_{12}	U_{13}	U_{23}
P1	135(5)	165(5)	164(5)	0*	18(4)	0*
P2	135(5)	155(5)	154(5)	0*	-10(4)	0*
S1	150(3)	158(3)	151(3)	-2(3)	-10(3)	-17(3)
N1	150(13)	145(13)	196(13)	16(10)	-4(11)	-9(11)
N2	164(14)	169(14)	300(16)	-8(11)	78(13)	29(13)
C1	187(23)	239(25)	157(21)	0*	51(18)	0*
C2	130(21)	301(27)	185(23)	0*	48(18)	0*
C3	247(27)	343(31)	204(24)	0*	14(22)	0*
C4	165(22)	225(24)	235(24)	0*	-7(20)	0*

A3.2 Positional and thermal parameters ($\times 10^4$) for hydrogen atoms and C-H bond lengths (Å) for 1,5-$(Me_2PN)_2(SN)_2$

Atom	X/a	Y/b	Z/c	U	Atoms	Distance
H11	294	8509	-1376	197	C1-H11	1.0929
H12	1765	7500*	-1179	197	C1-H12	1.0661
H21	-1456	8377	306	219	C2-H21	0.9308
H22	-1176	7500*	1387	219	C2-H22	0.8842
H31	5000	8448	-1320	266	C3-H31	1.0211
H32	3529	7500*	-1606	266	C3-H32	1.1027
H41	1176	8372	4242	220	C4-H41	0.9144
H42	588	7500*	3340	220	C4-H42	0.9112

* Parameters are restricted by the symmetry of the crystal

APPENDIX 4

A4.1 Thermal parameters (x 10^3) for non-hydrogen atoms of $(Ph_2PN)_4(NS)_2^{2+}(Br_3^-)_2.CH_3CN$

Atom	U_{11}	U_{22}	U_{33}	U_{12}	U_{13}	U_{23}
Br1	86(2)	72(2)	79(1)	-4(1)	5(1)	16(1)
Br2	59(2)	86(2)	103(2)	-3(1)	4(1)	12(1)
Br3	133(2)	115(2)	131(2)	-19(2)	20(2)	-22(2)
Br4	76(2)	115(2)	146(2)	-7(2)	0(2)	30(2)
Br5	78(2)	101(2)	90(2)	24(2)	16(1)	28(1)
Br6	191(3)	122(2)	132(2)	30(2)	-9(2)	-11(2)
P1	35(3)	36(3)	53(3)	-1(3)	0(3)	3(3)
P2	42(3)	48(4)	44(3)	-4(3)	-1(3)	-3(3)
P3	45(3)	58(4)	51(3)	-5(3)	1(3)	-2(3)
P4	53(4)	40(3)	52(3)	-1(3)	9(3)	-5(3)
S1	51(3)	50(3)	47(3)	-4(3)	4(3)	10(3)
S2	54(3)	48(3)	50(3)	3(3)	0(3)	9(3)
N1	45(9)	41(9)	28(7)	0(7)	1(7)	12(6)
N2	22(8)	27(9)	48(8)	15(7)	-6(7)	13(7)
N3	65(10)	57(10)	27(8)	26(8)	-1(7)	3(7)
N4	51(9)	11(8)	34(8)	3(7)	1(7)	-1(6)
N5	24(8)	72(11)	60(10)	3(9)	13(8)	3(8)
N6	42(8)	27(8)	28(7)	-12(7)	6(7)	-11(6)
N7[a]	107(14)	68(12)	72(12)	13(11)	-9(11)	-27(10)

Atom	U	Atom	U	Atom	U	Atom	U
C11	37(5)	C31	42(5)	C51	56(5)	C71	59(5)
C12	66(6)	C32	53(5)	C52	97(7)	C72	95(7)
C13	67(6)	C33	84(6)	C53	131(9)	C73	128(8)
C14	79(6)	C34	60(5)	C54	155(10)	C74	108(8)
C15	109(8)	C35	68(6)	C55	168(10)	C75	134(9)
C16	71(6)	C36	58(5)	C56	93(7)	C76	89(7)
C21	39(5)	C41	46(5)	C61	52(5)	C81	52(5)
C22	63(6)	C42	73(6)	C62	85(6)	C82	154(10)
C23	88(7)	C43	75(6)	C63	106(7)	C83	175(11)
C24	82(6)	C44	99(7)	C64	123(8)	C84	101(7)
C25	98(7)	C45	85(6)	C65	103(7)	C85	77(6)
C26	68(6)	C46	89(6)	C66	75(6)	C86	70(6)
C1[a]	121(10)						
C2[a]	127(8)						

[a] solvent molecule CH_3CN

A4.2 Positional and thermal parameters (x 10^4) for hydrogen atoms of $(Ph_2PN)_4(NS)_2^{2+}(Br_3^-)_2.CH_3CN$

Atom	x/a	y/b	z/c	U	Atom	x/a	y/b	z/c	U
H12	2572	7296	2313	770	H52	6842	8985	4749	1130
H13	2008	8868	2216	810	H53	7223	10524	4517	1580
H14	2750	10085	2038	1000	H54	6929	11149	3672	1800
H15	4119	10063	2126	1210	H55	6214	10272	2968	1880
H16	4742	8519	2152	830	H56	5964	8610	3166	1060
H22	3735	7003	1167	760	H62	7680	7035	4151	1010
H23	3311	6130	349	1050	H63	8559	6391	4795	1210
H24	3294	4484	455	920	H64	8197	6030	5684	1350
H25	3666	3661	1245	1250	H65	6867	6170	5935	1100
H26	39 3	4632	2064	720	H66	5942	6774	5260	820
H32	7563	6069	2579	650	H72	4992	9483	4598	1100
H33	8554	7228	2461	940	H73	4671	11115	4491	1510
H34	8359	8648	1970	700	H74	3892	11606	3770	1110
H35	7027	9094	1743	770	H75	3093	10529	3306	1680
H36	6047	7936	1847	700	H76	3378	8871	3892	1050
H42	5734	6346	1135	850	H82	4314	6353	4983	1780
H43	5688	5287	382	760	H83	3387	5750	5615	2040
H44	5703	3651	554	1180	H84	2203	6637	5683	1110
H45	5900	3045	1448	1110	H85	1882	7780	5093	830
H46	5966	4137	2200	1010	H86	2790	8268	4404	780

A4.3 Bond lengths (Å) and angles (Deg) for the phenyl groups of $(Ph_2PN)_4(NS)_2^{2+}(Br_3^-)_2$

Atoms	Distance	Atoms	Distance
C11-C12	1.43(2)	C31-C32	1.43(2)
C12-C13	1.43(2)	C32-C33	1.39(2)
C13-C14	1.27(3)	C33-C34	1.39(2)
C14-C15	1.39(3)	C34-C35	1.39(2)
C15-C16	1.41(3)	C35-C36	1.41(2)
C16-C11	1.36(2)	C36-C31	1.32(2)
C21-C22	1.33(2)	C41-C42	1.39(2)
C22-C23	1.42(2)	C42-C43	1.36(2)
C23-C24	1.38(3)	C43-C44	1.37(3)
C24-C25	1.35(3)	C44-C45	1.36(3)
C25-C26	1.42(2)	C45-C46	1.39(2)
C26-C21	1.41(2)	C46-C41	1.35(2)
C51-C52	1.38(2)	C71-C72	1.34(3)
C52-C53	1.38(3)	C72-C73	1.42(3)
C53-C54	1.31(3)	C73-C74	1.29(3)

cont'd ...

A4.3 (continued)

Atoms	Distance	Atoms	Distance
C54-C55	1.39(4)	C74-C75	1.33(3)
C55-C56	1.44(3)	C75-C76	1.42(3)
C56-C51	1.34(3)	C76-C71	1.36(2)
C61-C62	1.40(2)	C81-C82	1.31(3)
C62-C63	1.37(3)	C82-C83	1.40(4)
C63-C64	1.33(3)	C83-C84	1.40(3)
C64-C65	1.39(3)	C84-C85	1.26(3)
C65-C66	1.41(2)	C85-C86	1.42(2)
C66-C61	1.38(2)	C86-C81	1.36(2)

Atoms	Angle	Atoms	Angle
P1-C11-C12	117(1)	P3-C51-C52	118(1)
P1-C11-C16	121(1)	P3-C51-C56	119(1)
C16-C11-C12	121(1)	C56-C51-C52	123(2)
C11-C12-C13	116(1)	C51-C52-C53	118(2)
C12-C13-C14	120(2)	C52-C53-C54	121(2)
C13-C14-C15	126(2)	C53-C54-C55	123(2)
C14-C15-C16	116(2)	C54-C55-C56	116(2)
C15-C16-C11	120(2)	C55-C56-C51	119(2)
P1-C21-C22	122(1)	P3-C61-C62	122(1)
P1-C21-C26	121(1)	P3-C61-C66	122(1)
C26-C21-C22	116(1)	C66-C61-C62	116(1)
C21-C22-C23	126(2)	C61-C62-C63	122(2)
C22-C23-C24	113(1)	C62-C63-C64	122(2)
C23-C24-C25	128(2)	C63-C64-C65	120(2)
C24-C25-C26	114(2)	C64-C65-C66	119(2)
C25-C26-C2	123(1)	C65-C66-C61	121(2)
P2-C31-C32	119(1)	P4-C71-C72	119(1)
P2-C31 C36	120(1)	P4-C71-C76	121(1)
C36-C31-C32	120(1)	C76-C71-C72	120(2)
C31-C32-C33	115(1)	C71-C72-C73	119(2)
C32-C33-C34	126(2)	C72-C73-C74	120(2)
C33-C34-C35	117(1)	C73-C74-C75	122(2)
C34-C35-C36	118(1)	C74-C75-C76	119(2)
C35-C36-C31	124(1)	C75-C76-C71	119(2)
P2-C41-C42	118(1)	P4-C81-C82	122(1)
P2-C41-C46	123(1)	P4-C81-C86	120(1)
C46-C41-C42	119(1)	C86-C81-C82	117(2)
C41-C42-C43	119(1)	C81-C82-C83	125(2)
C42-C43-C44	120(1)	C82-C83-C84	114(2)
C43-C44-C45	122(2)	C83-C84-C85	124(2)
C44-C45-C46	117(2)	C84-C85-C86	120(2)
C45-C46-C41	123(1)	C85-C86-C81	120(1)

APPENDIX 5

A5.1 Thermal parameters (x 10^4) for non-hydrogen atoms of

1,5-$(Ph_2PN)_2(NSBr)_2$

Atom	U_{11}	U_{22}	U_{33}	U_{12}	U_{13}	U_{23}
Br1	92(2)	45(2)	46(2)	3(2)	27(2)	7(2)
Br2	71(2)	51(2)	51(2)	1(2)	25(2)	6(2)
S1	47(4)	25(4)	37(4)	-6(4)	13(3)	-11(3)
S2	21(3)	38(4)	47(4)	-8(3)	13(3)	-10(4)
P1	40(4)	32(4)	42(4)	0(4)	6(3)	6(4)
P2	24(3)	40(4)	30(3)	-2(4)	13(3)	2(3)
N1	11(8)	67(15)	55(11)	-6(10)	9(7)	-14(10)
N2	55(11)	22(11)	53(13)	-3(9)	19(9)	-15(9)
N3	58(11)	34(12)	20(8)	15(10)	-1(7)	-3(8)
N4	3(6)	73(15)	33(11)	-2(9)	9(7)	-1(10)

Atom	U	Atom	U	Atom	U	Atom	U
C11	21(4)	C21	37(7)	C31	42(7)	C41	52(7)
C12	49(5)	C22	40(5)	C32	46(6)	C42	58(8)
C13	51(5)	C23	40(5)	C33	86(9)	C43	61(7)
C14	55(6)	C24	53(4)	C34	67(5)	C44	49(5)
C15	48(6)	C25	54(5)	C35	73(6)	C45	58(5)
C16	41(6)	C26	43(7)	C36	82(11)	C46	41(5)

A5.2 Positional and thermal parameters (x 10^4) for hydrogen

1,5-$(Ph_2PN)_2(NSBr)_2$

Atom	x/a	y/b	z/c	U	Atom	x/a	y/b	z/c	U
H12	4587	5756	7844	490	H32	9188	1741	8766	510
H13	3528	5682	8818	590	H33	11079	187	9063	910
H14	2175	3384	8820	610	H34	10369	-1603	9247	700
H15	2011	641	7832	500	H35	10728	-3643	7941	750
H16	2955	1025	6811	420	H36	9399	-1966	6944	690
H22	3831	2798	4847	470	H42	10017	4083	6423	550
H23	2452	4196	3751	430	H43	11320	3944	5531	630
H24	2120	7076	3861	560	H44	10930	2299	4487	490
H25	2801	8683	5108	600	H45	9467	-36	4304	600
H26	3884	6990	6328	460	H46	8272	-274	5205	430